PROLINE-CE

WORKPACKAGE T2, ACTIVITY T2.3

OUTLINING OF LESSONS LEARNT AND RESULTING RECOMMENDATIONS

D.T2.3.3 PA REPORTS ABOUT CLIMATE CHANGE ISSUES IN PILOTS

TRANSNATIONAL REPORT

Lead Institution	PP13 - CMCC Foundation
Contributor/s	See next page
Lead Author/s	Guido Rianna
Date last release	December 6, 2018

Contributors, name and surname	Institution
Roland Koeck	PP3, LP/PP1 - University of Natural Resources and Life Sciences, Department of Forest- and Soil Sciences, Institute of Silviculture
Markus Hochleitner	PP3 - Municipality of the city of Waidhofen/Ybbs, Water Works
Gerhard Kuschnig	PP2 - Municipality of the city of Vienna, Vienna Water
Elisabeth Gerhardt	Federal Research and Training Centre for Forests, Natural Hazards and Landscape
Hubert Siegel	LP/PP1 - Austrian Federal Ministry of Agriculture, Forestry, Environment and Water Management; Forest Department
Joanna Czekaj	PP11 - GPW S.A.
Mirosława Skrzypczak	PP11 - GPW S.A.
Krzysztof Skotak	IOŚ – PIB
Rafał Ulańczyk	IOŚ – PIB
Ewa Łupikasza	Jars Sp. zoo
Magdolna Ambrus	PP7 - General Directorate of Water Management
Róbert Hegyi	PP7 - General Directorate of Water Management
Janka Mezei	KSzI Ltd.
Erika Kissné Jáger	KSzI Ltd.
Márton Ganszky	KSzI Ltd.
Bence Kisgyörgy	KSzI Ltd.
Veronika Kiss	KSzI Ltd.
Ágnes Tahy	PP7 - General Directorate of Water Management
Daniel Bittner	PP12 - Technical University of Munich
Gabriele Chiogna	PP12 - Technical University of Munich
Hagen Verch	PP12 - Technical University of Munich
Markus Disse	PP12 - Technical University of Munich
Daniel Bittner	PP12 - Technical University of Munich

Gabriele Chiogna	PP12 - Technical University of Munich
Hagen Verch	PP12 - Technical University of Munich
Markus Disse	PP12 - Technical University of Munich
Josip Terzić	PP8 - Croatian Geological Survey, Department of Hydrogeology and Engineering Geology
Ivana Boljat	PP8 - Croatian Geological Survey, Department of Hydrogeology and Engineering Geology
Ivona Baničck	PP8 - Croatian Geological Survey, Department of Hydrogeology and Engineering Geology
Matko Patekar	PP8 - Croatian Geological Survey, Department of Hydrogeology and Engineering Geology
Daria Čupić	AP17 - Croatian Waters
Barbara Čenčur Curk	PP4 - University of Ljubljana, Faculty of Natural Sciences and Engineering, Ljubljana, Slovenia
Jerca Praprotnik Kastelic	PP4 - University of Ljubljana, Faculty of Natural Sciences and Engineering, Ljubljana, Slovenia
Primož Banovec	PP4 - University of Ljubljana, Faculty of Civil and Geodetic Engineering, Ljubljana, Slovenia
Ajda Cilenšek	PP4 - University of Ljubljana, Faculty of Civil and Geodetic Engineering, Ljubljana, Slovenia
Matej Cerk	PP4 - University of Ljubljana, Faculty of Civil and Geodetic Engineering, Ljubljana, Slovenia
Branka Bračič Železnik	PP5 - Public Water Utility JP VO-KA, Ljubljana, Slovenia
Guido Rianna	PP13 - CMCC Foundation
Veronica Villani	PP13 - CMCC Foundation
Nicola Ciro Zollo	PP13 - CMCC Foundation
Angela Rizzo	PP13 - CMCC Foundation

Table of Contents

1. Introduction

The Report T2.3.3 “PA Reports about climate change issues in pilots” is aimed to:

- provide a frame about potential changes that Central Europe (CE) area could experience in weather forcing recognized of interest for water protection purposes, under the effect of Climate Changes (CC);
- characterize the Pilot Action site from a climate viewpoint considering past experiences and/or data from PROLINE CE.

The work is aimed to display and evaluate:

i) what are the climate conditions currently observed on Central Europe domain as returned by E-OBS gridded dataset;

ii) the potential variations that the domain could experience on short and long-time horizon under the effect of climate changes; In this regard, several weather variables are taken into account: seasonal temperature and cumulative precipitation values, consecutive dry and wet days and maximum daily precipitations;

iii) what are the current State-Of-The-Art (SOTA) for each Pilot Action site from the climate to the hydrological viewpoint

iv) the potential differences between PROLINE CE approach and current SOTA.

Despite the considerable limitations associated with simplifications, they are assumed as proxy for expeditious evaluations about future changes in quantity and quality of water resources and occurrence and severity of hydrological/hydraulic hazards. In order to take into account, the high uncertainties currently associated to climate projections (increasingly larger for further future period of interest), the findings provided by an ensemble of different climate modelling chains included in EURO-CORDEX initiative are considered and characterized by very high horizontal resolution (0.11°, about 12 km over the Europe).

In the following, first, an overview about current conditions is reported using E-OBS dataset on reference period 1971-2000; after, the related climate zonation is shown recurring to widely used classification proposed by Koppen & Geiger (Koppen & Geiger, 1954; 1961). Furthermore, the main elements and approaches currently used to perform climate projections at regional scale are introduced and variations in different weather patterns are displayed on short (2021-2050) and long-time horizon (2071-2100) under two different scenarios of greenhouse gases and aerosols concentrations. Finally, an overview about the different Pilot Actions are introduced, considering both SOTA data and data from EURO-CORDEX initiative with the aim of understanding the difference between SOTA and EURO-CORDEX data and eventually indicating if current state of knowledge could satisfy the main issues for each Pilot Action.

2. Summary of pilot actions and pilot sites

Pilot actions and pilot sites respectively are classified according to their geographic specification, natural site characteristics (aquifer type) and main land use (Table 1) into three clusters (Pilot Action Cluster, PAC):

- PAC1: Mountain forest and grassland sites
- PAC2: Plain agriculture/grassland/wetland sites
- PAC3: Special sites (riparian strips)

Table 1: Pilot Actions and Pilot Sites respectively, classified into three clusters according to land uses and geographic scope.

PILOT ACTION CLUSTER 1 (PAC1) Mountain forest and grassland sites	**PA1.1 Catchment area of the Vienna Water Supply, AT1** Drinking water source: Karst aquifer
	PA1.2 Catchment area of Waidhofen/Ybbs, AT2 Drinking water source: Fractured aquifer
PILOT ACTION CLUSTER 2 (PAC2) Plain agriculture/ grassland/ wetland sites	**PA2.1 Well field Dravlje valley in Ljubljana, SI** Drinking water source: Porous aquifer
	PA2.2 Water reservoir Kozłowa Góra, PL Drinking water source: Surface water
	PA2.3 Tisza catchment area, HU1 Drinking water source: Surface water
	PA2.4 Groundwater protection in karst area, HR **2.4.1 - South Dalmatia: Prud, Klokun and Mandina spring** **2.4.2 - Imotsko polje springs** Drinking water source: Karst aquifer
	PA2.5 Neufahrn bei Freising, GER Drinking water source: Porous aquifer
PILOT ACTION CLUSTER 3 (PAC3) Special sites (riparian strips)	**PA3.1 Po river basin, IT** Drinking water source: Bank filtration
	PA3.2 Along Danube Bend, HU2 Drinking water source: Bank filtration

3. National policies on climate change

Since 2005, the European Commission is heavily engaged in efforts to improve the adaptation to changes in Europe's climate. As a result, a number of policies and strategies on adapting to climate change were proposed and adopted.

The Commission's 2009 White Paper "Adapting to climate change: towards a European framework for action" sets out a framework to reduce the EU's vulnerability to the impact of climate change and was designed to evolve as further evidence became available.

Later, in April 2013, the European Commission adopted the EU strategy on adaptation to climate change, which aims to make Europe more climate-resilient and to enhance the preparedness and capacity of all governance levels to respond to the impacts of climate change. The strategy has been welcomed by the EU Member States, which have accepted it at national level.

Following the limited participation in the Kyoto Protocol, which was ratified in 1997 during the 3rd Conference of the Parties (COP3) but entered into force only in 2005, the European Union has worked on the construction of a broad coalition of developed and developing countries in favour of ambitious objectives. This coalition has led to the positive result of the Paris conference. In fact, the EU was the first major economy to submit its intended contribution to the Paris Agreement in March 2015, which represent the first-ever universal, legally binding global climate deal to combat climate change and adapt to its effects. The Agreement was adopted in December 2015 during the Paris Climate Conference (21st Conference of the Parties - COP21). The final Agreement is based on three pillars: 1) increasing efforts for mitigation to limit the global warming within the 2°C but with the desirable target of 1.5°C; 2) favouring the mainstreaming of adaptation initiatives at local level; 3) putting in place proper financial instruments to support developing countries for coping with climate change's impacts.

In 2015, the 2030 Agenda for Sustainable Development and the 17 Sustainable Development Goals (SDG), articulated in 169 Targets to be reached by 2030, were adopted by the United Nations General Assembly. SDG raising the issue of adaptation to climate change and, among these, Goal 13 demands urgent action to combat climate change and its impacts. The 2030 Agenda for Sustainable Development provides an overarching framework connecting the Climate Change Adaptation targets and commitments with poverty reduction, economic growth, social inclusion and environmental protection. Nevertheless, the issues related to Climate Change are highly recalled in many other SDGs for example related to ensure water in every part of the world and to any community or to build more resilient urban centres. In particular, Goal 6 aims to ensure availability and sustainable management of water and sanitation for all. In order to achieve this goal, it is necessary to improve water quality by reducing pollution, eliminating dumping and minimizing release of hazardous chemicals and materials (Target 6.3), increase water-use efficiency and ensure sustainable withdrawals (Target 6.4), and protect and restore water-related ecosystems, including mountains, forests, wetlands, rivers, aquifers and lakes.

Recently, the European Commission has published a report about the evaluation of the implementation of the EU Strategy on adaptation to climate change (COM, 2018) from which emerged that

the commission has further consolidated adaptation in its legislative proposal for a common agricultural policy. In this policy climate adaptation, ecosystem services, biodiversity protection, and habitat conservation are some of the main objectives. In this framework, adaptation will feature in the long-term strategy, highlighting the need for EU companies and governments to plan for slow-onset impacts such water scarcity.

At national level, several policies have been adopted to ratify the international strategies for adapting to climate change effects. The national policies for each Pilot Action site are synthetized in Table 2.

Table 2: National policies on climate change for each Pilot Action site.

PA1.1 Catchment area of the Vienna Water Supply, AT1 **PA1.2 Catchment area of Waidhofen/Ybbs, AT2**	The Austrian Strategy for Adaptation to Climate Change was adopted by the Federal Government in 2017 supplemented by a comprehensive Action Plan as a guideline for the implementation of the recommendations for action (14 fields of activity). On the basis of new scientific findings, key findings from the 2015 progress report (of the first Adaptation Strategy 2012) and current political developments, this strategy was fundamentally updated and further developed in 2016. All affected ministries, the federal states, as well as interest groups, stakeholders and NGOs were involved in the work.
PA2.1 Well field Dravlje valley in Ljubljana, SI	Strategic Framework for Adaptation to Climate Change was accepted by Slovenian Government in 2016 (MOP, 2016): • Its general objective is reducing exposure to climate change impacts, reducing sensitivity and vulnerability caused by these impacts, and increasing the resilience and adaptability of society. • In order to monitor the established objective, a vulnerability indicator for climate change will be introduced. Implementation will be monitored through the preparation of a regular biennial report and regular updating of steps and guidelines. • A long-term upgrade and integration of existing databases and their accessibility is foreseen to support decision making. In the area regarding water resources data, is evaluated that complementation is needed by better assessing impacts on good water status and that individual data sets should be connected with data from other sectors and spatially between different planning units (municipalities, regions, country). The Framework Programme for Transition to a Green Economy, adopted in October 2015 together with Plan of Governmental Activities for 2015-2016, refers to the need for integration in sectoral strategies. It links climate adaptation particularly with the objectives of

	biodiversity conservation, green jobs creation, sustainable urban development, and green agricultural practices
PA2.2 Water reservoir Kozłowa Góra, PL	Polish National Strategy for Adaptation to Climate Change by 2020 with the perspective by 2030 (SPA 2020). • It was emanated as a respond to The European Commission's "*The White Paper: Adapting to climate change: Towards a European framework for action*". Its goal is to develop a strategy of adaptation for sectors and regions vulnerable to climate change was established on 19th May 2010 as a part of a broader research project named KLIMADA, which covers the period up to 2070
PA2.3 Tisza catchment area, HU1 **PA3.2 Along Danube Bend, HU2**	Kyoto Protocol: accepted and promulgated by the Hungarian Parliament in the 2007 Act LX: it stipulated the creation of the National Climate Change Strategy (NÉS). The 29/2008. (III.20.) Parliament regulation defines a framework for measures planned for 2008-2025 • The objectives of NÉS were implemented by the National Climate Change Program. The objects and purposes of the Hungarian Government's NÉS include the decrease of the consumption of fossil fuels, the start of a civic initiative for energy efficiency, the constrain of the current level of energy consumption, the increase of the share of renewable energy sources and the development of public transportation. NÉS incorporates the National Decarbonisation Plan, which targets for action, priorities and directions for greenhouse gas emission reduction, in line with new requirements, by 2050 National Water Strategy (2013) • Its goal is to ensure the quantitative and qualitative protection of water, the need to reduce and prevent the harmful effects of water use (including drinking water supply, industrial and irrigation water extraction, ecological water needs) generated from surpluses or shortages of water. There are also actions to promote the economical utilization of drinking water, even raising the possibility of limiting water use
P2.4 Groundwater protection in karst area, HR	Decision on the Acceptance of the Fifth National Report of the Republic of Croatia under the United Nations Framework Convention on Climate Change (OG 24/10) Decision on Adoption of the Air Protection, Ozone Layer and Mitigation of Climate Change in the Republic of Croatia for the Period 2013 – 2017 (OG 139/13)

2.4.1 - South Dalmatia: Prud, Klokun and Mandina spring **2.4.2 - Imotsko polje springs**	Decision on the adoption of the Sixth National Report of the Republic of Croatia under the United Nations Framework Convention on Climate Change (OG 18/14) Strengthening the capacities of the Ministry of Environment and Energy for adaptation to climate change (May 2016 - November 2017) • It was initialized by the Croatian Ministry of Environment and Energy with the main purpose was to draw up a draft of the National Climate Change Adjustment Strategy for the period up to 2040 with a view for 2070 and an Action Plan draft National Adaptation Strategy • It defined the priority measures and activities for the most vulnerable sectors such as hydrology and water resources, agriculture, forestry, biological diversity and natural ecosystems, coastal area management, tourism and human health Adjustment Strategy • Its goals are to reduce the vulnerability of social and natural systems to negative climate change impacts (i.e., strengthening their recovery rate, as well as to gather all relevant stakeholders in order to facilitate strong support for the implementation of joint actions and a more proactive approach to the problematics) and to integrate the adjustment procedures into existing policies, programmes and plans that are conducted on all management levels
PA2.5 Neufahrn bei Freising, GER	At national level: National Adaptation Strategy (DAS) adopted on 17 December 2008. National Adaptation Plan (NAP) adopted on 31 August 2011. • The goal is to reduce greenhouse gas emissions by 80% to 95% until 2050 with respect to emissions in 1990; two interim goals are defined for 2020[1] and 2030, where greenhouse gas emissions should at least be reduced by 40% and 55%, respectively

[1] In the framework of the coalition negotiations of the newly constituted grand coalition of the German federal government, the negotiating partners agreed that the 2020 targets are not achievable. They decided to create a set of measures in order to achieve the 2020 climate protection targets at the beginning of the 2020's. When that new set of measures will be issued by the current federal government and which particular measures this set will contain is still questionable (Spiegel Online, 2018).

	• The share in gross final energy consumption from renewable energies should be increased to 18%, 30% and 60% in 2020, 2030 and 2050 At local level (Bavaria area): Bavarian climate protection 2050 • It follows the same goals as defined by the European Union and Germany Bavarian Climate Program 2020 • Released in 2007 by the Bavarian State Ministry of the Environment and Consumer Protections, its program includes principles and targets of climate policy, reduction of greenhouse gas emissions, as well as adaptation strategies in different sectors and research and development Climate Policy Programme Bavaria 2050 Detailed program published in 2015 and updated in 2017; it includes a comprehensive overview of climate impacts and measures related to the Bavarian climate policy
PA3.1 Po river basin, IT	National Strategy for climate change adaptation • Defined in 2015 by the Italian Ministry of the Environment on the basis of European Commission COM (2013) 216 final "An EU Strategy on adaptation to climate change" and also considering the Environmental European Agency report "National adaptation policy processes in European countries" (Report No. 4/2014) First draft for public consultation of the National Plan for Climate Change Adaptation Regional Administrations in Northern Italy have started working on climate change, intending to put in action national guidelines and results to draw regional and local strategies, plans rules and regulations to increase climatic knowledge, modelling and simulation and to set up efficient actions for mitigation and adaptation processes[2]. Ongoing activities include: • verifying if current legislation, sectoral and territorial policies and governance instruments may have alone, or together, CC mitigation and/or CC adaptation effects,

[2] In 2014, Lombardia Region started with the implementation of a process for the construction of a Regional climate change adaptation Strategy; Emilia Romagna Region started in 2015 a path toward a unitary strategy for climate change mitigation and adaptation; in 2017, also Piemonte Region set up a Strategy to face climate change

	• evaluating if these effects may satisfy the actual CC mitigation and adaptation targets even compared with international agreements • project where necessary additional measure and relate indicators

4. General overview on the Central Europe domain

4.1. Selecting climate indicators

In recent years, several literature works provided exhaustive investigations about the expected impacts of CC on water resources and hydrological hazards at global (e.g. Hirayabashi et al., 2013), continental (e.g. Alfieri et al., 2015; Royas et al., 2012) or on areas included in CE domain (e.g. Vezzoli et al., 2015 for Po River Basin). Such studies usually adopt complex and time-consuming simulation chains in which hydrological and or hydraulic models use as inputs the data provided by climate simulations. They usually focus only on one of two topics covered by the project (drinking water protection or flood hazard) often adopting approaches and assumptions not easily managed by stakeholders and communities.
Then, in this work, an expeditious approach is preferred; it simply identifies a set of weather forcing that can be assumed as "proxies" to provide an assessment about the potential effects of Climate Changes on drinking water resources and hydrological hazard in Central Europe. They include seasonal cumulative rainfall and average temperature values respectively assumed as main drivers for water input and output (through evapotranspiration); moreover, three indices are selected among the 27 proposed by CCl/CLIVAR/JCOMM Expert Team (ET) on Climate Change Detection and Indices (ETCCDI) as recognized of higher interest for the topics covered by the Project; namely:

- Rx1day: yearly maximum 1-day precipitation;
- CDD (Consecutive Dry Days): Maximum length of dry spell, maximum number of consecutive days with precipitation (RR) < 1mm;
- CWD (Consecutive Wet Days): Maximum length of wet spell, maximum number of consecutive days with RR ≥ 1mm.

Such indicators are assumed related to events inducing hydrological hazards (according the geomorphological and land use features of affected areas) (Rx1d) and to precipitation patterns strongly affecting the effective amount of water entering the soil or recharging surface water bodies. Nevertheless, it is worth recalling that ETCCDI indicators are designed to detect "moderately extreme weather events" (Wehner, 2013) then characterized by return time periods usually less than 10 years. For much rarer (more severe) phenomena, it is necessary to recur to extreme value statistical theories. In last years, such techniques have been widely adopted to assess in steady conditions return periods of fixed Extreme Weather Events while, in recent times, numerous approaches have been proposed to account for non-stationary conditions potentially induced by climate changes.

4.2. Dataset

To provide an overview about current conditions, E-OBS dataset is used. E-OBS gridded data set (Haylock et al., 2008) contains daily maps of gridded data spanning the period from 1 January 1950 to the present, at four different grid resolutions for five weather variables (daily mean temperature TG, daily minimum temperature TN, daily maximum temperature TX, daily precipitation sum RR and daily averaged sea level pressure PP). It was developed within the European Union Framework 6 ENSEMBLES project (van der Linden and Mitchell, 2009) with the main goal to support validation of Regional Climate Models (RCMs) and improve understanding of climate change impacts.

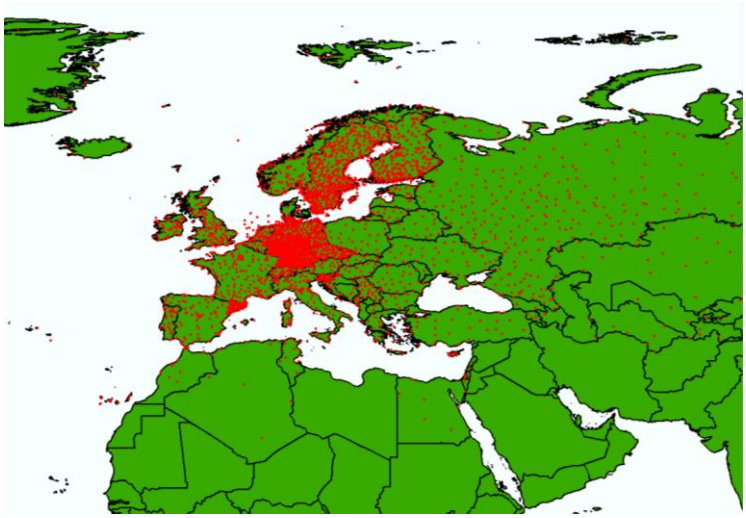

Figure 1: Distribution of weather stations providing data for E-OBS gridded dataset; focus on Europe area.

The data used are provided from the European Climate Assessment & Dataset (ECA&D), (Klein Tank et al., 2002; Klok and Klein Tank, 2008) with about 11,400 stations (update December 2017, Figure 1) and gradually expanding. Data are monthly updated thanks to National Meteorological and Hydrological Services (NMHSs), individual researchers affiliated with a university, global data centres like the National Climatic Data Center (NOAA, Asheville, USA) or the synoptic messages from the Global Telecommunication System (van der Schrier et al., 2013). Specifically, in this work, version 16.0 is adopted with 0.25◦ × 0.25◦ regular longitude-latitude.

During recent years, several researches using the dataset attempted giving caveats about potential inaccuracies and constraints associated to it; for example, according van der Schrier et al. (2013) uncertainties due to urbanization, statistical interpolation, and the potential inhomogeneity drives the total uncertainty estimate. Hofstra et al. (2009) carry out an analysis about the homogeneity of the gridded data revealing that it is primarily induced by inhomogeneity in the underlying station data (e.g. break point detection); moreover, the comparison with much denser station return, on several areas, significant differences in precipitation (usually biased toward lower for E-OBS) while correlations overall are high. In this regard, Figure 1 show how the density of stations from which the gridded dataset is retrieved is highly variable across the Europe inducing larger uncertainties in areas less covered by observations (e.g. Southern Italy).

Finally, Turco et al. (2013), investigating Great Alpine Region and NW Italy, display how most E-OBS gridpoint series should to be shifted back by 1 day to have maximum overlap of the measurement period. Moreover, temporal and spatial similarities of most indices are higher adopting NWIOI (Ronchi et al., 2008; AAVV, 2011) and MAP (Frei and Schar, 1998) than between MAP or the NWIOI and EOBS.

In this work, the performed analysis considers Central Europe domain over 1971-2000 time span. The period is selected accounting for World Meteorological Organization (WMO) indications according which such length allows properly taking into account interannual variability limiting, at the same time, the arising of statistically significant trend in weather pattern. Moreover, the same time span is used as reference for comparing climate simulations in Section 3.
In order to put in place effective and adequate adaptation counter measurements, the assessments about future evolutions of weather forcing and associated hydrologic variables have a crucial role. In this regard, the modelling chains usually carried out include three elements:

1) Based on assumptions about future evolutions of economic development/growth and demographic changes at global and regional scale, Integrated Assessment Models (IAM) provide evaluations for future concentrations of greenhouse gases (GHG), aerosols, chemically active gases (greenhouse gases and aerosols) and changes in land use on next centuries. In this regard, Intergovernmental Panel on Climate Change (IPCC) has selected four reference standard pathways (commonly known as RCP Representative Concentration Pathways) allowing subsequent analysis by means of Climate models (CMs) following reference assumptions about baselines and starting points and permitting the comparisons among climate projections. The four pathways respectively estimate an increase in radiative forcing levels of 8.5, 6, 4.5 and 2.6 W/m2, by the end of the century compared to pre-industrial era (1750). Of course, the first one is recognized as more pessimistic (but business as usual) and the last one more optimistic and feasible only assuming high mitigation counter-measurements (Figure 2).

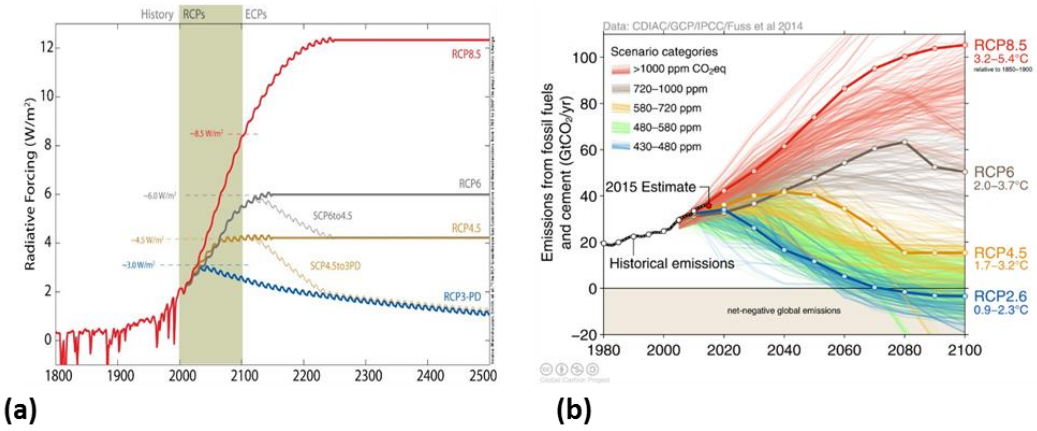

Figure 2: (a) expected trends in radiative forcing following the different RCPs (Meinshausen et al., 2011); (b) assessed increases in global temperature and emissions under the different concentration scenarios.

(2) Such assessments are used as forcing for Earth System Models (ESMs). They are numerical models aimed to assess the impacts on the climate system of variations of greenhouse gases. Nevertheless, due to their coarse horizontal resolution (at the moment, hardly exceeding 70-80km) they are able to simulate only large-scale atmospheric state (IPCC, 2014). Numerous studies (e.g. Breugem 2007; IPCC, 2014) show that they are able to reproduce the climate and the global response to the changes of GHG with higher reliability for some variables (temperature) and lower for others

(precipitation). However, despite significant developments in recent years, because of the horizontal resolutions today permitted, these models are inadequate for estimates of trends and impacts at the local/regional level for which the features of the area (distance from the sea, topography) are crucial (even with respect of large-scale atmospheric circulation).

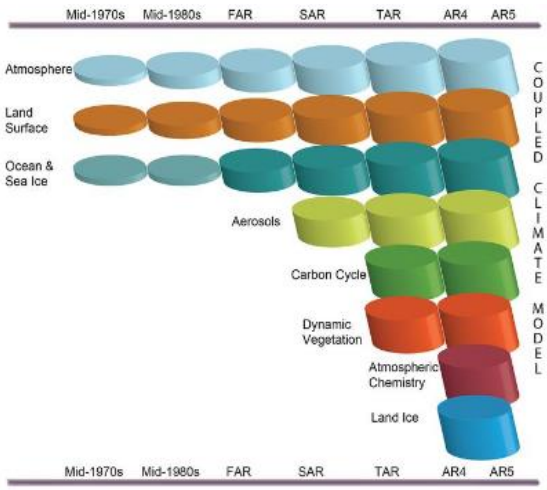

Figure 3: The evolution of Global models in terms of considered physical dynamics (from Wilby, 2017).

(3) For these reasons, several downscaling techniques were developed in last years; they largely differ for computational costs, prerequisites and limitations; they are classifiable as "statistical" and "dynamical" approaches. The first ones adopt frameworks based on empirical statistical relationships between "predictors" large-scale and “predictand” local climate variables, calibrated and validated on observed data and then applied to ESM variables. They require limited computational burden and also allow analysis at station scale but need long series of observed data for the definition of the statistical relationships. The latter ones involve the use of climate models at limited area and highest resolution (RCM Regional Climate Model) nested for the area of interest on the global model from which they draw the boundary conditions. Currently adopted resolutions, in the order of 10 km, on the one hand, allow a better resolution of the orography and, on the other one, solve a substantial fraction of the local atmospheric phenomena. Moreover, different experiments have proven their good capability in reproducing regional climate variability and changes (Feser, 2011). Even if this refinement makes it possible to accurately evaluate a remarkable fraction of weather patterns, dynamical approaches may misrepresent orography, land surface feedbacks and sub-grid processes, thus inducing biases preventing their direct use for impact analysis (Maraun, 2016; Maraun et al., 2015). To overcome this issue, different approaches, known as Bias Correction (BC) methods, have been proposed in recent years (Lafon et al., 2013; Teutschbein et al., 2012). They can be defined as statistical regression models calibrated for current periods in order to detect and correct biases, which are assumed to systematically affect the climate simulations. Although the advantages, limitations and warnings regarding their adoption are widely debated in recent literature (Ehret et al., 2012), they are currently recognized as a necessary stage in producing weather variables to use as inputs for impact-predictive tools. On the other side, in order to evaluate uncertainties associated to different realizations of climate experiments and favour the comparison among the simulations, in last years, several consortiums have promoted “ensemble” initiatives. Among these ones, in more recent years, the WCRP Coordinated Regional Downscaling Experiment (CORDEX) project (Giorgi et al. 2009) has been established; it provides a global coordination for Regional Climate Downscaling in order to improve climate change adaptation measurements and impact assessments. In this report, climate projections included in EURO-CORDEX ensemble at the highest available resolution (0.11°) are considered (Table 3).

Table 3: Available EURO-CORDEX simulations at a 0.11° resolution (~12km) over Europe (EURO-CORDEX ensemble); they are identified reporting providing institution, driving ESM model and adopted RCMs.

Code	Institution	Driving model	RCM
1	CLMcom	CNRM-CM5_r1i1p1	CCLM4-8-17_v1
2	CNRM	CNRM-CM5_r1i1p1	Aladin53
3	RMIB-Ugent	CNRM-CM5_r1i1p1	Alaro
4	SMHI	CNRM-CM5_r1i1p1	RCA4_v1
5	KNMI	EC-EARTH	RACMO22E_v1
6	DMI	EC-EARTH	HIRHAM5_v1
7	CLMcom	EC-EARTH	CCLM4-8-17_v1
8	KNMI	EC-EARTH	RACMO22E_v1
9	SMHI	EC-EARTH	RCA4_v1
10	IPSL-INERIS	IPSL-CM5A-MR_r1i1p1	WRF331F_v1
11	SMHI	IPSL-CM5A-MR_r1i1p1	RCA4_v1
12	CLMcom	HadGEM2-ES	CCLM4-8-17_v1
13	KNMI	HadGEM2-ES	RACMO22E_v1
14	SMHI	HadGEM2-ES	RCA4_v1
15	CLMcom	MPI-ESM-LR_r1i1p1	CCLM4-8-17_v1
16	MPI-CSC	MPI-ESM-LR_r1i1p1	REMO2009
17	SMHI	MPI-ESM-LR_r1i1p1	RCA4_v1
18	MPI-CSC	MPI-ESM-LR_r1i1p1	REMO2009
19	DMI	NorESM1-M	HIRHAM5

4.3. Current conditions

Figure 4a shows data concerning seasonal average temperature (in green, PASs are identified). The maps clearly highlight spatial patterns across the Region; during Winter (December-January-February, DJF) lower values are primarily observed in high altitude areas (values lower than -3°C) as Alps and Carpathian Mts while, on plain sites, the latitude tends to regulate values (higher for Mediterranean countries with values ranging between 3° and 10°C). During the Summer (June-July-August, JJA) large parts of the domain experience values crossing the 20°C while, in alpine areas values remain between 3° and 10°C. It worth stressing that reported values are main function of horizontal resolution of E-OBS datasets while locally they could result significantly different.

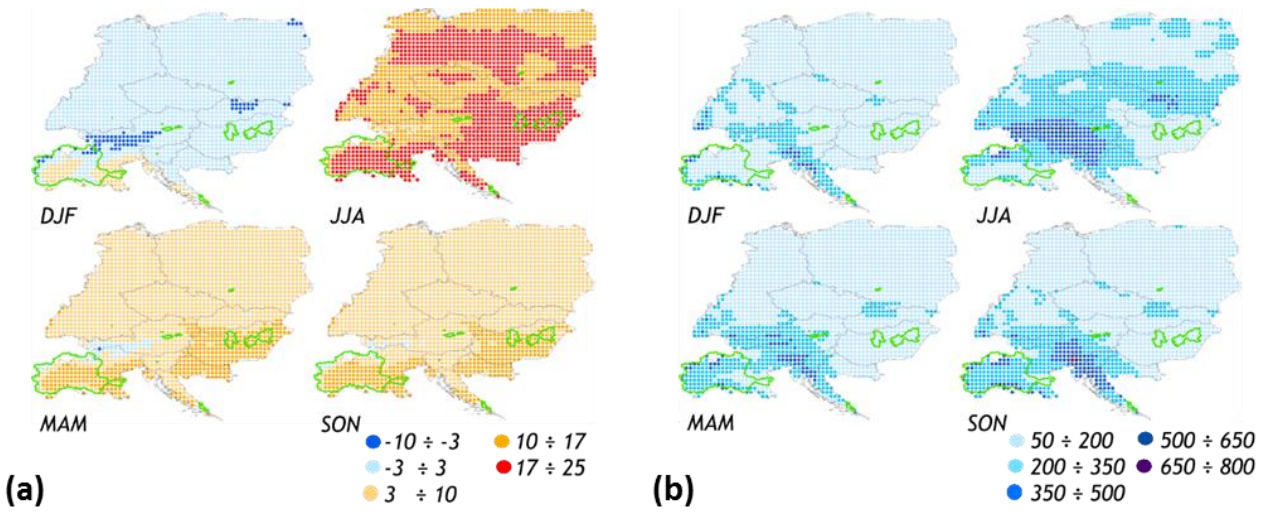

Figure 4: (a) seasonal temperature values on CE domain as reported in E-OBS gridded dataset (1971-2000 period, data reported in Celsius degrees); (b) seasonal cumulative precipitation values on CE domain as reported in E-OBS gridded dataset (1971-2000 period, data reported in millimetres/season).

During the intermediate seasons, Spring (March-April-May, MMA) and Autumn (September-October-November, SON) the Alpine Regions maintain values lower than 0°C (on wider area in MMA) while clear North-South growth gradients are detectable with northernmost areas characterized by values lower than 10°C, on average, and the Southernmost with higher values.
Concerning PASs, the extension and the orography of PA3.1 entail that different thermometric regimes coexist (Alpine, Po Valley); on the other hand, the other PASs appear according E-OBS dataset characterized by a substantial homogeneity.

Figure 4b shows data concerning seasonal cumulative precipitation. Variations among the seasons appear less pronounced compared to what has been observed for temperature. During DJF, the higher values are monitored on Alpine, Apennine and High Adriatic areas (up to 600 mm/season) (PAS 3.1; 2.1) while on a large part of the domain, precipitation does not exceed 200 mm/season according E-OBS dataset; in such areas, several PASs are totally included (1.1; 1.2; 2.3; 3.2; 2.5).

During the summer, on a large part of CE, higher values are observed; in particular, in the NE part of alpine Region, seasonal precipitation may arrive at about 650 mm/season. In this case, the lower values are detected for Hungarian and Croatian PASs (3.2; 2.3; 2.4) while for Slovenian (2.1) and Austrian (1.1.1) PASs significant values are retrievable (up to 500mm/season). Again, Italian test case result characterized by large spatial variability while, for the remaining ones, seasonal values do not exceed 350mm/season.
For intermediate seasons, similar patterns arise with higher values observed, for SON, in NE part of Great Alpine Region and Liguria Apennines (up to 800mm/season). In this perspective, it is interesting to note how Hungarian test cases result characterized by moderate values during all the seasons.

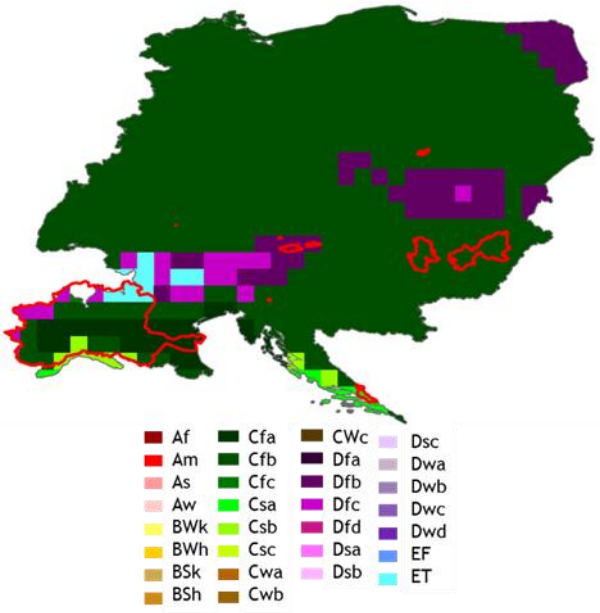

1st	2nd	3rd	Description	Criteria*
A			Tropical	$T_{cold} \geq 18$
	f		- Rainforest	$P_{dry} \geq 60$
	m		- Monsoon	Not (Af) & $P_{dry} \geq 100-MAP/25$
	w		- Savannah	Not (Af) & $P_{dry} < 100-MAP/25$
B			Arid	$MAP < 10 \times P_{threshold}$
	W		- Desert	$MAP < 5 \times P_{threshold}$
	S		- Steppe	$MAP \geq 5 \times P_{threshold}$
		h	- Hot	$MAT \geq 18$
		k	- Cold	$MAT < 18$
C			Temperate	$T_{hot} > 10$ & $0 < T_{cold} < 18$
	s		- Dry Summer	$P_{sdry} < 40$ & $P_{sdry} < P_{wwet}/3$
	w		- Dry Winter	$P_{wdry} < P_{swet}/10$
	f		- Without dry season	Not (Cs) or (Cw)
		a	- Hot Summer	$T_{hot} \geq 22$
		b	- Warm Summer	Not (a) & $T_{mon10} \geq 4$
		c	- Cold Summer	Not (a or b) & $1 \leq T_{mon10} < 4$
D			Cold	$T_{hot} > 10$ & $T_{cold} \leq 0$
	s		- Dry Summer	$P_{sdry} < 40$ & $P_{sdry} < P_{wwet}/3$
	w		- Dry Winter	$P_{wdry} < P_{swet}/10$
	f		- Without dry season	Not (Ds) or (Dw)
		a	- Hot Summer	$T_{hot} \geq 22$
		b	- Warm Summer	Not (a) & $T_{mon10} \geq 4$
		c	- Cold Summer	Not (a, b or d)
		d	- Very Cold Winter	Not (a or b) & $T_{cold} < -38$
E			Polar	$T_{hot} < 10$
	T		- Tundra	$T_{hot} > 0$
	F		- Frost	$T_{hot} \leq 0$

Figure 5: Koppen-Geiger classification according Rubel & Kottek (2010); in legend, all the classes proposed by K-G are reported. PASs reported in red.

MAP = mean annual precipitation, MAT = mean annual temperature, Thot = temperature of the hottest month, Tcold = temperature of the coldest month, Tmon10 = number of months where the temperature is above 10, Pdry = precipitation of the driest month, Psdry = precipitation of the driest month in summer, Pwdry = precipitation of the driest month in winter, Pswet = precipitation of the wettest month in summer, Pwwet = precipitation of the wettest month in winter, Pthreshold = varies according to the following rules (if 70% of MAP occurs in winter then Pthreshold = 2 x MAT, if 70% of MAP occurs in summer then Pthreshold = 2 x MAT + 28, otherwise Pthreshold = 2 x MAT + 14). Summer (winter) is defined as the warmer (cooler) six month period of ONDJFM and AMJJAS.

In order to provide a synthetic characterization of climate features retrievable in the CE domain, the widely adopted climate classification proposed by Koppen (1900) and updated by Geiger (1961) is displayed (it is commonly known as Koppen-Geiger, K-G, classification). K-G is primarily based on five vegetation groups identified by the French botanist De Candolle: the equatorial zone (A), the arid zone (B), the warm temperate zone (C), the snow zone (D) and the polar zone (E). Furthermore, a second letter in the classification considers the precipitation (e.g. Df for snow and fully humid), a third letter the air temperature (e.g. Dfc for snow, fully humid with cool summer) (Kottek et al., 2006); in this perspective, the transition values among the classes are primarily determined through an expert judgment approach. Therefore, although more rigorous approaches have been argued and proposed in last years (Sanderson, 1999; Strahler, 1971; Peel et al., 2004), K-G continues to be broadly adopted in different application fields (Rubel & Kottek, 2011).

In this context, K-G classification proposed by Rubel & Kottek (2010) is adopted; they provided world maps for the observational period 1901-2002 adopting Climatic Research Unit (CRU) dataset of the University of East Anglia for the temperature (Mitchell and Jones, 2005) and the Global

Precipitation Climatology Centre (GPCC) provided by the German Weather Service for the precipitation (Fuchs, 2008). Both are available on a regular 0.5-degree grid and monthly temporal resolution. Furthermore, the Rubel & Kottek (2010) analysis provides assessments about future shifts in classification (2003–2100), under the effect of climate changes, recurring to climate projections included in Tyndall Centre for Climate Change Research dataset, TYN SC 2.03 (Mitchell et al., 2004) including 20 global simulations under different emission scenarios. The results are provided for time spans 25 years long; for consistency with what previously reported, the findings for 1976-2000 are displayed in Figure 5 (in red, are reported PAS). Specifically, on CE domain, Rubel & Kottek (2010) identify seven classes:

- Cfb: temperate oceanic climate; in it, Hungarian (2.3; 3.2), Polish (2.2), Slovenian (2.1) and German (2.5) PASs fall
- Dfb: warm-summer humid continental climate; in it, Austrian PASs fall (1.1; 1.2)
- Cfa: humid subtropical climate
- Csb: warm-summer Mediterranean climate; in it, Croatian PASs fall (2.4)
- Csa: hot-summer Mediterranean climate
- Dfc: subarctic climate
- ET: Tundra

In this sense, the large variability characterizing Italian PAS is confirmed; indeed, in it, five classes are included (ET, Dfc, Csb, Cfb, Cfa).

Figure 6 displays the spatial distribution of the three indicators above introduced (CDD, CWD, Rx1D) for CE domain (reference period 1971-2000). The first two should provide a characterization of the precipitation distribution (in terms of interarrival time and event length) while the third one is assumed as rough proxy for the occurrence of hydrological hazards.

Concerning CDD, the higher values are observed in the Southern part of CE domain (PAS 3.1 and 2.4) and Hungary (PAS 2.3 and 3.2) where they can reach 40-46 days with the resulting higher probability of water shortage issues. On the other hand, the areas in which Austrian, German and Polish PASs are included, result less affected with values hardly exceeding 20 days. Furthermore, the larger CWD

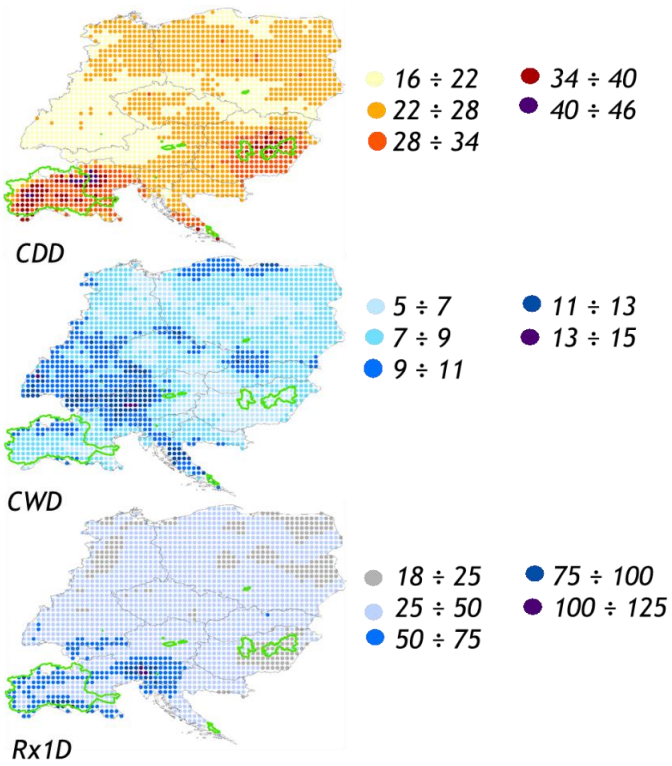

Figure 6: CDD (days, upper part), CWD (days, in the middle) and Rx1D (millimetres, in the bottom) values on CE domain as computed through E-OBS gridded dataset (1971-2000 period).

values are registered in high elevation areas (e.g. NE part of Alpine region) where they may arrive at 15 days; on the other side, on plain areas, they are usually limited to 5-7 days.
Finally, considering Rx1d, the lowest values (not exceeding 25 mm/day) are registered in some areas of the northern part of CE domain and Hungary (PAS 3.2 and 2.3 partly lie in such areas). On the main part of the domain, the values do not go beyond 50 mm/day while the higher values are retrievable in high altitude areas of Alps, Apennines and South Bavaria. In the specific, the peak values are observed again in east part of Alpine Region where they reach 100-125 mm.

4.4. Future conditions

In the following, variations on short time horizon (2021-2050 vs 1971-2000) and long-time horizon (2071-2100 vs 1971-2000) are displayed under two RCPs, RCP4.5 and RCP8.5. Currently, to this aim, nineteen simulations are available (details reported in Table 3). The same weather forcing considered in Section 2 are analysed; for each one (for the two time spans and two RCPs), the variations are displayed in terms of 25th, 50th (median value) and 75th distribution percentiles according the scheme reported in Table 4.

Table 4: Layout displaying the arrangement of the variation maps concerning climate projections.

2021-2050 vs 1971-2000	*a) RCP4.5 25th percentile*	*g) RCP8.5 25th percentile*
	b) RCP4.5 50th percentile	*h) RCP8.5 50th percentile*
	c) RCP4.5 75th percentile	*i) RCP8.5 75th percentile*
2071-2100 vs 1971-2000	*d) RCP4.5 25th percentile*	*j) RCP8.5 25th percentile*
	e) RCP4.5 50th percentile	*k) RCP8.5 50th percentile*
	f) RCP4.5 75th percentile	*l) RCP8.5 75th percentile*

Variations in DJF temperature

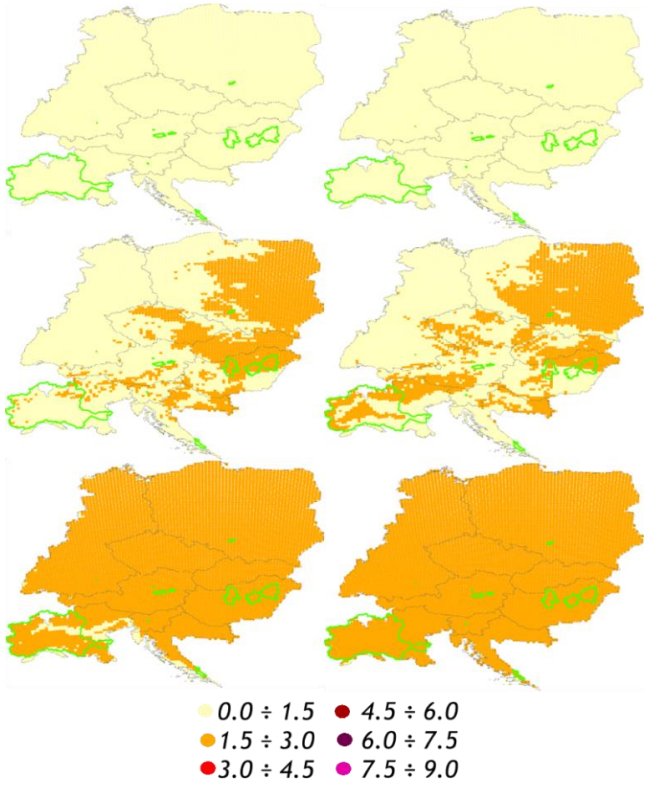

Figure 7: 2021-2050 vs 1971-2000. An increase in temperature is expected, for all seasons, under the two RCPs and the two-time horizons. For DJF, the increase returned as median value, is lower than 1.5°C on the western part of the domain while on the eastern part it could arrive at about 3°C. However, for 25th and 75th percentiles, increases appear quite homogeneous (up to 1.5°C and 3°C, respectively). Such findings show how, already on short term, snow precipitation and accumulation dynamics could be highly altered by expected warming. In this perspective, higher changes could occur in areas where, currently, average values are about 0°C.

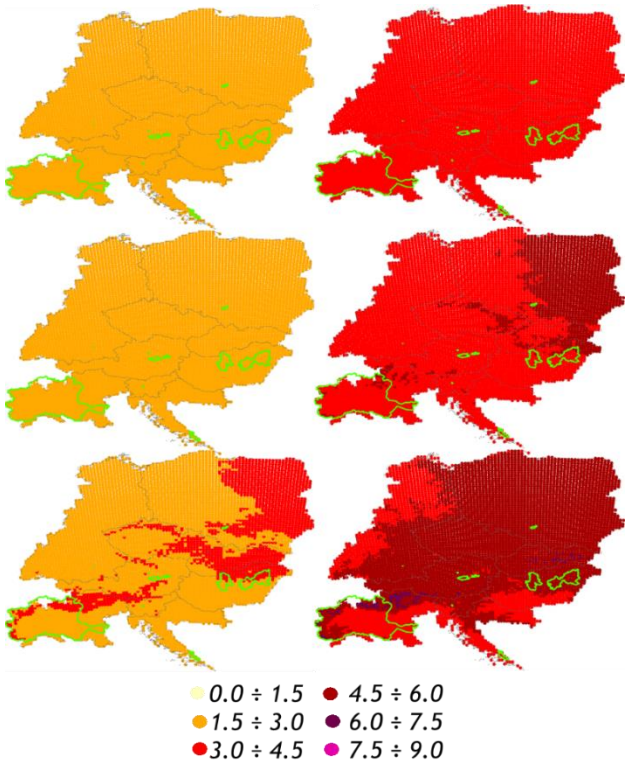

Figure 8: 2071-2100 vs 1971-2000. Two elements clearly arise by the findings on long time horizon; first, on average, much higher increases values are expected; furthermore, the severity of RCP strongly regulates the magnitude of variations. As median value, the increase does not exceed the 3°C under RCP4.5 while it could be about 4.5°C under RCP8.5 (larger values are detected in Eastern portion of the CE domain, up to 5-6°C). It is interesting noting how the variations returned by 25th-75th percentiles result quite close to values retrieved by the median one (higher increase expected on Alps with values, in Eastern part, ranging from 6 to 7.5°C). Under such results, snow dynamics could be totally upset by such increases.

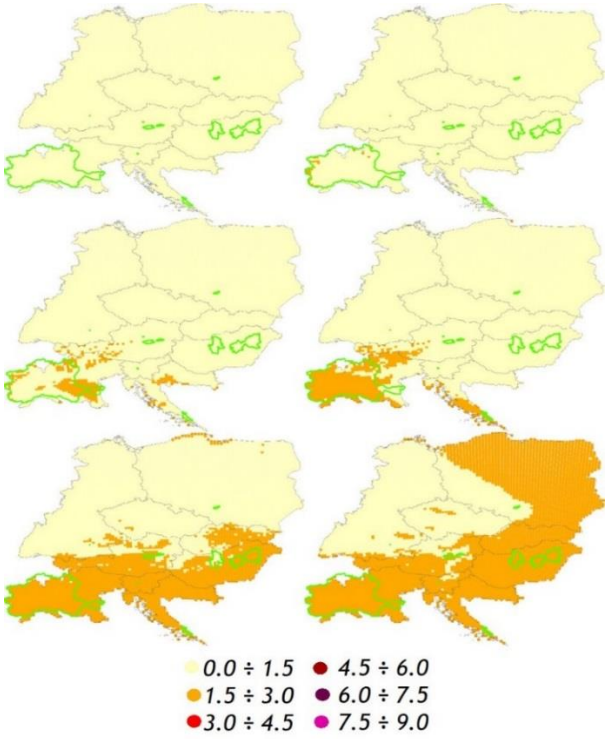

Figure 9: 2021-2050 vs 1971-2000. For JJA, on short time horizon, similar increase values are expected using EURO-CORDEX ensembles. However, significant variations characterize the spatial patterns: in general, higher values are constantly retrieved for the Southern part of the domain (Italy and Balkan countries); the two RCPs give similar findings also if the areas where the increases could exceed 1.5°C result quite larger under RCP8.5 (e.g., for 75th percentile, also the Eastern part of CE domain is expected to experience increases up to 3°C). Such variations in temperature could lead to substantial increase in atmospheric evapotranspiration demand driven also by higher humidity deficits.

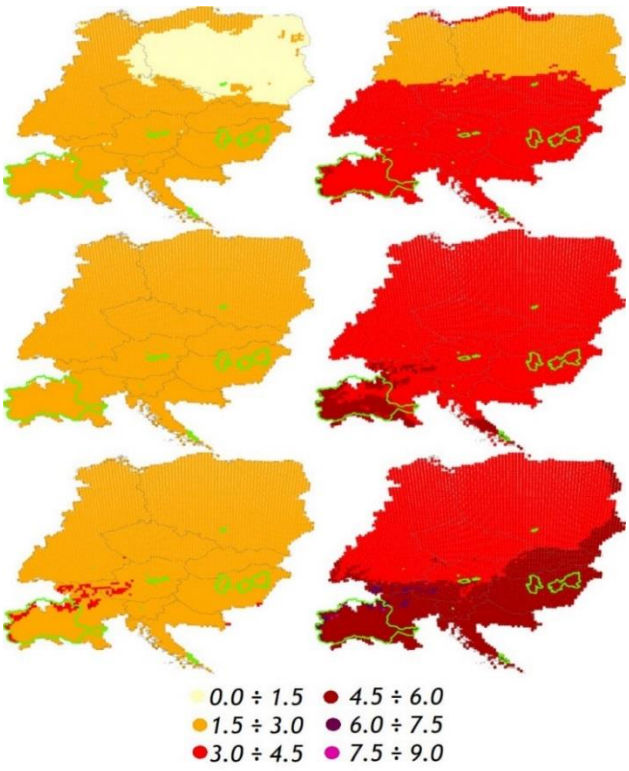

Figure 10: 2071-2100 vs 1971-2000. The two elements before stressed for DJF temperature are confirmed: the increases result main function of time horizon and RCP severity. Under RCP4.5 (RCP8.5), the increases are up to 3°C (6°C) with slight variations among the percentiles (with clear North-South increase gradient). Moreover, on the Alpine area, often larger values are returned with isolated peaks exceeding 8°C under RCP8.5; it could induce dramatic consequences also in current permafrost areas; concerning evapotranspiration, the increase in potential demand could significantly increase. Nevertheless, the actual evaporation should primarily account for the availability of soil water driven by rainfall cumulative values.

Variations in MAM temperature

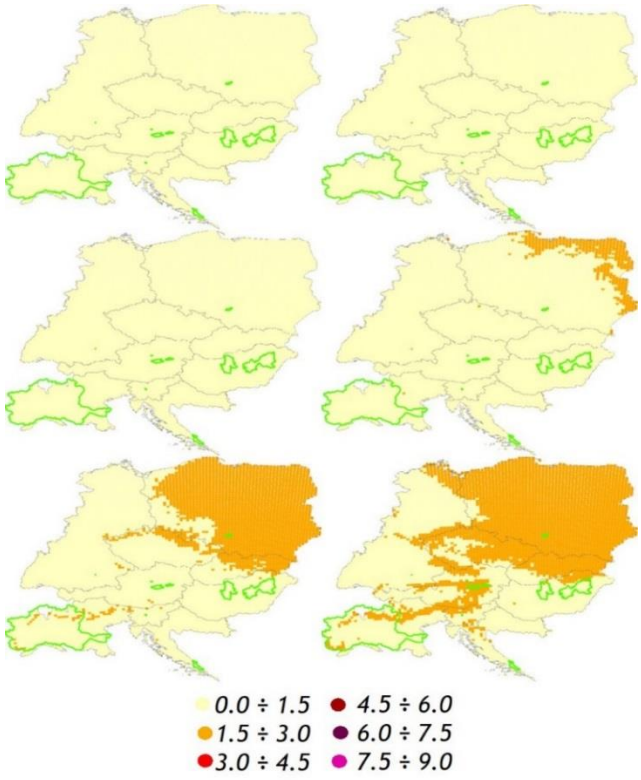

Figure 11: 2021-2050 vs 1971-2000. During MAM, on short-term horizon, the expected increases should not exceed, as median value, 1.5°C (in North-East part of the domain, under RCP8.5, higher increases are assessed). On the other hand, according 75th percentile, the part interested by larger increases result quite larger. Such increases could affect as snow persistency dynamics inducing significant variations in seasonal river discharge as, obviously, it could entail higher potential evaporation values.

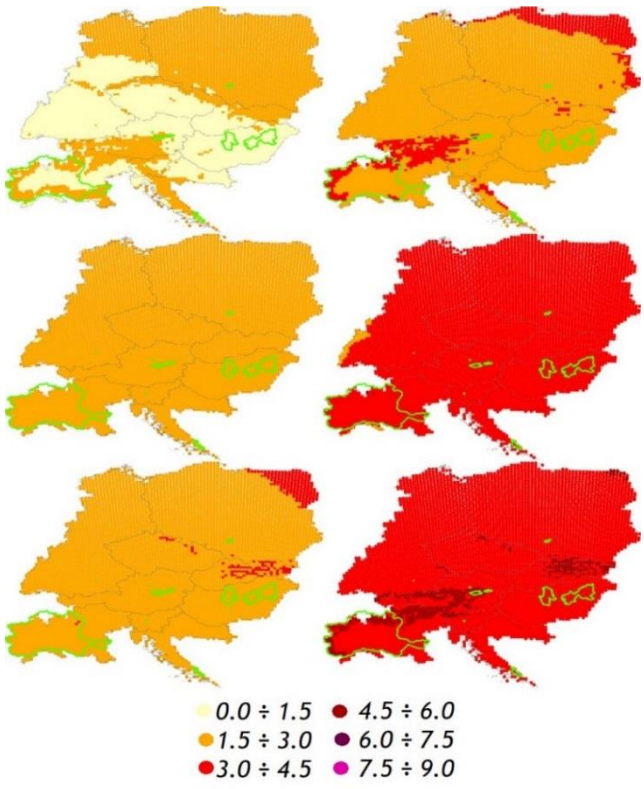

Figure 12: 2071-2100 vs 1971-2000. The increases expected on long term appear quite homogeneous over the domain (in special way, for 50th and 75th percentile). In general, the growth does not exceed 3°C under RCP4.5 and 4.5°C under RCP8.5; in this case, Alpine Region and some areas in Hungary could experience larger variations. As stressed before, the variations between RCPs result limited on short term and then the required adaptation measurements to face with such changes could be substantially equivalent while they could highly differ for long time targets in terms of interested areas, magnitude of variations and then required measures and costs.

Variations in SON temperature

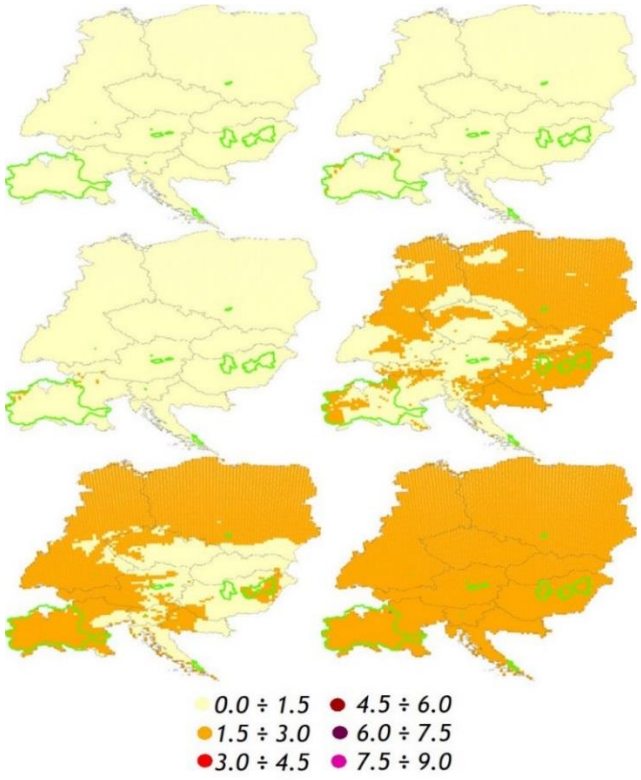

Figure 13: 2021-2050 vs 1971-2000.On short term, for SON, the median increases do not exceed 1.5°C under RCP4.5 while large values are expected under RCP8.5 (N-E domain, western Italy, Germany). The increases could maintain high the atmospheric demand after Summer season and delay the beginning of snow covering in high altitude areas. In general, the increases in air temperature are expected entailing substantial variations also in terms of rainfall patterns (see Figure 19-27, 32-33). Indeed, it leads to increase in atmospheric moisture retention requiring the accumulation of higher water contents to trigger precipitation events (Clapeyron equation).

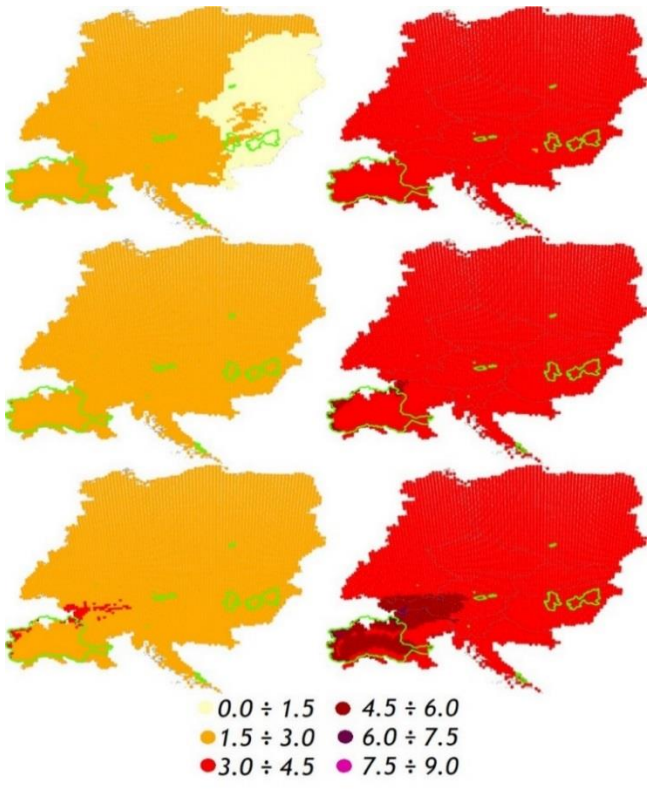

Figure 14: 2071-2100 vs 1971-2000. On farthest time horizon, the climate simulations forced by RCP4.5 reveal increases not exceeding 3°C while, under RCP8.5, it could arrive up to 4.5°C. It is interesting to note how, primarily for 75th percentile, the areas potentially affected by larger increases could correspond to Alpine Region (and Po Valley under RCP8.5). Such evaluations should be carefully taken into account by decision makers and water operators that, in last years, suffered the consequences of severe droughts led by increases in temperatures (during the entire year) and abrupt reductions in seasonal cumulative values.

Variations in DJF precipitation

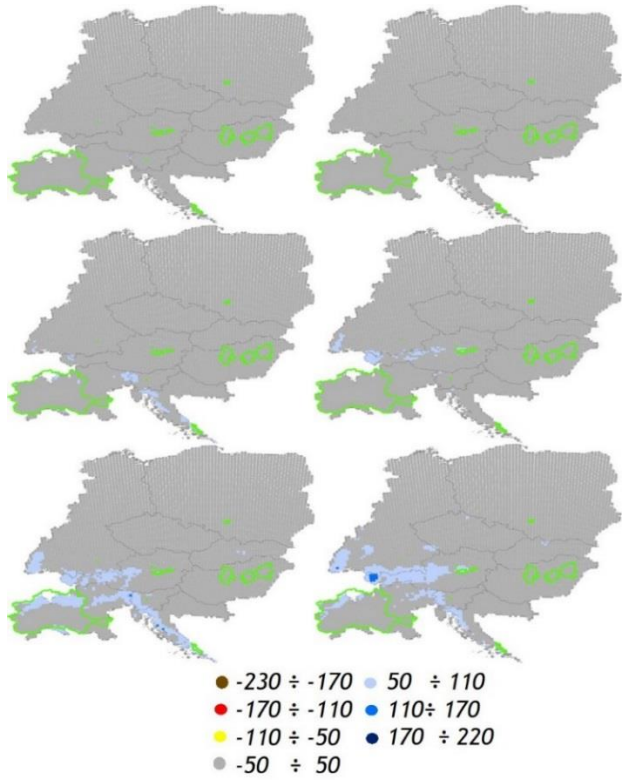

Figure 15: 2021-2050 vs 1971-2000.Concerning seasonal cumulative precipitation, in general, the tendencies revealed by climate simulations appear much less clear; the signals are contrasting for the different seasons and investigated areas. Moreover, findings displaying slight or no variations often result by "algebraic sum" of very different outputs provided by climate projections. For DJF, on short term, the variations appear quite limited. Only considering 75th percentile, on the Alpine arc, are estimated increases of about 50-100 mm/season; on the other side, no substantial decrease is estimated on the entire domain.

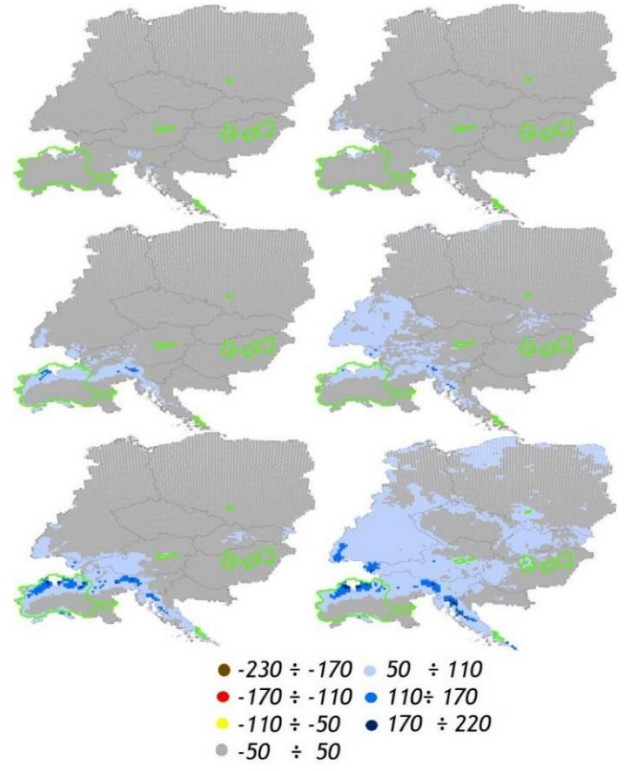

Figure 16: 2071-2100 vs 1971-2000. Concerning long time horizon, the climate simulations tend returning similar findings in terms of magnitude (higher increase on alpine region up to 220 mm/season) but not in extent of areas interested by increases: they are much larger under RCP8.5 (interesting primarily Germany, Austria and Balkan countries). On the other hand, Northeast part of the domain could result less interested by variations.

Variations in JJA precipitation

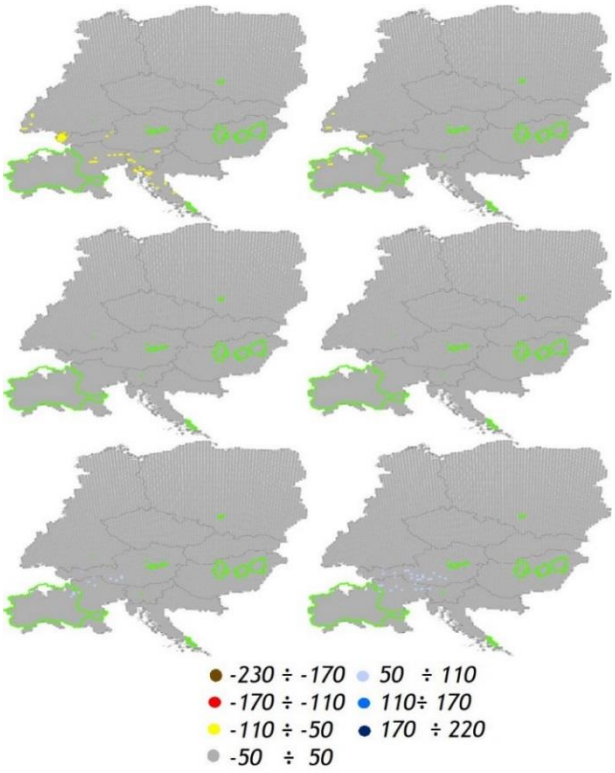

Figure 17: 2021-2050 vs 1971-2000. Concerning JJA, very slight variations could interest CE domain on short term horizon; then, the larger atmospheric demand driven by temperature increase (Figure 13) could entail a substantial reduction of soil water content with several consequences on different fields. For example, it could be necessary adopting more frequently irrigation practices (in special way, in south part of the domain where they are already widely utilized). On the other hand, in view of proper adaptation strategies, the selection of crops less water-demanding could be taken into consideration.

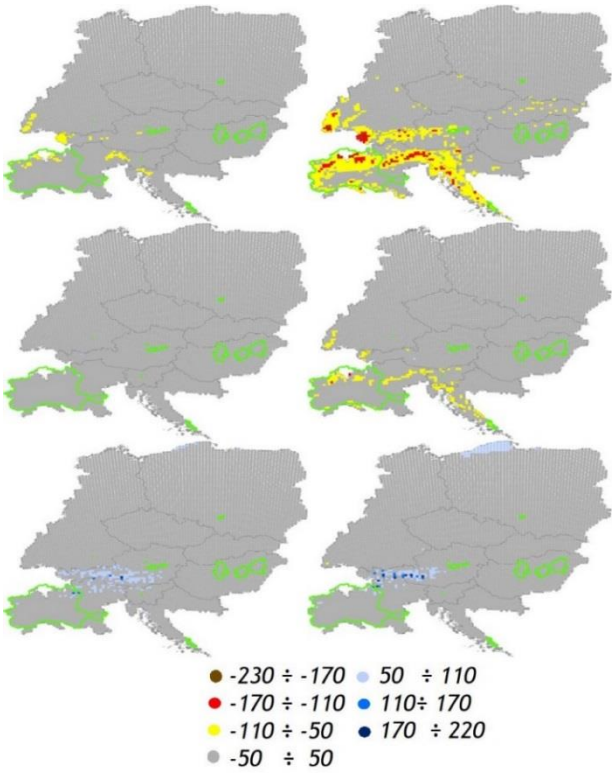

Figure 18: 2071-2100 vs 1971-2000. On long time horizon, the largest part of the domain appears slightly interested by variations in cumulative precipitations; however, contrasting findings characterize mainly the Alpine Region and Balkan countries under RCP8.5. They could experience substantial reductions according 25th and 50th percentile assessments while, on the other hand, mainly on Austrian Alps, moderate increases are assessed according 75th percentile. It confirms the great differences in output that currently could characterize climate projections.

Variations in MAM precipitation

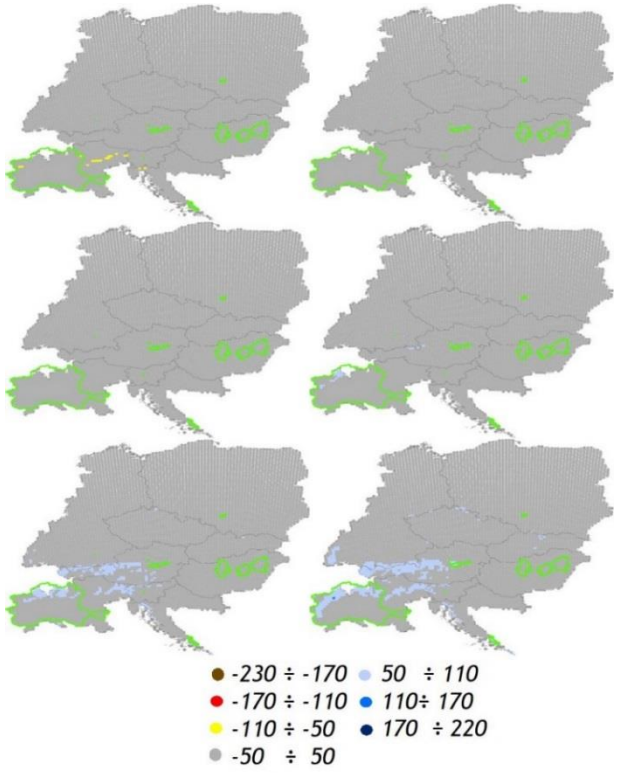

Figure 19: 2021-2050 vs 1971-2000. About MAM, on short term, moderate variations are returned only by 75th percentile assessments primarily on Alpine region and neighbouring areas. However, under both scenarios, the increases do not exceed 110 mm/season.

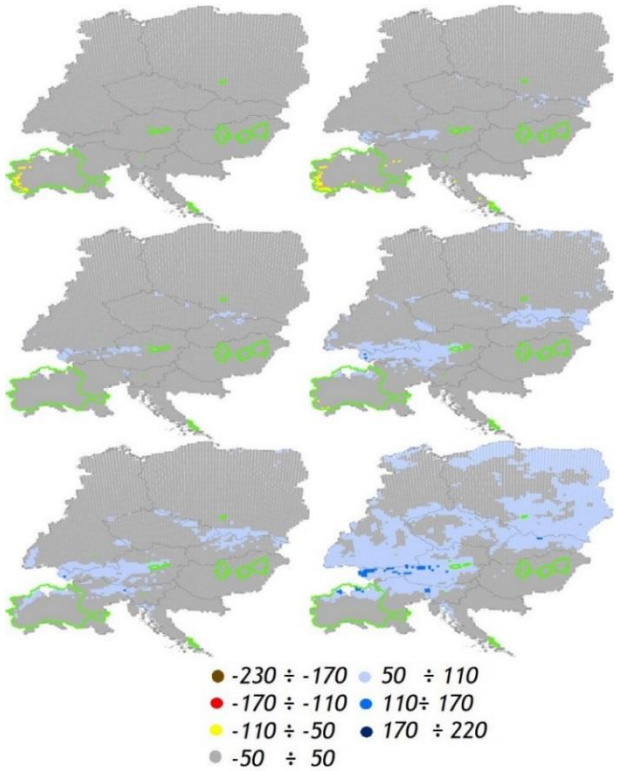

Figure 20: 2071-2100 vs 1971-2000. For MAM, on long time horizon, the larger part of the domain should be not affected by significant variations. In high altitude areas, however, variations up to 110 mm/season are evaluated as median values while they could interest larger parts according 75th percentile with peaks up to 170 mm/season. Again, in general terms, increasing signals are expected for the area.

Variations in SON precipitation

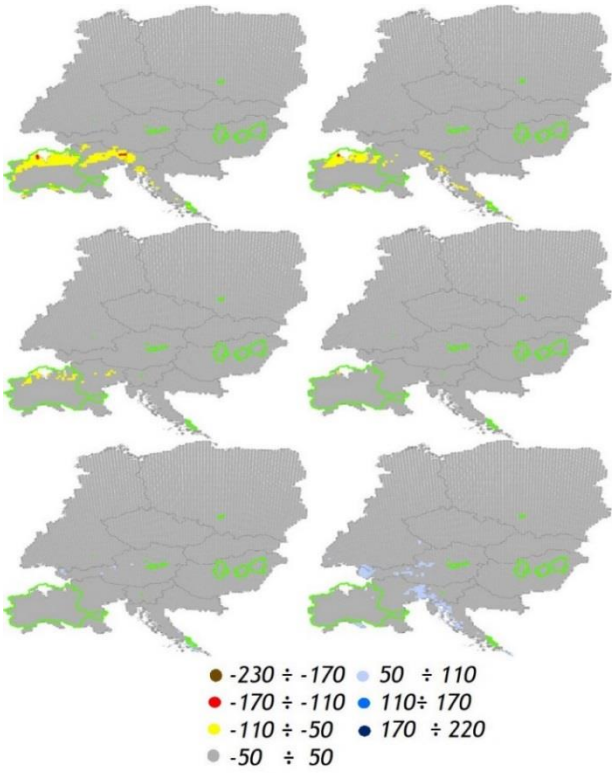

Figure 21: 2021-2050 vs 1971-2000. Concerning short term, for SON, contrasting findings already highlighted over the other seasons (in special way, Summer in Figure 21-22) are detectable. According 25th percentile evaluation, Alpine and Apennine regions could be interested by reductions, on average, about equal to 110 mm/season. The median values return very slight variations over all the domain under the two RCPs. Finally, very limited increases are retrieved considering RCP8.5 scenario in terms of 75th percentile.

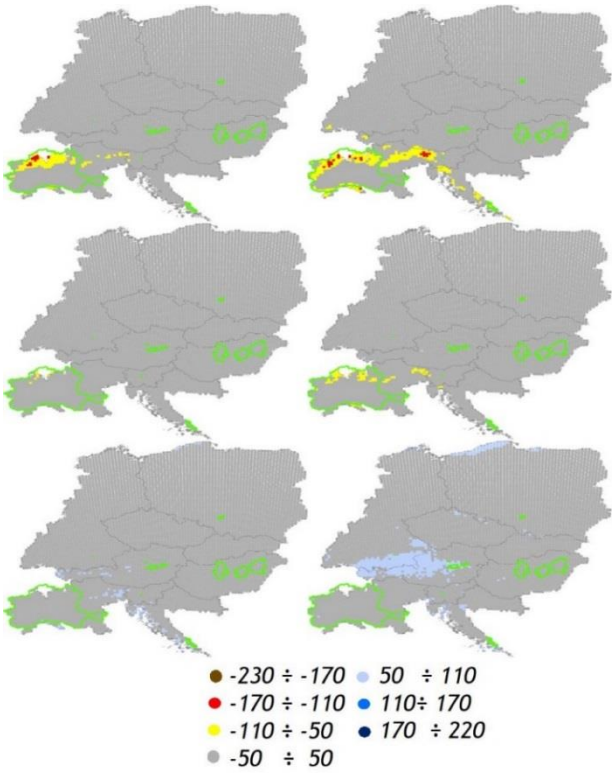

Figure 22: 2071-2100 vs 1971-2000. On long time horizon, the pattern before detected on short term more clearly arise: for 25th percentile, the reductions are expected affecting Alpine, Apennine and Balkan areas with reductions up to 170 mm/season. The median value returns very limited variations over all the domain while slight increases are assessed on borders among Germany, Austria and Italy and in extreme northern part of the domain (under RCP8.5 for 75th percentile).

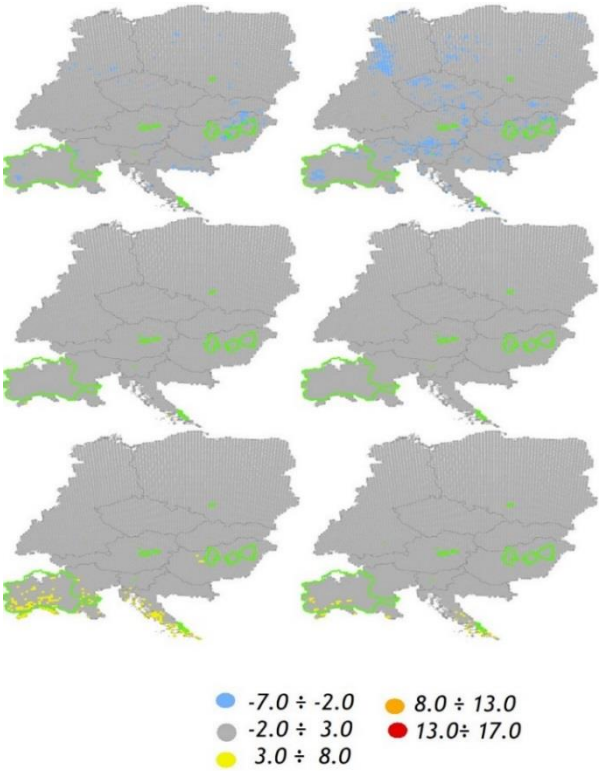

Figure 23: 2021-2050 vs 1971-2000. Concerning variations in CDD (Consecutive Dry Days), on short term, the median value returns limited variations over the entire domain. For 25th percentile, the areas interested by reductions result quite sparse over the CE domain (mainly under RCP8.5) while the increases returned by 75th percentile assessments are located in the Southern part of the domain (Italy and Balkan areas) with increases ranging, on average, between 3 and 8 days. In these areas, such result appears quite interesting considering the drought events recently affecting them and that could be exacerbated already on short time horizon according 75th percentile.

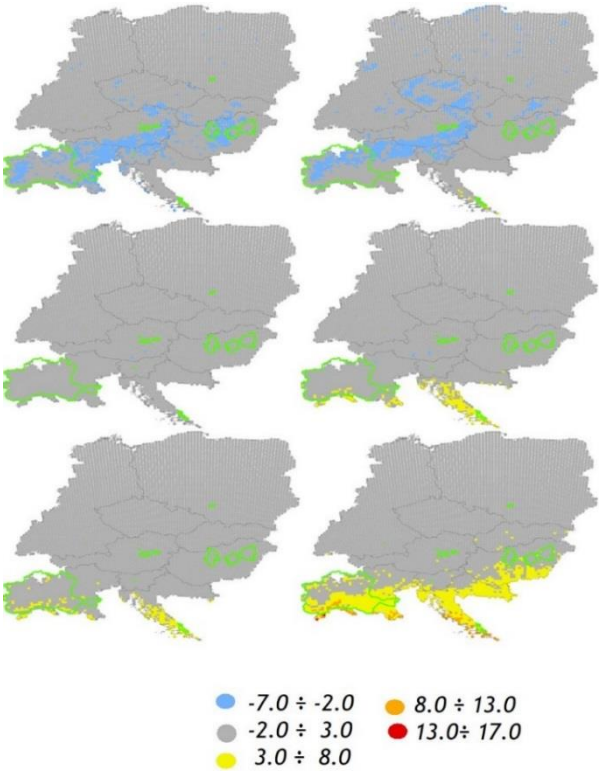

Figure 24: 2071-2100 vs 1971-2000. The spatial patterns already highlighted on short time horizon result substantially confirmed also on long time horizon; however, for 25th percentile, the areas interested by reductions result localized mainly on Alpine Region and Central part of the domain. For the median values, increases should interest only the areas located in the southern part of domain. Finally, larger areas are expected experiencing increases according 75th percentile with peaks also attaining 13 days.

Variations in CWD

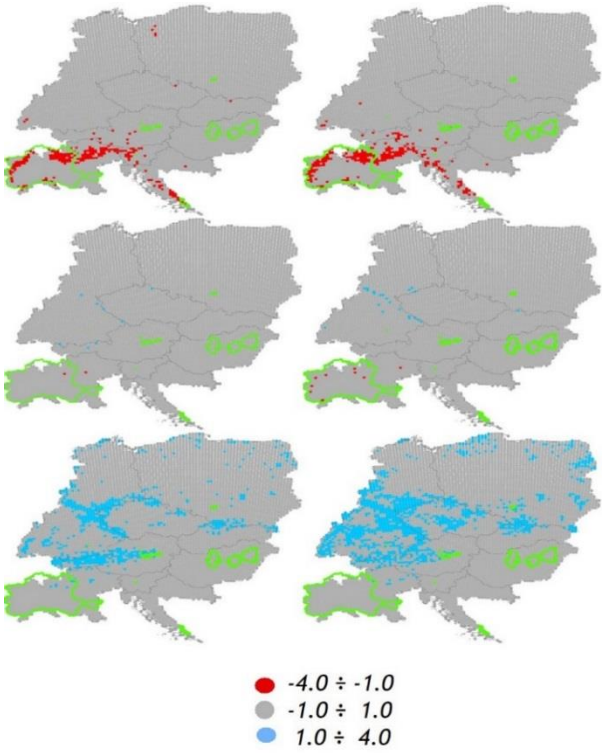

Figure 25: 2021-2050 vs 1971-2000. For what concern CWD (Consecutive Wet Days), the first element to stress is that expected variations stand in a range quite more limited than those considered for CDD (-4<CWD<4 vs -7<CDD<17). However, also for this indicator, not clear indications are retrievable: for 25th percentile, the reductions could primarily affect Alpine and Balkan regions. In terms of median value, significant variations appear very limited while, for 75th percentile, higher increases are assessed in special way in Northwestern part of the domain and high-altitude areas.

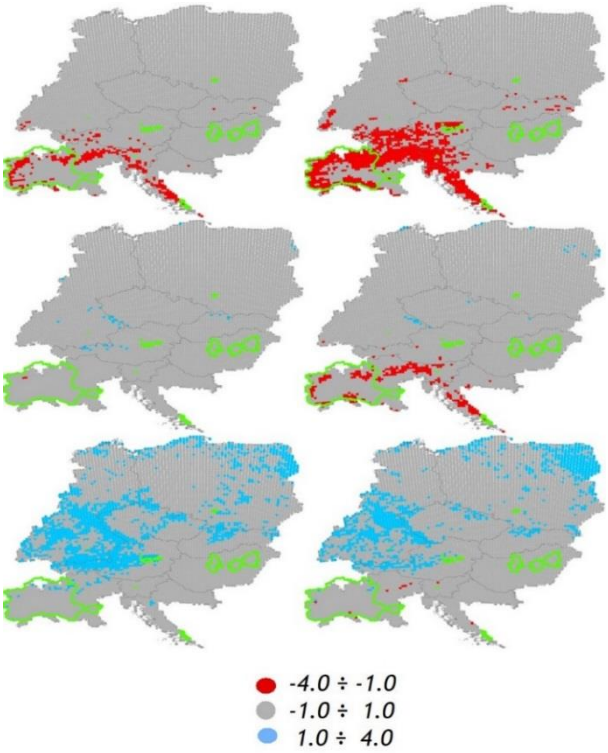

Figure 26: 2071-2100 vs 1971-2000. On long time horizon, similar patterns are retrieved. For 25th percentile, the areas potentially affected by reductions result quite larger than those expected on short time horizon. For median value, under RCP8.5, reductions are assessed over Italy and Balkan countries while increases are returned by 75th percentile over a large part of the domain.

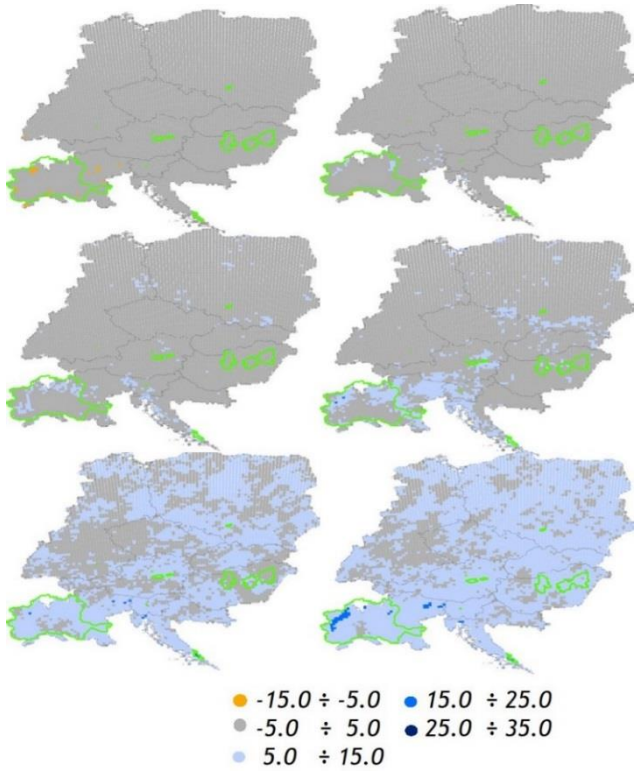

Figure 27: 2021-2050 vs 1971-2000. Concerning Rx1D, climate simulations provide clear increasing signals; on short time horizon, according median value, they primarily interest the southern part of the domain and high-altitude areas with values not exceeding 15 mm/day. For 75th percentile, the increases result quite generalized with limited part of the Alps that could experience growths up to 25 mm/day. It is worth recalling that Rx1D has been selected only as proxy for triggering of hydrological hazards. Their actual occurrence is strictly linked to geomorphological conditions of basins (extent, orography, land use/cover).

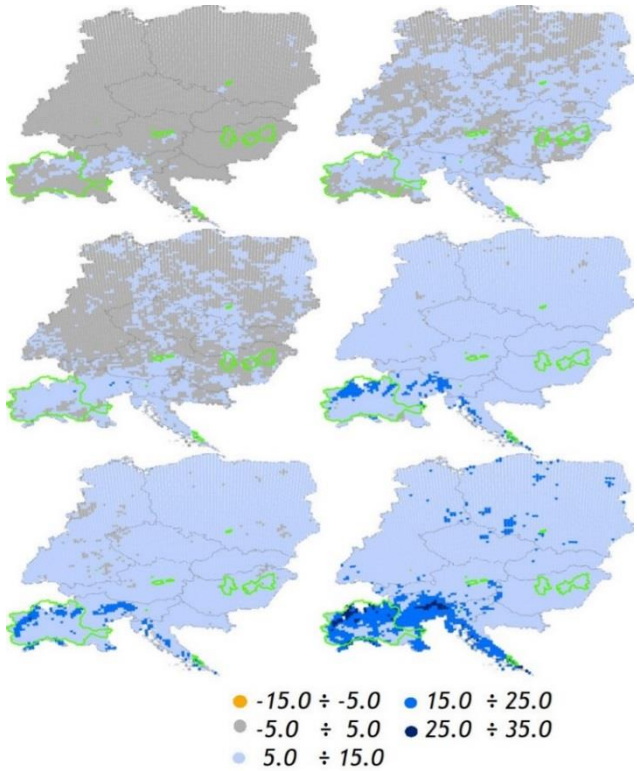

Figure 28: 2071-2100 vs 1971-2000. On long time horizon, the increasing before highlighted patterns result highly exacerbated over all the domain; in particular, over the Alps, generally the increase returned by median values assessments exceed 15 mm/day while, for 75th percentile, under RCP8.5, large part of Italian and Balkan territories could be interested by increases of about 15-25 mm/day with peaks attaining 25-35 mm/day on high altitude areas.

5. Pilot Actions (PAs) characterization

5.1. PA1.1 Catchment area of the Vienna Water Supply, AT1 and PA1.2 Catchment area of Waidhofen/Ybbs, AT2

5.1.1. Foreword

This section is about climate change issues in Pilot Action Cluster 1, the one considering the Pilot Action 1.1: Catchment area of the Vienna Water Supply, and Pilot Action 1.2: Catchment area of Waidhofen/Ybbs. Analysis are based on the study "H.P. Nachtnebel, T. Senoner, M. Herrnegger (2010). Final Report of Work package 3 - Climate Change, Chapter Austria. To be downloaded at: www-ccwaters.eu – Output Documentation, Work package 3".

The catchment considered in CC-Waters climate work is reported in Figure 29. The pilot area of Vienna Water is the catchment area of the water supply of the city of Vienna. The area is located in the Eastern Alps. On the other hand, the PA1.2 Waidhofen/Ybbs is not situated within the highlighted area but can be found in the western field of the northern-most areas of the analysed area.

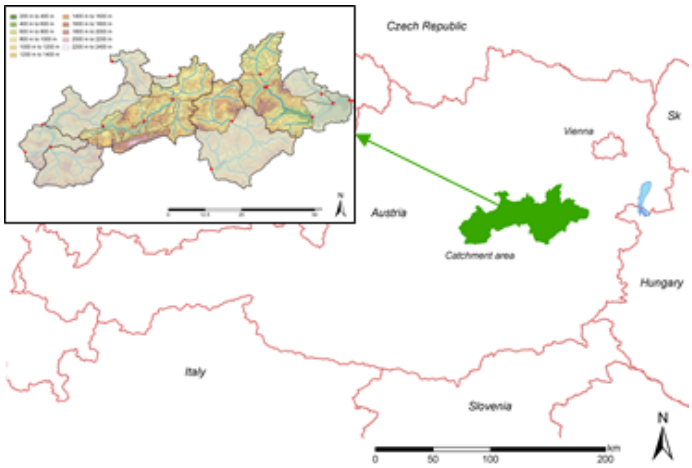

Figure 29: Location of the catchment area considered in CC-WaterS climate work with a zoom on the geological features of the area.

The main morphological features are karstic mountain ranges with high plateaus and steep slopes. Geologically, the area is dominated by Triassic carbonate rocks (Eastern Northern Calcareous Alps, limestone, dolomites, at the base impermeable shists). Soils in the area are mainly Rendzinas, loamy soils and immature soils (Rohböden). Land cover is dominated by forest ecosystems (mainly coniferous forests and deciduous and mixed forests; potentially deciduous forests would dominate) at higher elevations there is mountain pasture

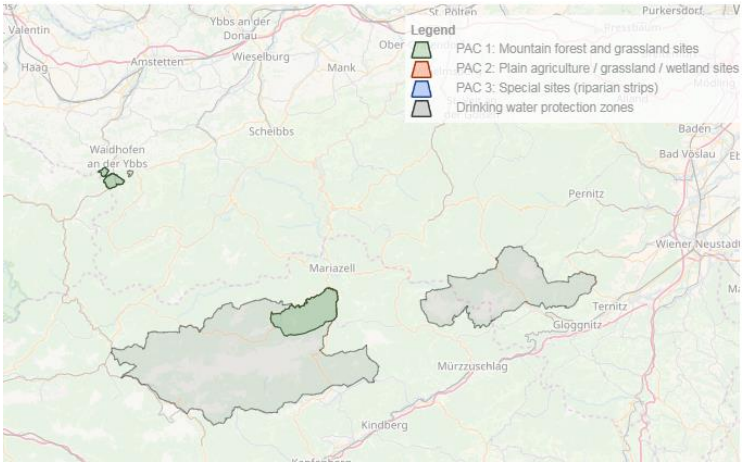

Figure 30: Location of the climate change scenario region, including PA1.1 and PA1.2.

and areas with poor vegetation. Settlement areas within the regions are small. Waidhofen/Ybbs as city within the area is located at the outer edge of the whole analysed region. Large parts of the region are legally decreed water protection areas (about 1010 km²), the PA Waidhofen/Ybbs will be the newest legally decreed water protection zone in the area. The main aquifers are karstic aquifers, with porous aquifers only in the valleys. Therefore, there is little or no surface flow from the mountain massifs – surface waters are mainly fed by spring water. Also, the water extracted for the transport to Vienna and Waidhofen/Ybbs comes from karstic springs. In the case of Vienna more than 90 % of the drinking water comes from tapped springs, only some minor wells contribute with water abstracted from porous aquifers in the valleys. In the case of Waidhofen/Ybbs 100 % of the supplied drinking water stems from the karstic alpine springs.

Figure 31: Water supply of Vienna with the two main transport pipelines (I. and II. Wiener Hochquellenleitung) from the Pilot areas.

Figure 31 shows a scheme of the extraction and transport network of the Vienna Water. A total amount of 437,000 m³ is diverted to Vienna on an average day.

As common in water supplies with karstic aquifers, the main supply problems arise from contaminations after storm events. Some of the springs react very quickly, while others show a slower reaction to rainfall and contamination. In general, there are no quantitative problems. Most springs show distinct seasonal flow pattern with low flows in winter, but this coincides with the time of the lowest demand.

5.1.2. Previous state-of-the-art framework

5.1.2.1. Current climate

Climate change data is not needed for PA1.1 city of Vienna and PA1.2 Waidhofen/Ybbs (Pilot Action Cluster 1), as those were already gathered and analysed in the course of the CC-WaterS project. All related reports are available, including the estimation of land-use related changes, like e.g. the changes in tree species diversity and distribution within the forest ecosystems according to the supposed climate change scenarios. The implications of climate change for the Best Practice implementation are integrated in all PROLINE-CE project activities.

In order to integrate the already analysed climate change data in PROLINE-CE it became necessary to make the CC-WaterS dataset available. In Work package 3 of CC-WaterS a huge area was analysed with regard to the climate scenarios, as the solely catchment area of the city of Vienna did not include enough runoff gauges for checking the created data sets. Hence, the analysed region was extended and includes both PAC1.1 (PA of the city of Vienna) and PAC1.2 (PA of the city of

Waidhofen/Ybbs). This situation makes it easier to provide the climate change scenarios for both PA within Pilot Action Cluster 1.

Figure 32 shows a map of the main measurement network in the test area (the core investigation area is highlighted in yellow). Red triangles are runoff gauges, green triangles measurements of spring discharge, which are part of the regular observation network of the Hydrographic Survey. Vienna Water measures runoff and especially spring discharge at some other locations, but not continuously. Also, the waterworks of Waidhofen/Ybbs have some own measurement stations. The depicted blue meteorological stations are stations of the regular governmental observation network (regional Hydrographic Survey and nationwide Meteorological Service) with long precipitation records. Therefore, these stations were used in the regionalization of precipitation (Figure 33). Long records of temperature are available at fewer stations. There are also some experimental stations that have been set up in research projects in the last years. Mean annual precipitation (MAP) ranges from 550 to almost 3000 mm (Figure 33) when regionalized for a 1x1 km grid with External Drift Kriging (EDK, Ahmed and De Marsily 1987). Due to sparse information from areas at high elevation these high values cannot really be verified. Regionalized precipitation published in the Hydrological Atlas of Austria (HAO) by Skoda and Lorenz (2003) just reaches 2000 mm (Figure 34), but for 6x6 km grid cells. Preliminary water balance simulation indicated that for the western areas with the highest precipitation the values might be correct (as simulated runoff was not overestimated using this precipitation input). In the eastern areas, however, – where EDK and Skoda & Lorenz results match better – water balance simulations indicated that the precipitation estimated with EDK might be too high.

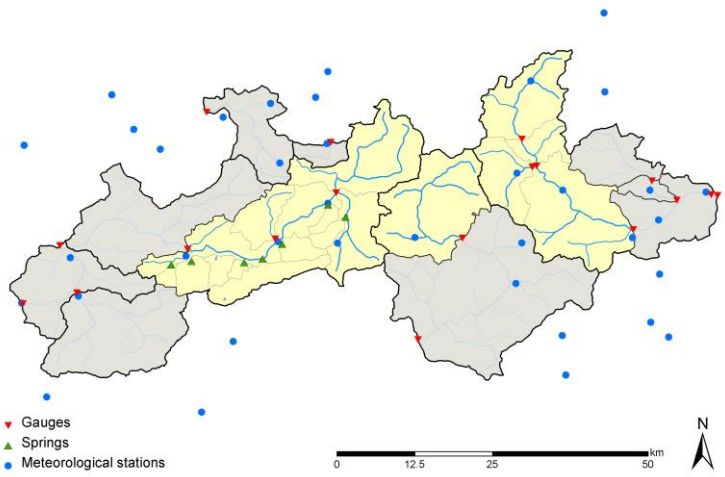

Figure 32: Meteorological stations, runoff gauges and monitored springs in the test area.

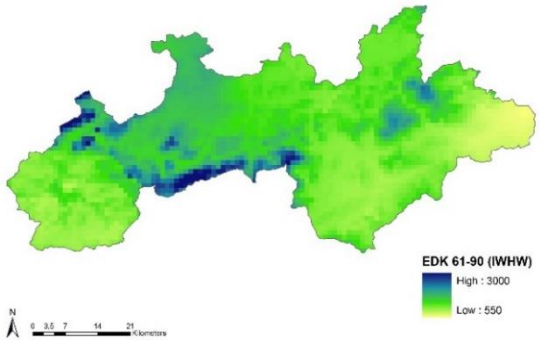

Figure 33: Mean annual precipitation 1961-1990, 1x1 km grid, regionalized with external drift kriging (EDK).

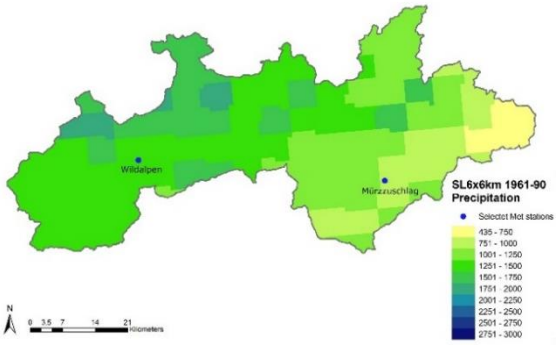

Figure 34: Mean annual precipitation 1961-1990, 6x6 km grid, regionalization by Skoda and Lorenz (2003).

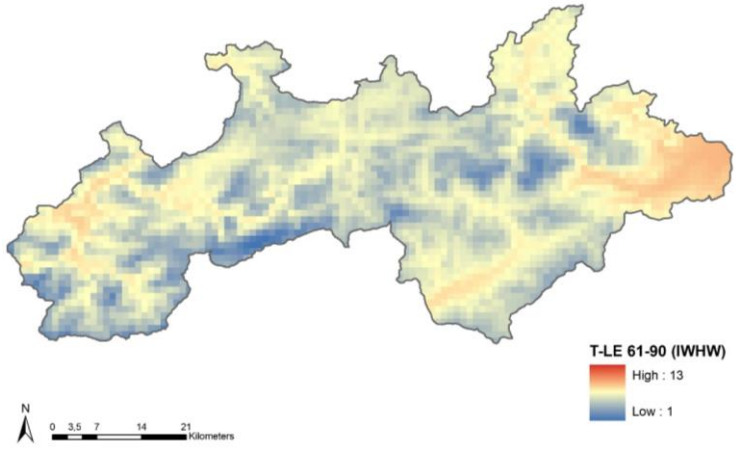

Figure 35: Mean daily temperature 1961-1990, 1x1 km grid, regionalized with a linear regression model with elevation.

Figure 35 reports the mean daily temperature over 1961-1990 properly regionalized for a 1x1 km grid with a linear regression model accounting for elevation. It points out that mean daily air temperature in the test area ranges from 1°C to 13°C. As air temperature distribution is strongly correlated with elevation, the map of regionalized mean daily temperature (Figure 29) mirrors topography.

With the aims of correcting precipitation and temperature time series of the selected RCMs, as a first trial the Europe-wide observation data set EOBS (Haylock et al. 2008) was considered. The control runs of all RCM simulations after the correction should have statistical characteristics very similar to that of the respective EOBS variable. To assess the quality of the corrected RCM data, some EOBS characteristics were compared to those of local observations.

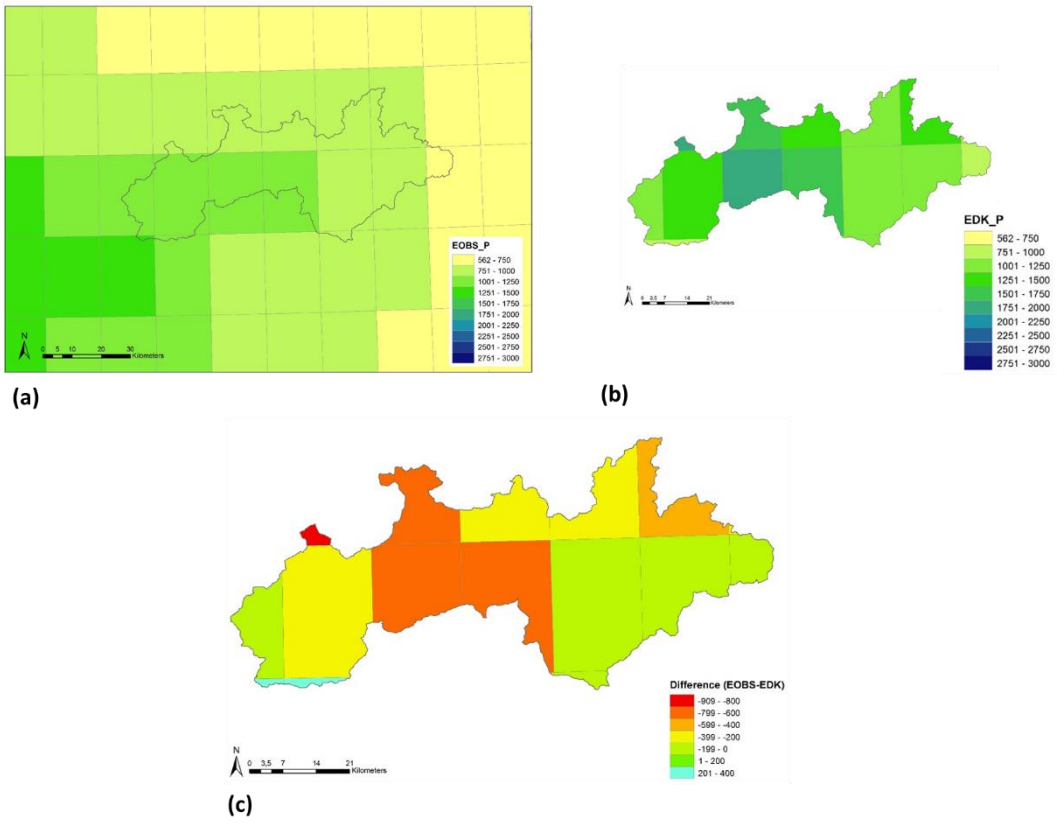

Figure 36: Mean annual precipitation (1961-1990) in EOBS data set (a), in local observations (EDK model regionalization upscaled to EOBS resolution) (b) and difference between the two (c) (all mm).

In this perspective, Figure 36 shows mean annual precipitation of the EOBS data set in the top picture, MAP of regionalized local observations, upscaled to EOBS resolution, in the middle picture, and the difference between the two in the bottom picture. The spatial pattern of EOBS precipitation is rather realistic, with higher values towards the central Alps in the south-west of the extent, and lower values in the eastern lowlands. The absolute values, however, are much too low. Comparing a local weather station data (Wildalpen) with the corresponding EOBS grid cell returns more deficiencies of the EOBS data set (Figure 37). Monthly mean precipitation again shows the underestimation of precipitation by EOBS, which is almost constant throughout the year. In the standard deviation the very high discrepancies in the winter months stand out. These are explained by the graph with the CDF of January precipitations, which shows that EOBS does not include any Januaries with more than 100 mm precipitation, while around 30 % of the observed January sums were higher than this value. Also, in July there is a considerable mismatch between the CDFs of Wildalpen and EOBS grid cell precipitation.

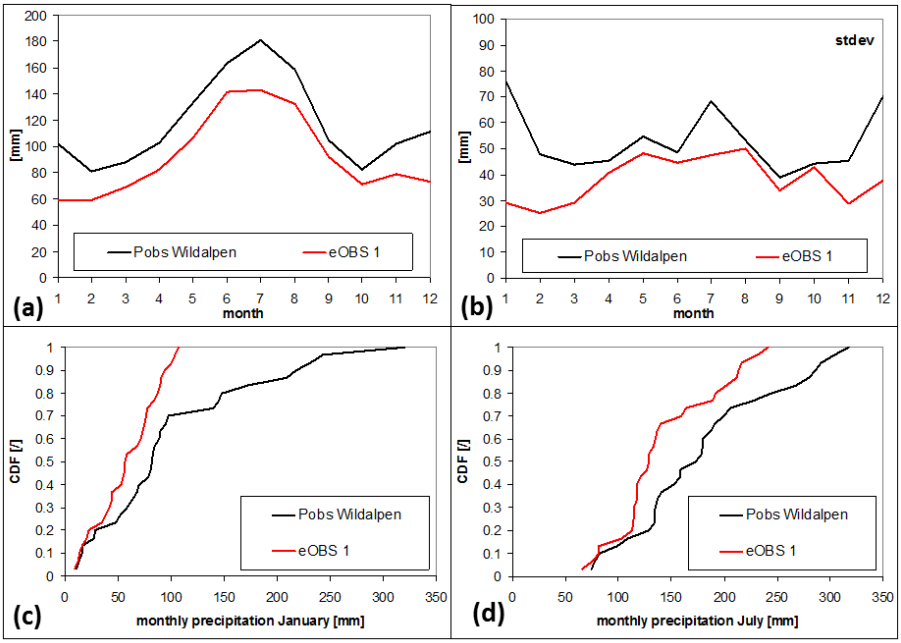

Figure 37: Monthly mean precipitation and standard deviation (1961-1990) in EOBS data set and local observation (a-b), and CDF of monthly precipitation for January and July (c-d).

Due to these considerable differences, another data set was adopted for bias correction of RCM precipitation in the Austrian test area. This data set by the ETH Zürich (Frei and Schär 2008) covers the entire Alpine region and uses more stations than the EOBS dataset. Figure 38 shows MAP of the ETHZ data set (which is also referred to as ALPIN data set), and the differences to the upscaled EDK regionalization of local observations. Larger parts of the test area have a MAP in the range of 1000-1250 mm in the ETHZ data set. Still, the ETHZ values are considerably lower than the EDK results. The comparison of station observations in Wildalpen and the closest ETHZ grid point, however, shows the better quality of the ETHZ data (Figure 39). Seasonality and variance are represented very well in the ETHZ time series, and so is the distribution of precipitation (now shown with the CDF of daily rainfall). While the areal comparison in Figure 38 included also a temporal mismatch (ETHZ means refer to 1971-1990 and EDK means to 19-1-1990), the comparison in Figure 39 is based on 1971-1990 data for both, local observation and ETHZ grid point.

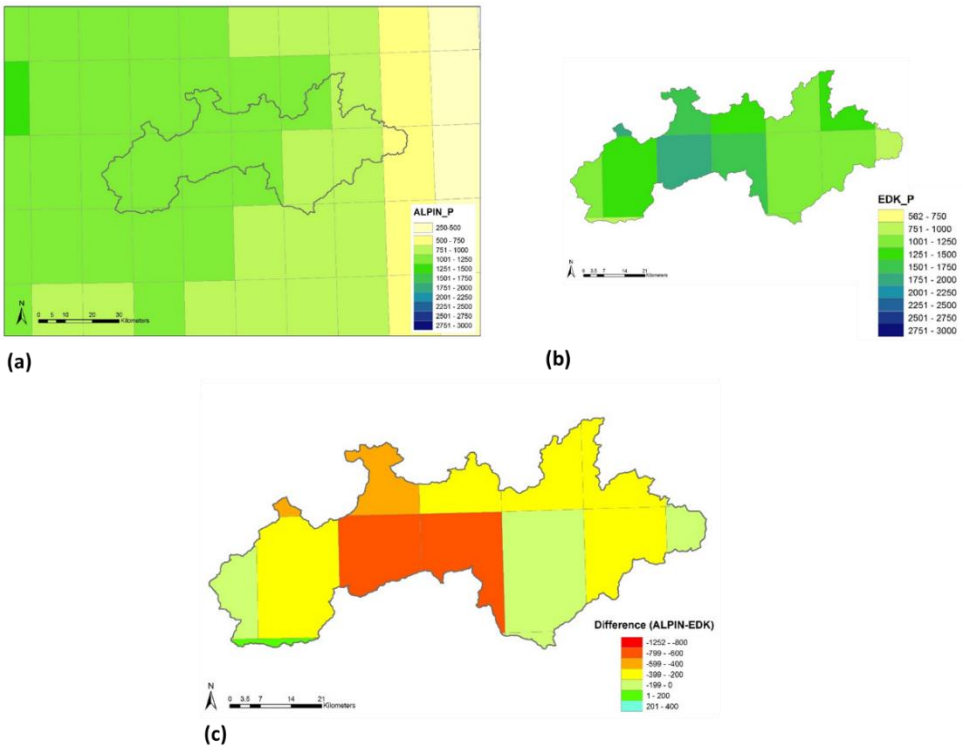

Figure 38: Mean annual precipitation (1971-1990) in ETHZ / ALPIN data set (a), in EDK (upscaled to EOBS / ETHZ resolution) (b) and difference between the two (c) (all mm).

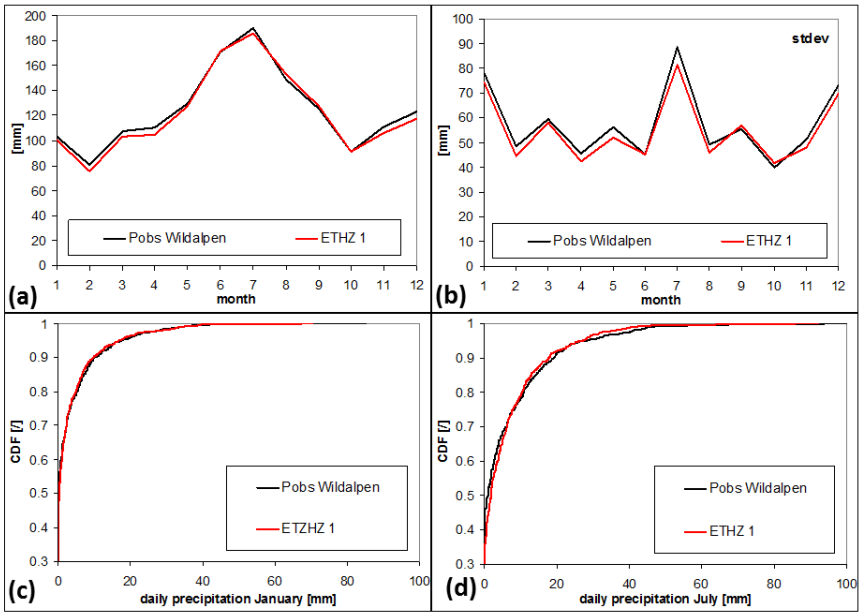

Figure 39: Monthly mean precipitation and standard deviation (1971-1990) in ETHZ / ALPIN data set and local observation (a-b), and CDF of daily precipitation for January and July (c-d).

Based on these results, the use of ETHZ precipitation data for bias correction of RCM precipitation seems justified. The fact that ETHZ precipitation is still too low in the areal mean has to be accounted for in the subsequent correction step. Also, the local distribution of precipitation within the 25km grid cells is approached.

The spatial distribution of mean daily air temperature in the EOBS data set generally reproduces the pattern caused by topography (Figure 40a-b). A comparison with the results of a regionalization of local observations with a model of linear regression with elevation, averaged for the resolution of the EOBS grid, shows a moderate overestimation of temperature in the EOBS data (Figure 40c). This can maybe be attributed to a generally lower elevation in the EOBS elevation model. The local distribution of temperature is calculated in a subsequent correction step. Remaining biases in temperature are also corrected in a later stage. Due to the larger influence of elevation differences, no comparison between one grid cell and one station is presented here.

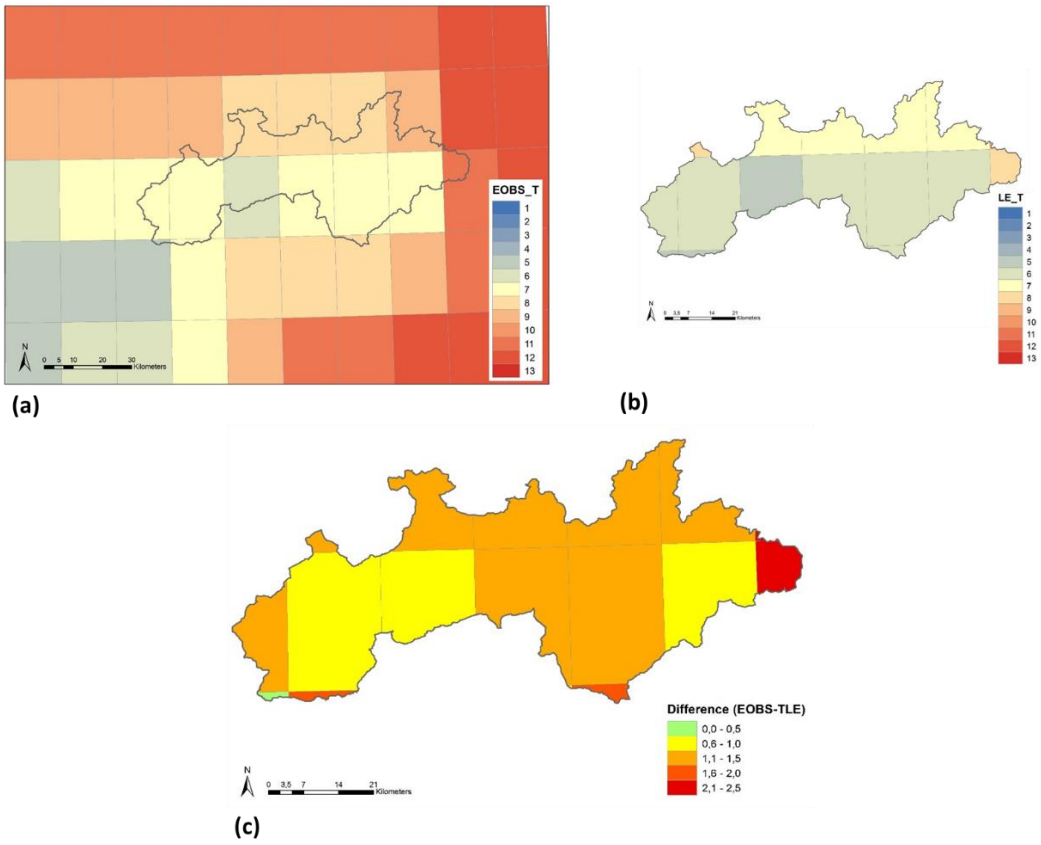

Figure 40: Mean daily air temperature (1961-1990) in EOBS data set (a), in local observations (LE model regionalization upscaled to EOBS resolution) (b) and differences between the two (c) (all °C).

5.1.2.2. Future climate

For climate change analysis, only one emission scenario, the A1B scenario (in line with the RCP4.5 as in IPCC AR/5), was selected in the framework of CC-WaterS project. To this aim, RCMs driven by different GCMs were selected: the RCM ALADIN driven by GCM ARPEGE, the RCM RegCM3 driven

by GCM ECHAM5-r3 and the RCM PROMES driven by GCM HadCM3Q0. In the following, such models are named according to the institute of origin respectively as CNRM, ICTP and UCLM.

The analysis of expected climate change is based on bias corrected RCM results, with the bias correction based on EOBS temperature and ETHZ / ALPIN precipitation. Subsequent correction steps of disaggregation to a 1x1 km grid and multiplicative correction did not alter the climate change signals, and therefore were not considered in this assessment of climate change in the Austrian test area. Climate change is analysed regarding the changes for the periods 2021-2050 and 2071-2100 compared to 1961-1990 for temperature and 1971-1990 for precipitation.

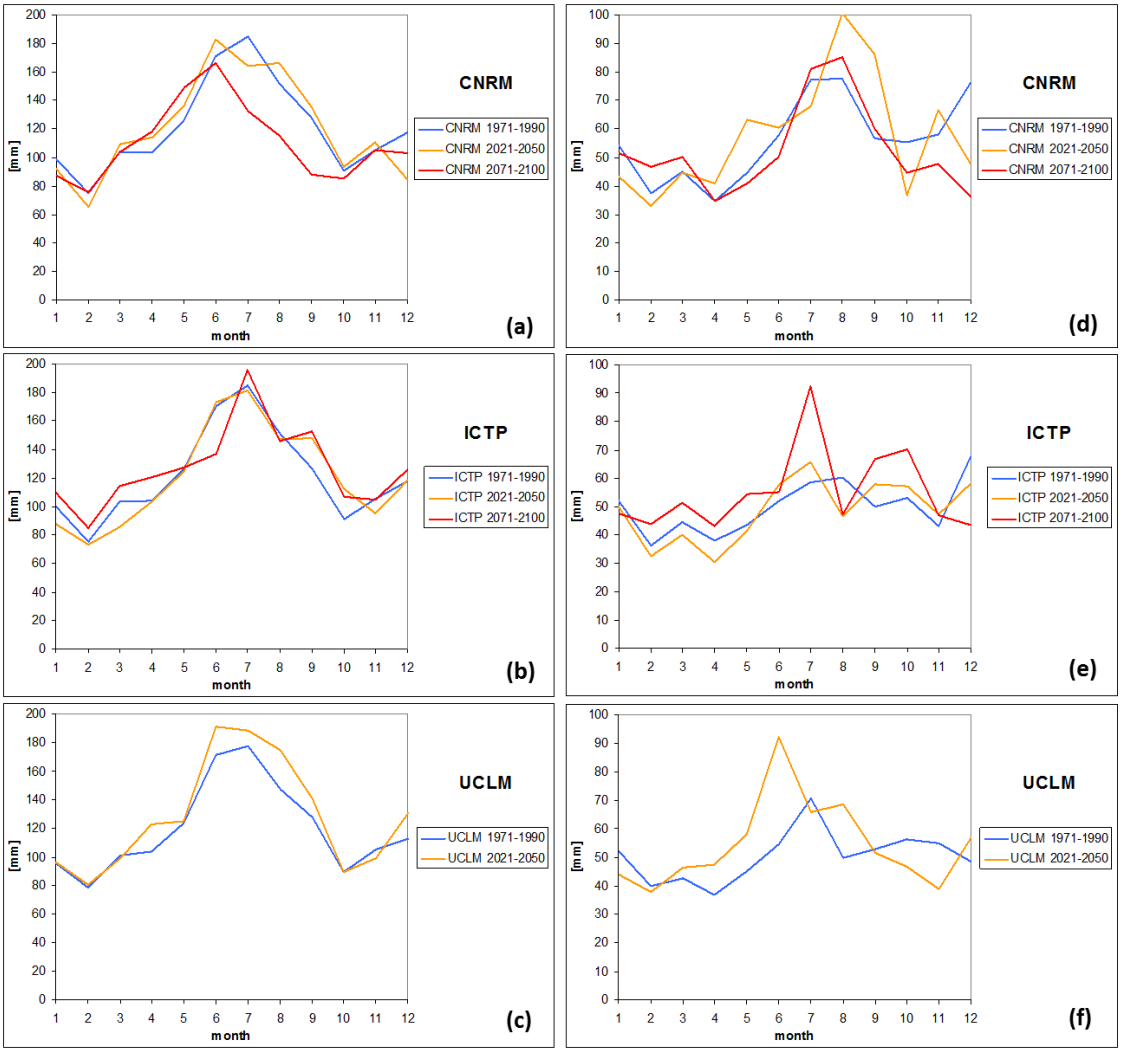

Figure 41: RCM mean monthly precipitation for the 30-year periods of 1961-1990, 2021-2050 and 2071-2100 (a-b-c); standard deviation of monthly RCM precipitation for the 30-year periods of 1961-1990, 2021-2050 and 2071-2100 (d-e-f).

Figure 41 show these changes for the grid cell closest to Wildalpen, which was used in previous analysis above. For precipitation, no clear trend can be deduced from the joint analysis of the three RCM (Figure 41a-b-c). While CNRM and ICTP show no pronounced change for 2021-2050, UCLM predicts an increase in precipitation, mainly in summer. For the period of 2071-2100, CNRM

estimates a strong decrease in summer precipitation and a minor increase in spring precipitation. ICTP predicts a general, but small increase in precipitation. Also, in precipitation variance no sharp change can be expected (Figure 41d-e-f). Only for the summer months all three models show an increase of standard deviation of monthly rainfall, but the increase is calculated for August in CNRM, July in ICTP, and June in UCLM, with no apparent change in the other months in all models.

Expectedly, all three RCMs show a clear trend of increasing temperature in the 21st century. The increase from 1961-90 to 2021-50 is slightly higher with the UCLM model than with the other two, and this model also shows an especially high increase in January and February (Figure 42a-b-c). The annual mean increase in temperature between these two periods is 1.5°C with CNRM, 1.1°C with ICTP and 2.2°C with UCLM.

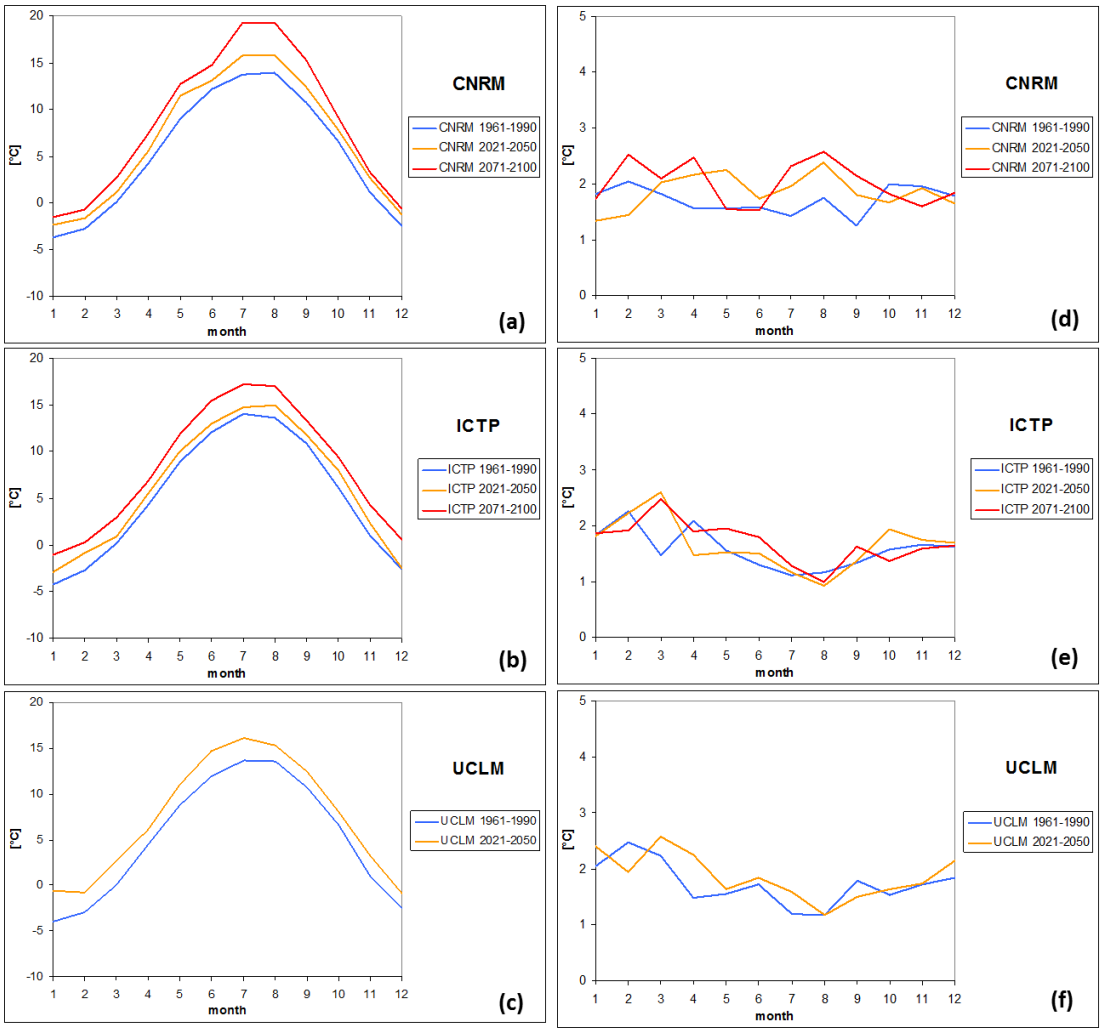

Figure 42: RCM mean monthly temperature for the 30- year periods of 1961-1990, 2021-2050 and 2071-2100 (a-b-c); standard deviation of RCM monthly temperature for the 30-year periods of 1961-1990, 2021-2050 and 2071-2100 (d-e-f)

For the period of 2071-2100 CNRM predicts a distinct peak of increase in the summer months. The mean increase of temperature relative to 1961-90 is expected to be 3.2°C with CNRM and 3.3°C with ICTP (Figure 42a-b-c).

Figure 42d-e-f show no clear tendency with respect to standard deviation of monthly temperature. CNRM predicts a slight increase in standard deviation, the other models rather not.

The analysis of results has to be based on long time-periods (e.g. decades or 30-year segments) to obtain a clear climate signal, otherwise short-term variations can also be caused by sampling issues because of the "randomness" in the weather (Deque et al., 2007).

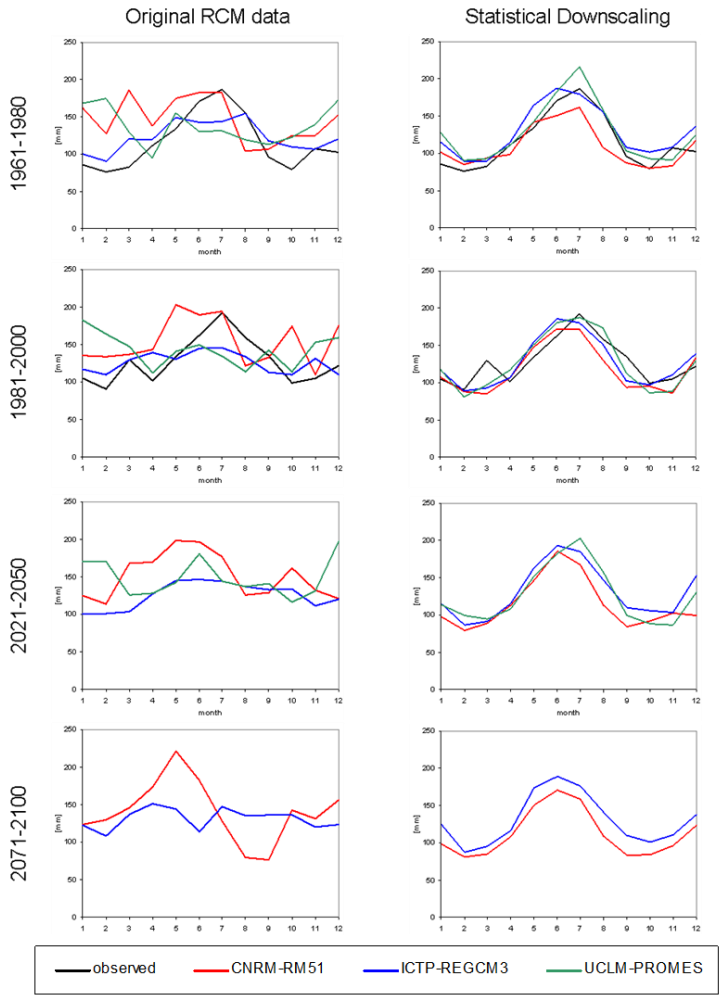

Figure 43: Seasonal monthly precipitation of different periods: original RCM data (left panel) and statistical downscaling results (right panel).

Results for seasonality in monthly precipitation are presented in Figure 43 for the periods 1961-1980 (calibration period), 1981-2000 (independent evaluation period), and the future periods 2021-2050 and 2071-2100. For the past periods a comparison with observed precipitation data is possible. The original RCM data show very poor performance. The results of the statistical downscaling reproduce seasonality well, both in the calibration and evaluation periods. For future precipitation the original RCM data exhibit some interesting trends: For the CNRM model a strong seasonality (with a peak in May) develops for future precipitation from almost no seasonality in the past. An opposing trend develops for the ICTP model: the weak seasonality in the past completely disappears in the future. Such changes in seasonality are not visible in the results of the statistical downscaling: in all periods the seasonality in precipitation is quite similar.

5.1.3. PROLINE CE development for PA1.1

This section shows the variations in seasonal precipitation (Table 5), seasonal temperature (Table 6) and yearly Rx1day, CDD and CWD (Table 7) for the Pilot Action 1.1: Catchment area of the Vienna Water Supply, AT1. The variations are obtained considering only the EURO-CORDEX data (§4.2). In this case, as a reference, the data of Figure 41 (for seasonal precipitation) and Figure 42 (for seasonal temperature). These data refer to three RCMs under the A1B emission scenario

(in line with the RCP4.5 concentration scenario as in IPCC AR/5), then a comparison can be established only for RCP4.5 EURO-CORDEX data.

Table 5: Changes in seasonal precipitation (mm) in PA1.1 with EURO-CORDEX projections.

		RCP4.5						RCP8.5					
		2021-2050 distribution percentiles			2071-2100 distribution percentiles			2021-2050 distribution percentiles			2071-2100 distribution percentiles		
		50th	25th	75th	50th	25th	75th	50th	25th	75th	50th	25th	75th
Changes in seasonal precipitation (mm)	winter	23.3	-3.9	37.7	26.6	2.4	39.4	34.1	1.3	49.8	40.6	13.8	57.6
	spring	19.0	13.1	38.8	44.8	32.2	65.6	34.3	25.2	52.3	62.1	43.5	78.5
	summer	0.4	-30.5	18.3	8.3	-15.9	30.4	16.8	-27.0	22.5	-10.4	-55.2	22.2
	autumn	12.8	-2.8	24.0	18.8	-1.1	37.2	17.4	-0.2	37.3	35.7	2.2	48.4

In terms of seasonal precipitation, the EURO-CORDEX models return:

- increasing of seasonal precipitation in winter and spring, emphasized on the base of RCP scenarios, over 2021-2050
- increasing of seasonal precipitation in spring (up to 60 mm as median value) with a decrease in summer over 2021-2050

In a qualitative way, by comparing data of Figure 41 with data in Table 5, similar trends can be detectable but with different absolute value.

Table 6: Changes in seasonal temperature (°C) in PA1.1 with EURO-CORDEX projections.

		RCP4.5						RCP8.5					
		2021-2050 distribution percentiles			2071-2100 distribution percentiles			2021-2050 distribution percentiles			2071-2100 distribution percentiles		
		50th	25th	75th	50th	25th	75th	50th	25th	75th	50th	25th	75th
Changes in seasonal temperature (°C)	winter	1.4	1.0	1.7	2.1	1.9	2.7	1.5	0.9	1.6	4.2	3.6	5.0
	spring	1.1	0.7	1.4	2.3	1.6	2.5	1.2	1.1	1.6	4.0	3.1	4.5
	summer	1.3	1.2	1.6	1.9	1.8	2.4	1.3	1.2	1.6	3.7	3.5	4.5
	autumn	1.0	0.8	1.5	2.2	1.7	2.6	1.4	1.0	1.8	3.7	3.4	4.3

In terms of seasonal temperature, the EURO-CORDEX models return:

- a general increase of seasonal temperature for all the seasons with values up to 4 °C for RCP8.5 scenario

In a qualitative way, by comparing data of Figure 42 with data in Table 6, similar trends can be detectable but values are different since the State-of-the-art points out increase in temperature compared with current period of 1-2°C in winter-later autumn-early spring and value higher than 5°C in summer for 2071-2100.

Table 7: Changes in yearly Rx1day (mm/day), CDD (-) and CWD (-) in PA1.1 with EURO-CORDEX projections.

		RCP4.5						RCP8.5					
		2021-2050 distribution percentiles			2071-2100 distribution percentiles			2021-2050 distribution percentiles			2071-2100 distribution percentiles		
		50th	25th	75th	50th	25th	75th	50th	25th	75th	50th	25th	75th
Changes in Rx1day (mm)	yearly	2.0	-1.3	4.5	4.5	2.0	6.7	2.9	-0.4	6.1	8.1	5.2	10.8
Changes in CDD (-)		-0.4	-1.2	0.7	-0.2	-1.4	1.3	0.1	-0.7	0.6	0.5	-0.5	1.1
Changes in CWD (-)		0.8	-0.4	1.0	1.0	-0.1	1.5	0.4	-0.5	1.0	-0.1	-1.2	0.5

In terms of yearly Rx1day, the EURO-CORDEX models return:

- no evident variations general increase for all the seasons over 2021-2050
- a slight increase in Rx1day over 2071-2050 with higher values for RCP8.5

In terms of yearly CDD and CWD, the variations are very low and so negligible.

5.1.4. PROLINE CE development for PA1.2

This section shows the variations in seasonal precipitation (Table 8), seasonal temperature (Table 9) and yearly Rx1day, CDD and CWD (Table 10) for the Pilot Action 1.2: Catchment area of Waidhofen/Ybbs, AT2. The variations are obtained considering only the EURO-CORDEX data (§4.2).

Table 8: Changes in seasonal precipitation (mm) in PA1.2 with EURO-CORDEX projections.

		RCP4.5						RCP8.5					
		2021-2050 distribution percentiles			2071-2100 distribution percentiles			2021-2050 distribution percentiles			2071-2100 distribution percentiles		
		50th	25th	75th	50th	25th	75th	50th	25th	75th	50th	25th	75th
Changes in seasonal precipitation (mm)	winter	18.4	-1.8	29.6	21.6	12.6	35.6	27.9	8.0	41.3	35.0	20.4	45.0
	spring	17.7	7.6	31.5	26.8	17.4	42.5	26.9	18.8	34.5	37.4	21.4	54.7
	summer	-4.0	-9.8	18.8	17.7	-8.5	37.5	9.5	-2.4	20.6	10.7	-33.5	33.3
	autumn	11.3	-4.5	17.1	12.4	0.5	23.8	19.6	-2.3	32.0	30.4	1.4	49.8

In terms of seasonal precipitation, the same considerations for data in Table 8 as reported in §5.1.3 are retrievable even if this area seems to be featured by slight increases on average of seasonal precipitation.

Table 9: Changes in seasonal temperature (°C) in PA1.2 with EURO-CORDEX projections.

		RCP4.5						RCP8.5					
		2021-2050 distribution percentiles			2071-2100 distribution percentiles			2021-2050 distribution percentiles			2071-2100 distribution percentiles		
		50th	25th	75th	50th	25th	75th	50th	25th	75th	50th	25th	75th
Changes in seasonal temperature (°C)	winter	1.3	1.1	1.8	2.3	2.1	2.8	1.4	0.9	1.9	4.2	3.8	4.8
	spring	0.9	0.7	1.3	2.2	1.4	2.7	1.3	1.0	1.5	3.5	2.7	4.1
	summer	1.2	1.1	1.5	1.9	1.6	2.5	1.3	1.1	1.5	3.6	3.2	4.2
	autumn	1.1	0.9	1.5	2.3	1.6	2.6	1.4	0.9	1.9	3.8	3.2	4.4

In terms of seasonal temperature, the EURO-CORDEX models return:

- a general increase of seasonal temperature for all the seasons with values up to 4 °C for RCP8.5 scenario especially in winter

Table 10: Changes in yearly Rx1day (mm/day), CDD (-) and CWD (-) in PA1.2 with EURO-CORDEX projections.

		RCP4.5						RCP8.5					
		2021-2050 distribution percentiles			2071-2100 distribution percentiles			2021-2050 distribution percentiles			2071-2100 distribution percentiles		
		50th	25th	75th	50th	25th	75th	50th	25th	75th	50th	25th	75th
Changes in Rx1day (mm)	yearly	2.9	-0.1	6.4	4.1	2.7	5.5	4.4	1.6	6.4	10.0	7.0	12.5
Changes in CDD (-)		0.0	-1.0	0.8	0.2	-1.3	1.7	0.1	-0.7	0.6	0.5	-0.5	1.1
Changes in CWD (-)		0.5	-0.4	0.9	0.4	-0.3	1.1	0.4	-0.5	1.0	-0.1	-1.2	0.5

In terms of yearly Rx1day, the EURO-CORDEX models return:

- an overall increase compared to current condition (about 10 mm for RPC8.5 for far time horizon

In terms of yearly CDD and CWD, the variations are very low and so negligible.

5.2. PA2.1 Well field Dravlje valley in Ljubljana, SI

5.2.1. Foreword

This section is about climate change issues in Pilot Action 2.1: Well field Dravlje valley in Ljubljana. Slovenian pilot action area is located in the central part of Slovenia, next to western Ljubljana bypass in the Dravlje Valley. Climate data representative for the study area were selected by 3x3 grid mesh (T1 to T9; Figure 44). Study area is located in the centred grid (T5). Further analysis of temperature, evapotranspiration and precipitation data was focused on the model grid T5, located nearest to the pilot area location in the Dravlje valley.

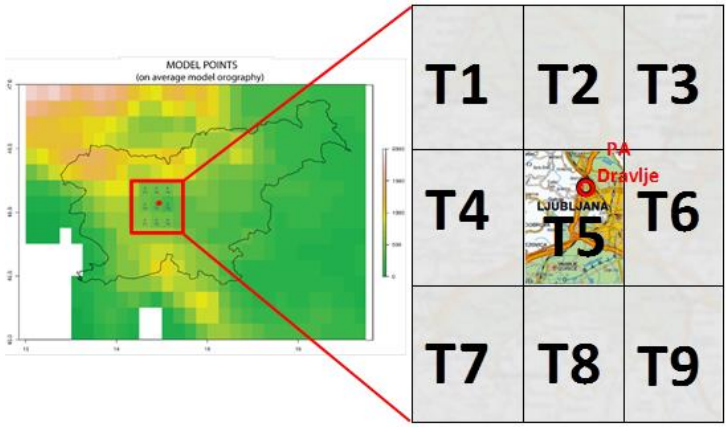

Figure 44: Analysed area with location of the pilot area (PA).

For hydraulic, hydrological and hydrogeological modelling of climate change scenarios daily precipitation and temperature data with bias correction are applied. For PA 2.1 climate change data are provided by the Slovenian Environment Agency (2017). Specifically, model data for six RCMs under the RCP4.5 and RCP8.5 scenarios are considered for 9 selected grids (Figure 44).

Table 11: List of models adopted in the analysis for the global model (GCM) and regional model (RCM); the last column identifies the corresponding for Table 3.

	GCM	*RCM*	*#*
M1	CNRM-CERFACS-CNRM-CM5	CLMcom-CCLM4	1
M2	MPI-M-MPI-ESM-LR	CLMcom-CCLM4	15
M3	ICHEC-EC-EARTH	DMI-HIRHAM5	6
M4	IPSL-IPSL-CM5A-MR	IPSL-INERIS	10
M5	MOHC-HadGEM2-ES	KNMI-RACMO22E	13
M6	MPI-M-MPI-ESM-LR	SMHI-RCA4	17

The Slovenian Environment Agency selected Regional Climate Models from the EUROCORDEX database, which the most properly describe Slovenian climate (Table 11). Model temperature and precipitation data was corrected to remove the systematic error using the quantile mapping method. Modelled data were compared with measured data of precipitation and temperature in the period 1981-2010. Before the comparison, the data were interpolated with kriging into the grid mesh (resolutions 0.125°). The comparative period was 1981-2010 (calibration period), the calculation was made for each of the periods 2021-2050 (the 'near future' period), and 2071-2100 (the 'far future' period) separately. Precipitation was corrected using the quantile mapping method directly, and the temperature was separated by four precipitation classes, the first of which was precipitation free,

while the others were divided by the terciles of the distribution of rainfall. The corrections were carried out by model points spatially independently.

The potential reference evapotranspiration is calculated from the model data of the highest and lowest daily air temperature, average daily humidity, short-wave solar radiation and surface wind velocity according to the Penman-Monteith equation (Allen et al. 1998).

5.2.2. Previous state-of-the-art framework

5.2.2.1. Current and future climate

Temperature data cover period from 1981 to 2100 and focus on the spatial grid T5 (*Figure 44;* pilot area location). The used models M1 to M6 (Table 11) indicate the combination of the global and regional model. Temperature data were corrected according to the precipitation - four precipitation classes (one precipitation free, others divided by the terciles of the distribution of rainfall). Average yearly temperature in the period of 119 years showed temperature rising through years for all six models for both scenarios: RCP4.5 (Figure 45a) and RCP8.5 (Figure 46a).

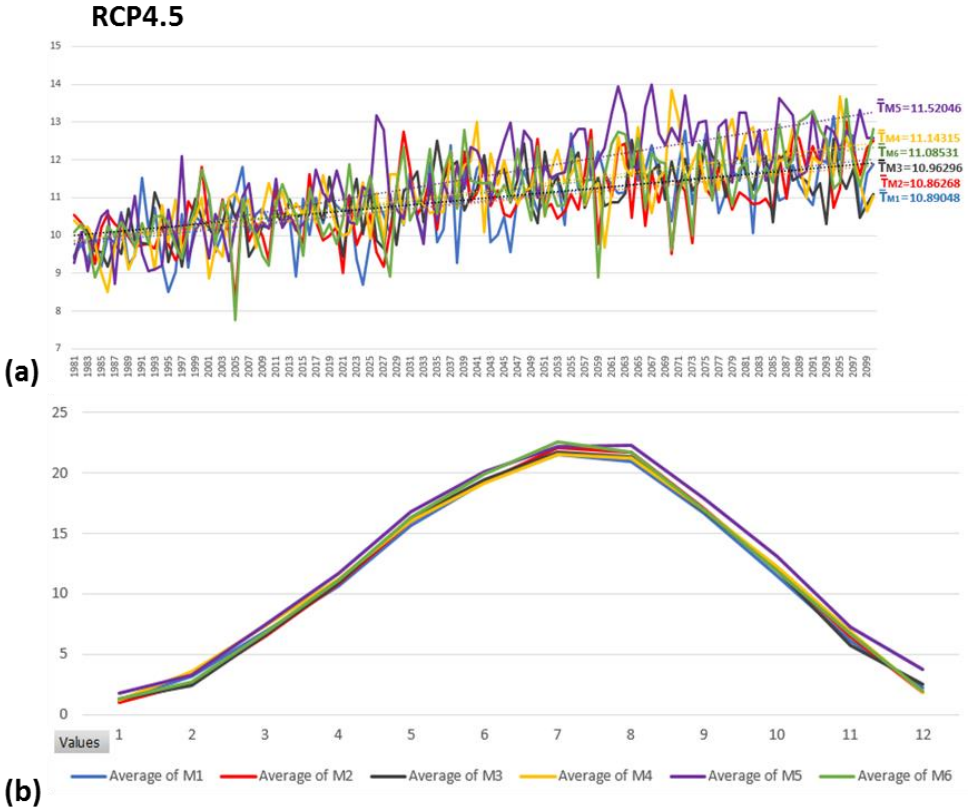

Figure 45: Yearly temperature (a) and average monthly temperature (b) for T5 area for all 6 models under RCP4.5 scenario.

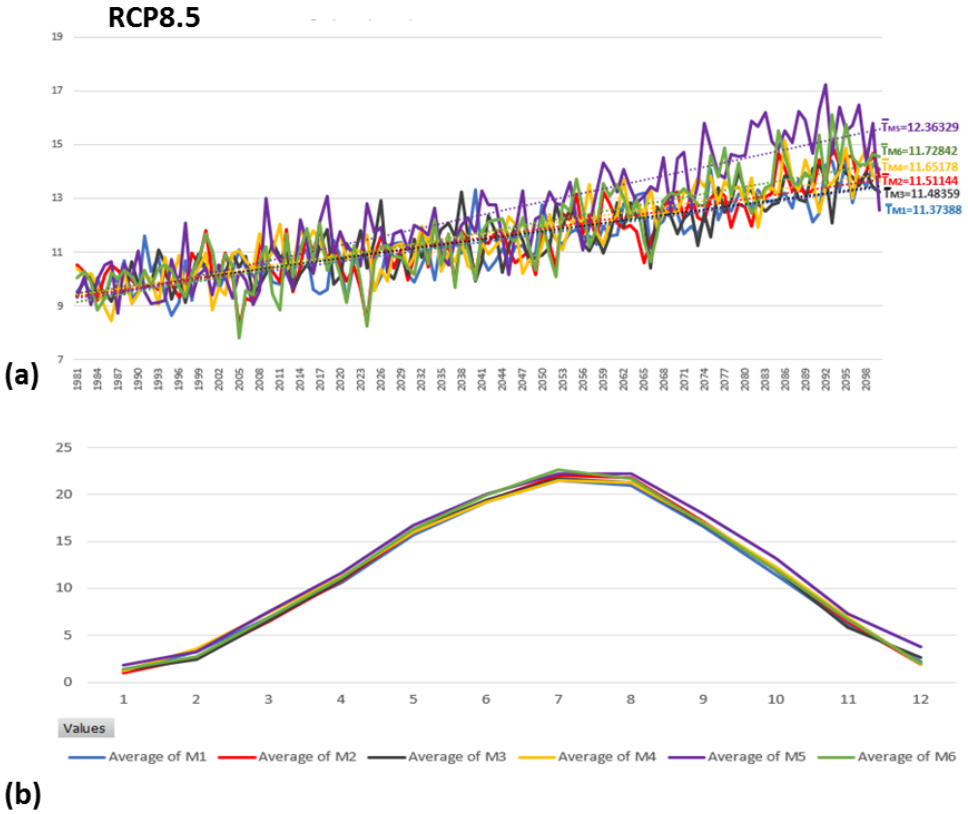

Figure 46: Yearly temperature (a) and average monthly temperature (b) for T5 area for all 6 models under RCP8.5 scenario.

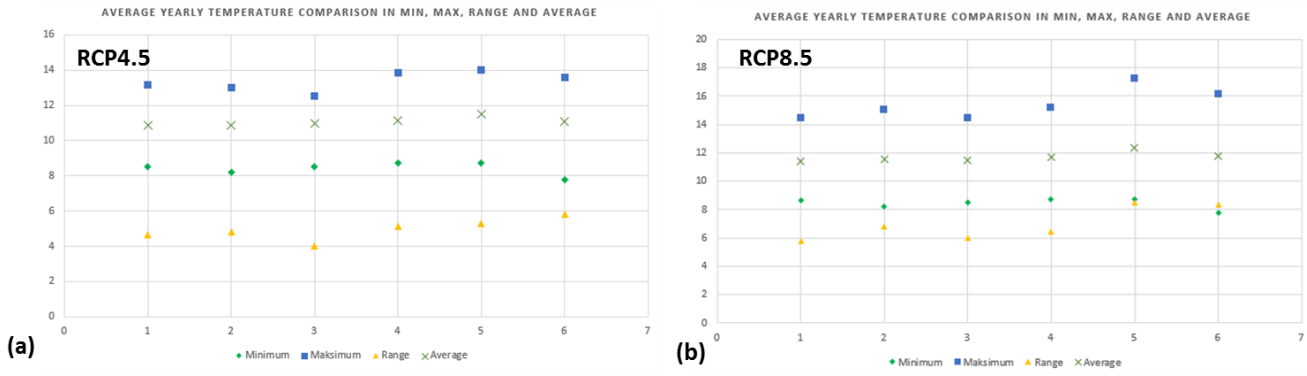

Figure 47: Comparison between average yearly temperature data (minimum, maximum, range and average) between RCP4.5 (a) and RCP8.5 (b) scenarios.

The average of average yearly temperature for each model was in the interval of one degree (from 10.9 to 11.5°C or from 11.4 to 12.4°C). The distribution of average monthly temperatures for all the six models through a year is shown in Figure 45a and Figure 46b, while Figure 47 compares the average yearly temperature between both RCPs.

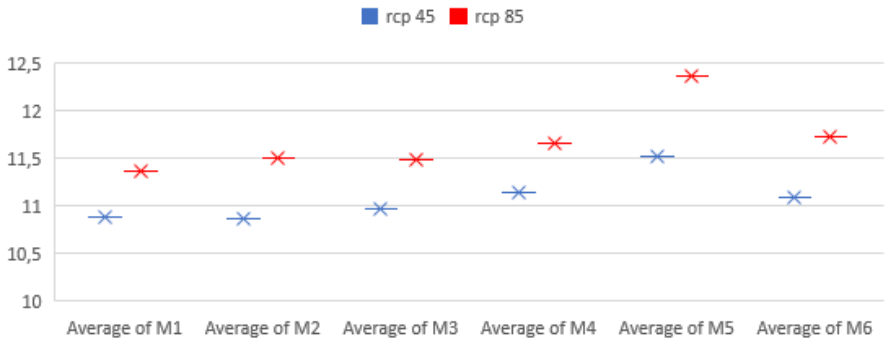

Figure 48: Average temperature comparison between scenarios and models.

The following Figures show predicted temperature change during Winter, Spring, Summer And autumn periods for both scenarios and the comparison between them.

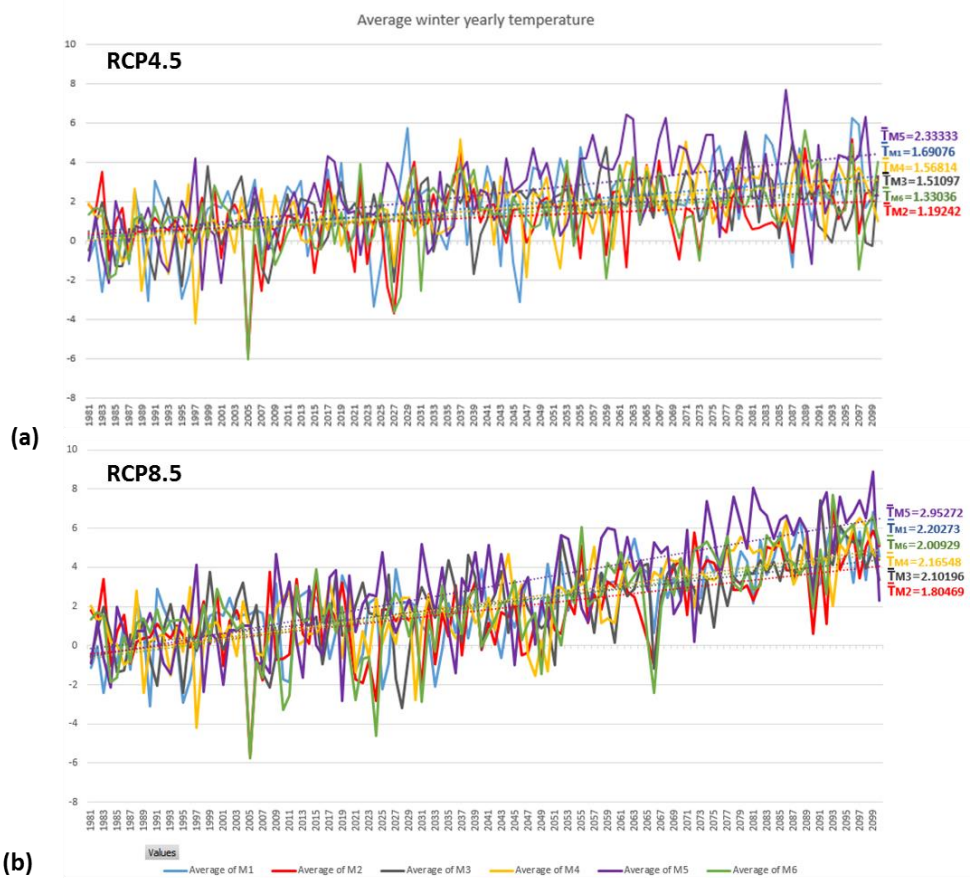

Figure 49: Winter yearly temperature for RCP4.5 (a) and RCP8.5 (b) scenarios.

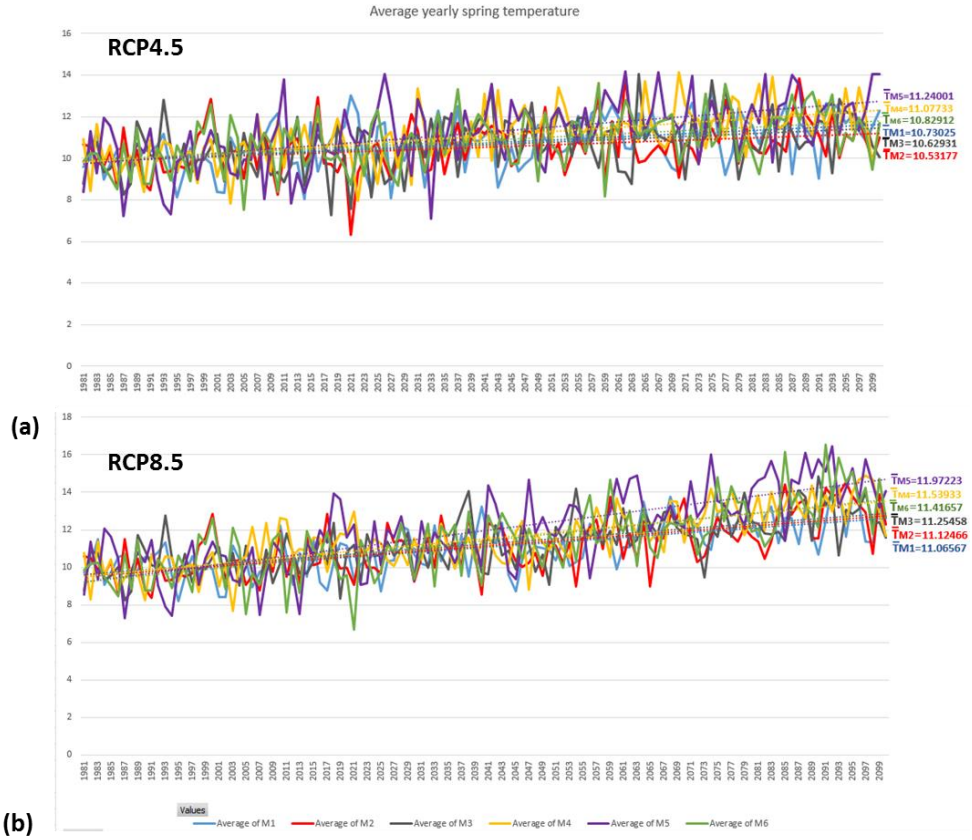

Figure 50: Spring yearly temperature for RCP4.5 (a) and RCP8.5 (b) scenarios.

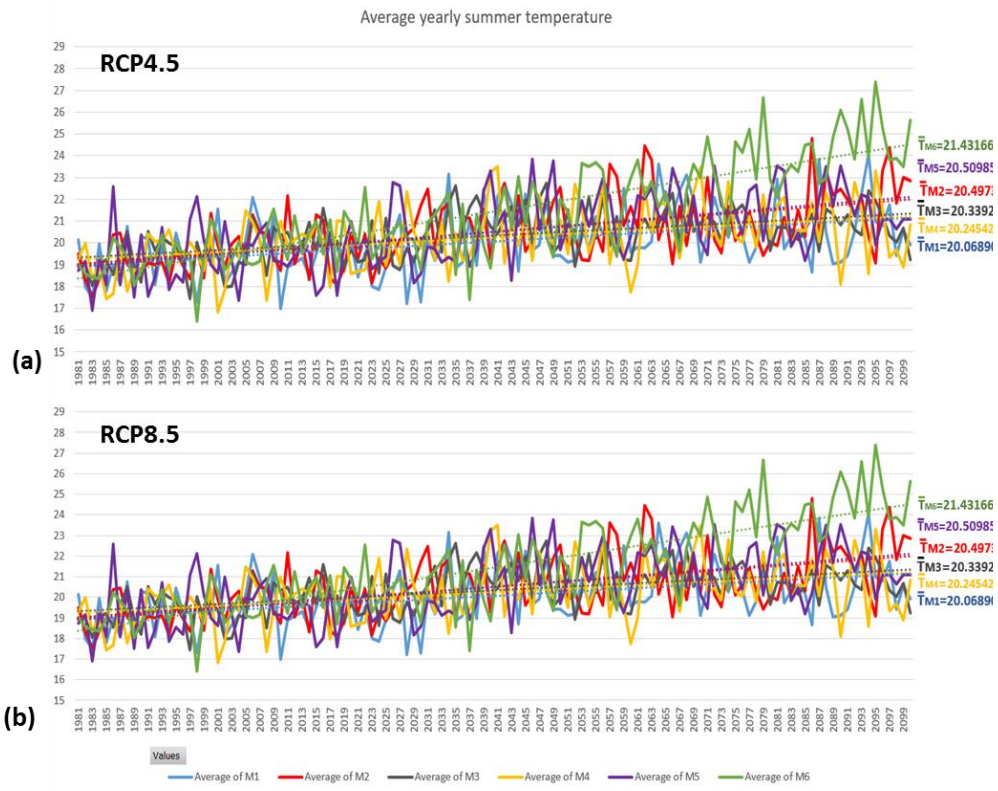

Figure 51: Summer yearly temperature for RCP4.5 (a) and RCP8.5 (b) scenarios.

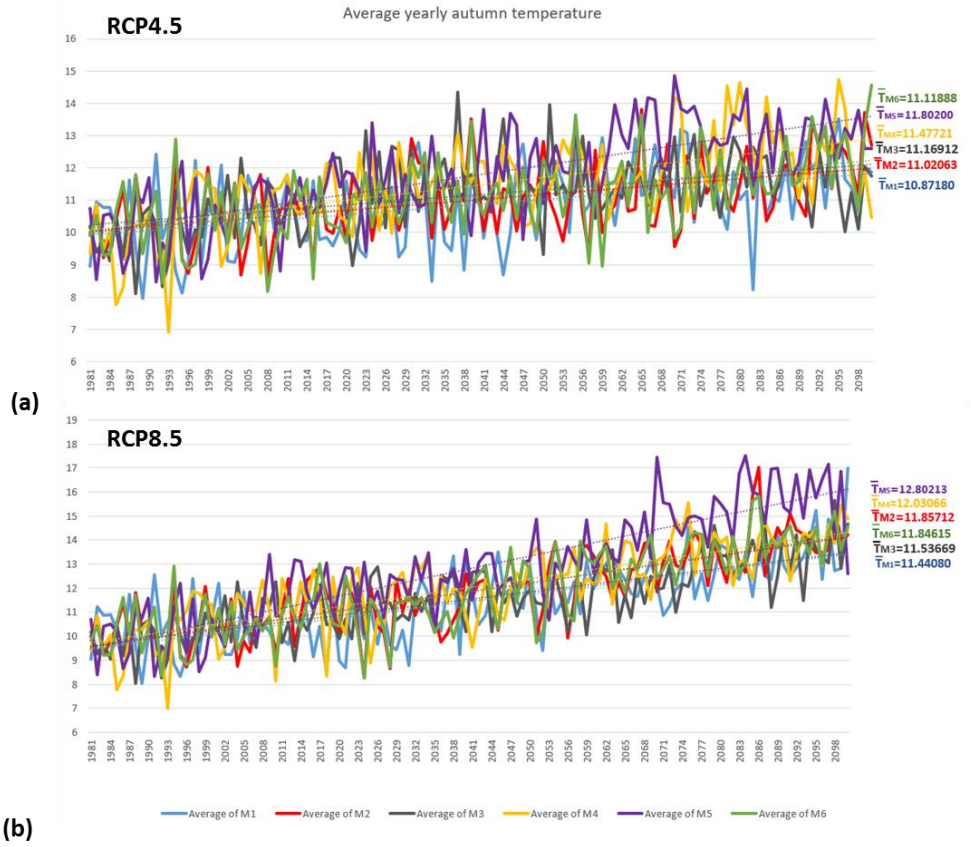

Figure 52: Autumn yearly temperature for RCP4.5 (a) and RCP8.5 (b) scenarios.

- December, January and February were defined as Winter period. The calculated average temperature range in the Winter period is from 1.2 to 2.3°C for RCP4.5 scenario and 1.8 to 2.9°C for RCP8.5 scenario
- March, April and May were defined as Spring period. The calculated average temperature range in the Spring period is from 10.6 to 11.2°C for RCP4.5 scenario and 11.1 to 12.0°C for RCP8.5 scenario
- June, July and August were defined as Summer period. The calculated average temperature range in the Summer period is from 20.1 to 21.4°C for RCP4.5 scenario and 20.6 to 21.5°C for RCP 8.5 scenario
- September, October and November were defined as Autumn period. The calculated average temperature range in the Autumn period is from 10.9 to 11.1°C for RCP4.5 scenario and 11.4 to 12.8°C for RCP8.5 scenario

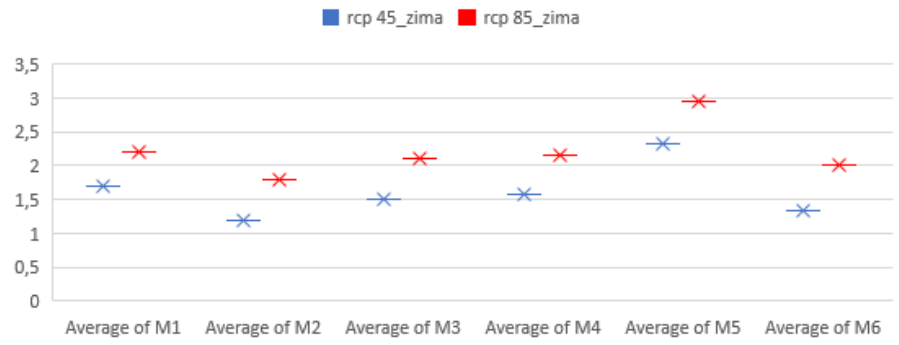

Figure 53: Average Winter temperature comparison between scenarios and models.

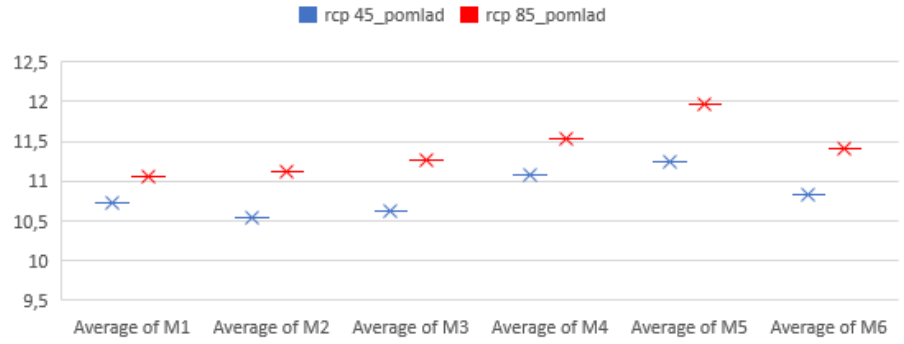

Figure 54: Average Spring temperature comparison between scenarios and models.

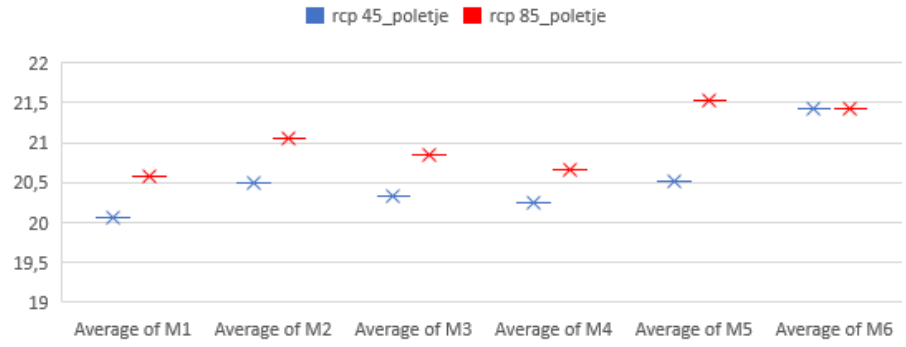

Figure 55: Average Summer temperature comparison between scenarios and models.

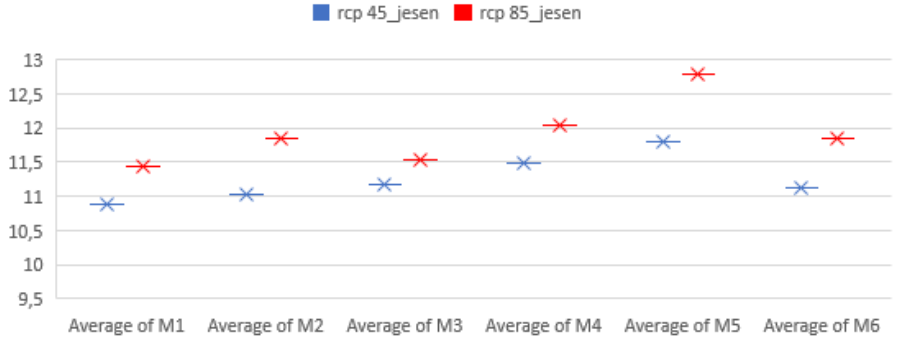

Figure 56: Average Autumn temperature comparison between scenarios and models.

Concerning analysis of precipitation data, they refer to the period from 1981 to 2100 and focus on the spatial grid T5 (*Figure 44;* pilot area location). The used models M1 to M6 (Table 11) indicate

the combination of the global and regional model. Precipitation was corrected using the quantile mapping method directly and is expresses in mm. Yearly Precipitation data in the period of 119 years for all six models are shown in Figure 57 expressed in mm.

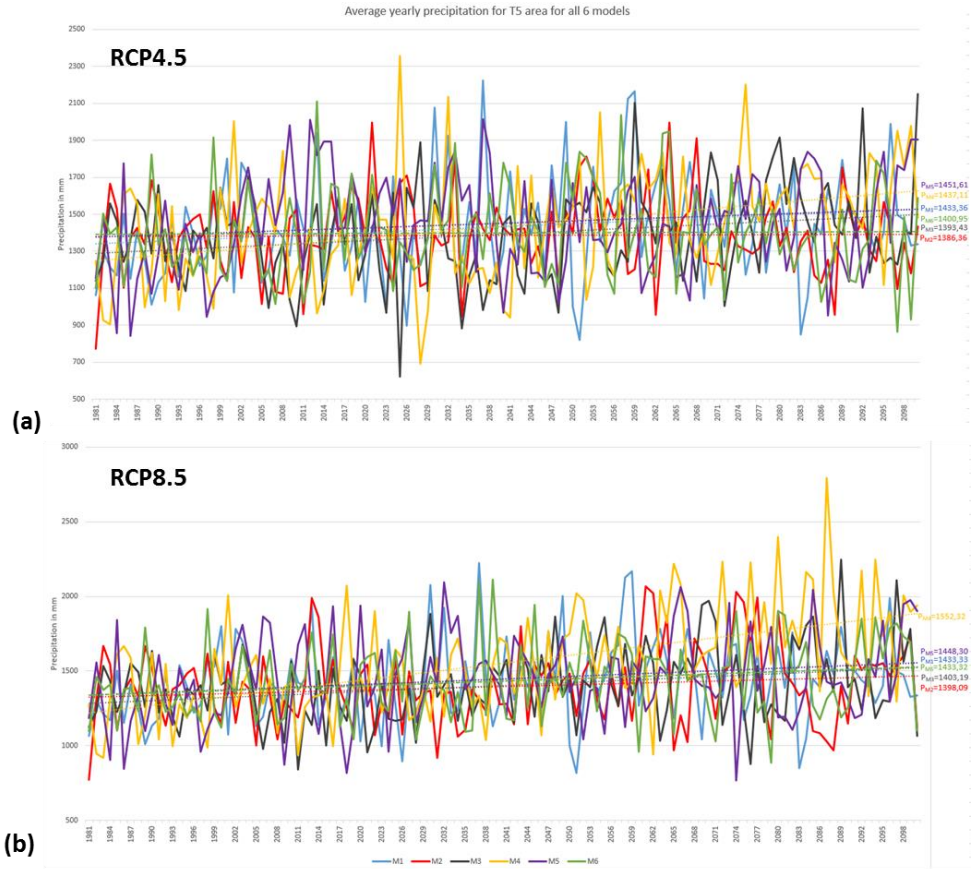

Figure 57: Yearly precipitation for T5 area for all 6 models under RCP4.5 (a) and RCP8.5 (b) scenarios.

Minimum, maximum, range and average values of average yearly precipitation data were calculated and are compared in Figure 58.

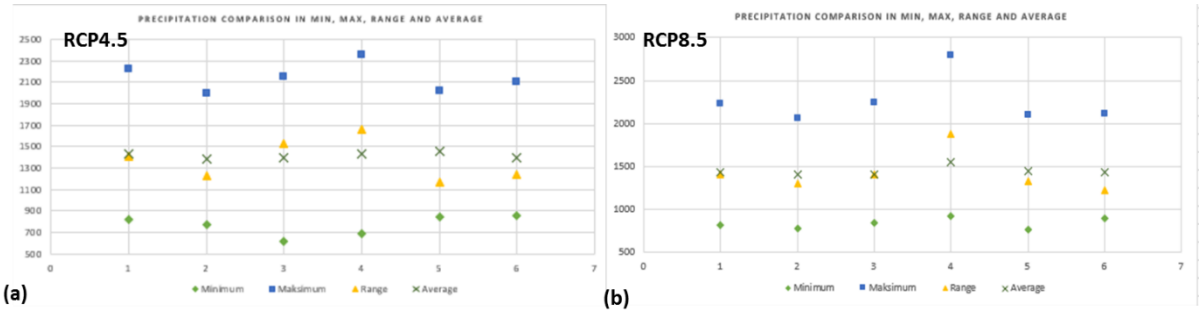

Figure 58: Comparison between average yearly models precipitation (minimum, maximum, range and average) between RCP4.5 (a) and RCP8.5 (b) scenarios.

The following Figures show predicted Rainfall change during Winter, Spring, Summer and Autumn periods for both scenarios and the comparison between them.

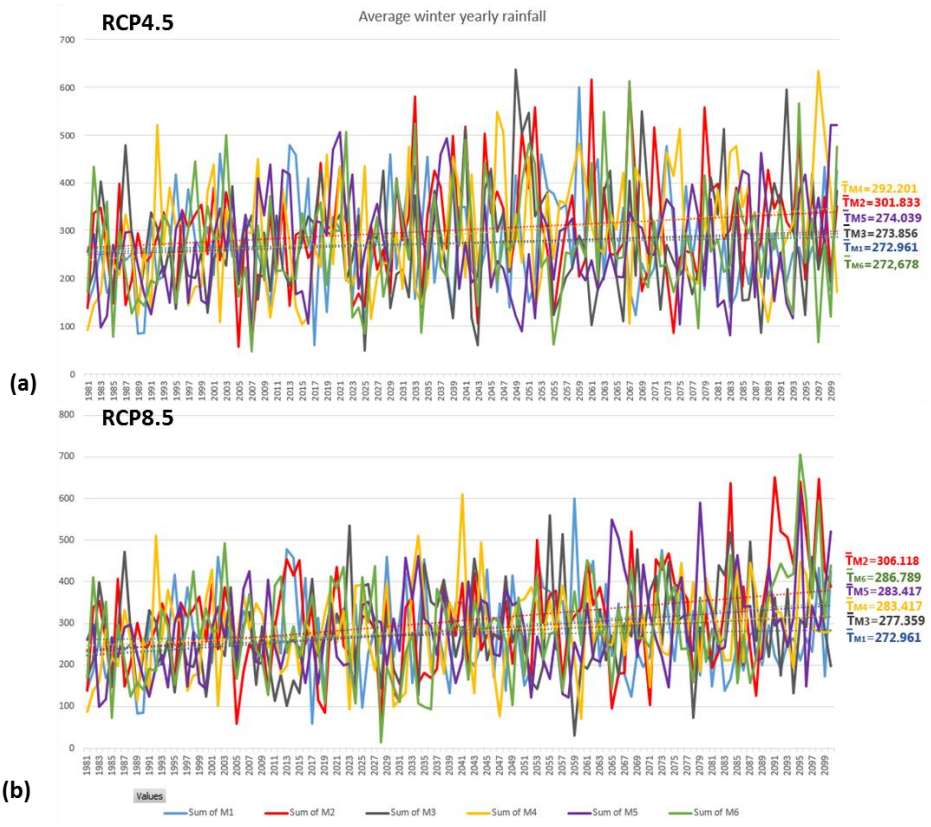

Figure 59: Winter yearly rainfall for RCP4.5 (a) and RCP8.5 (b) scenarios.

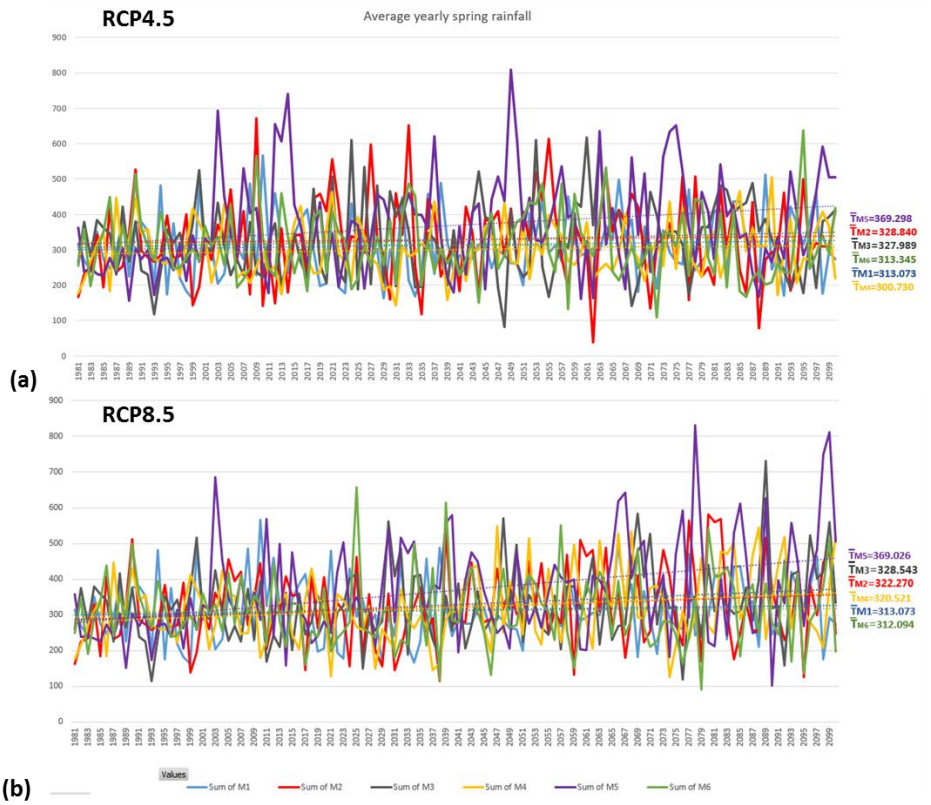

Figure 60: Spring yearly rainfall for RCP4.5 (a) and RCP8.5 (b) scenarios.

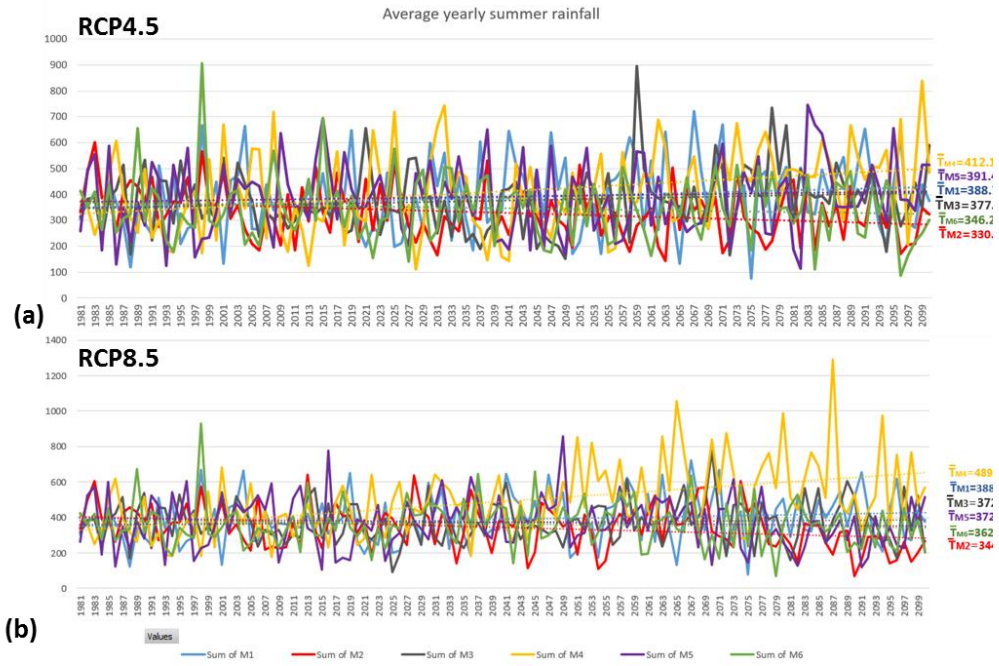

Figure 61: Summer yearly rainfall for RCP4.5 (a) and RCP8.5 (b) scenarios.

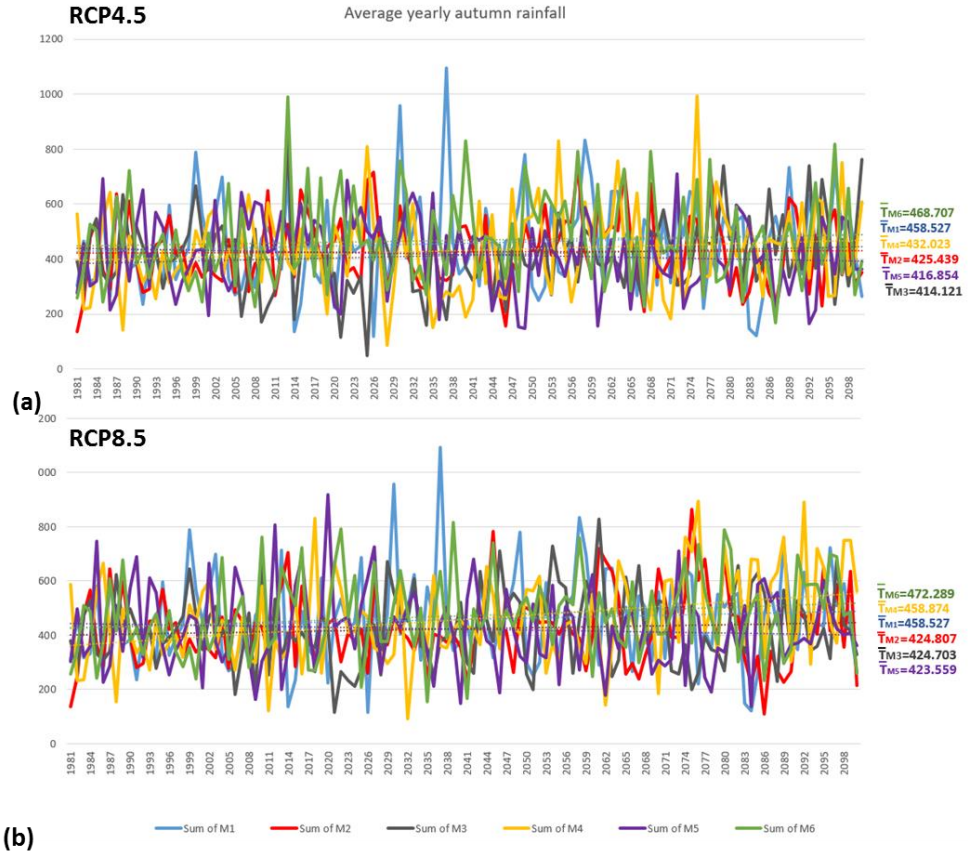

Figure 62: Autumn yearly rainfall for RCP4.5 (a) and RCP8.5 (b) scenarios.

- During Winter period, the calculated average rainfall range is from 273 mm to 292 mm for RCP 4.5 scenario and 273 mm to 306 mm for RCP8.5 scenario

- During Spring period, the calculated average rainfall range is from 301 mm to 370 mm for RCP 4.5 scenario and 312 mm to 369 mm for RCP8.5 scenario
- During Summer period, the calculated average rainfall range is from 330.25 mm to 412.15 mm for RCP 4.5 scenario and 344.90 mm to 489.55 mm for RCP8.5 scenario
- During Autumn period, the calculated average rainfall range is from 414.12.25 mm to 468.71 mm for RCP 4.5 scenario and 423.56 mm to 472.29 mm for RCP8.5 scenario

Finally, as for the Potential Evapotranspiration, data include period from 1981 to 2100, and focus on the spatial grid T5 (*Figure 44;* pilot area location). The used models M1 to M6 (Table 11) indicate the combination of the global and regional model.

The Potential Reference Evapotranspiration was calculated from the model data of maximum and minimum daily air temperature, average daily humidity, short-wave solar radiation and surface wind velocity according to the Penman-Monteith equation. Yearly Potential Evapotranspiration data in the period of 119 years for all six models are shown in Figure 63.

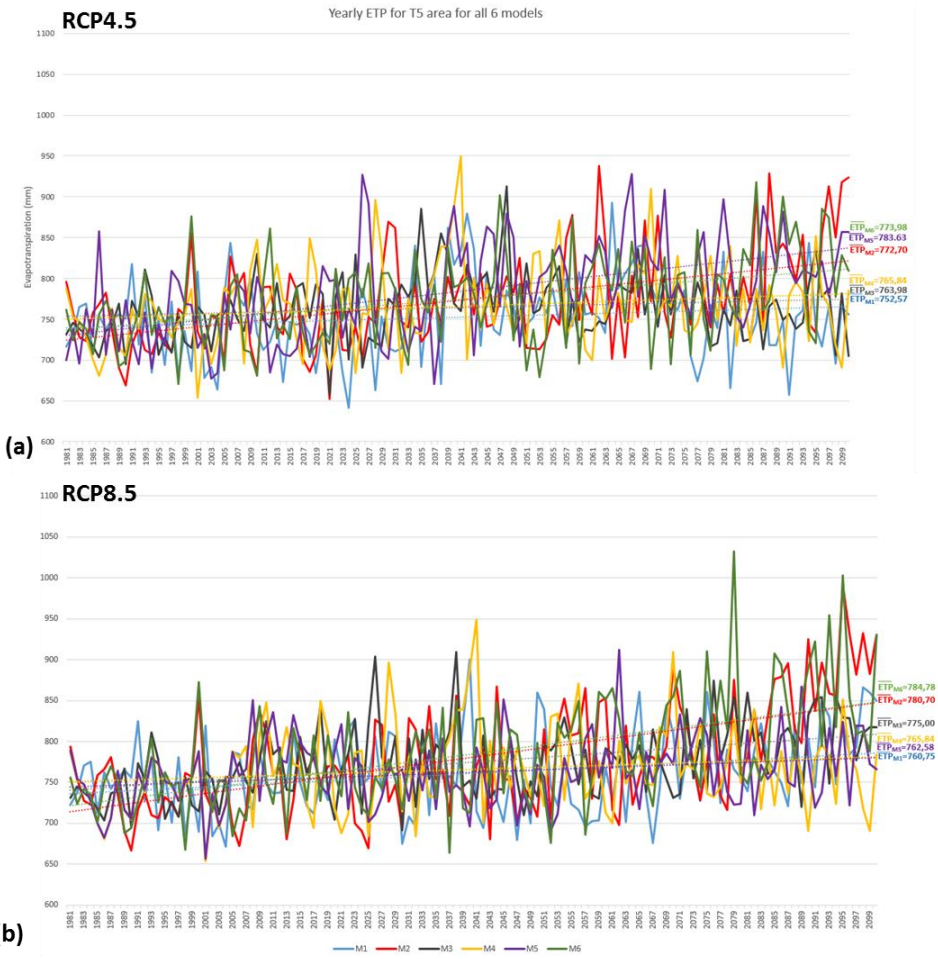

Figure 63: Yearly ETP for T5 area for all 6 models under RCP4.5 (a) and RCP8.5 (b) scenarios.

Minimum, Maximum, range and average values of average yearly Potential Evapotranspiration data for each model were calculated and are compared in Figure 64.

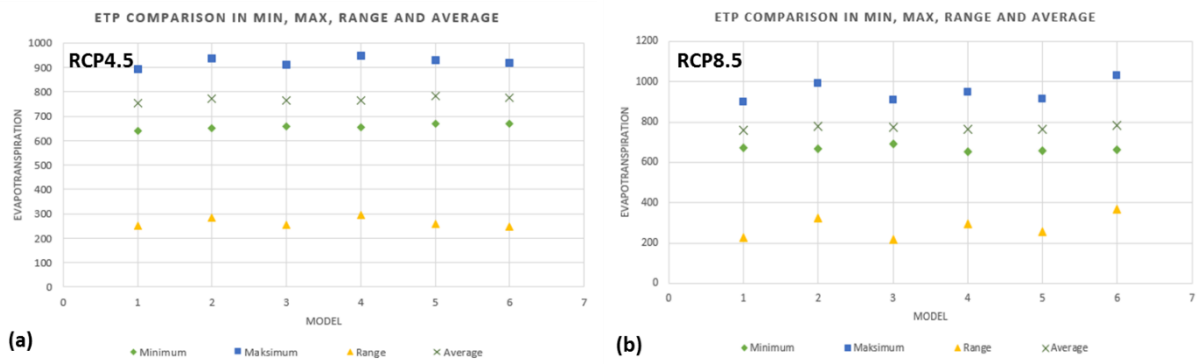

Figure 64: Comparison between average yearly models precipitation (minimum, maximum, range and average) between RCP4.5 (a) and RCP8.5 (b) scenarios.

5.2.3. PROLINE CE development for PA2.1

This section shows the variations in seasonal precipitation (Table 12), seasonal temperature (Table 13) and yearly Rx1day, CDD and CWD (Table 14) for the Pilot Action 2.1: Well field Dravlje valley in Ljubljana, SI. In the following State-Of-The-Art data and PROLINE data are compared considering RCP4.5 and RCP8.5 scenarios. In this sense, Table 12 points out the variations in seasonal precipitation (mm) for both State-Of-The-Art data and PROLINE data; for the former only the median values are reported while for the latter 25th and 75th values are shown.

Table 12: Changes in seasonal precipitation (mm) in PA2.1: comparison between State-of-the-art data (in light red) and PROLINE data (in light green).

		RCP4.5						RCP8.5					
		2021-2050 distribution percentiles			2071-2100 distribution percentiles			2021-2050 distribution percentiles			2071-2100 distribution percentiles		
		50th	25th	75th	50th	25th	75th	50th	25th	75th	50th	25th	75th
Changes in seasonal precipitation (mm)	winter	36.3			24.9			36.9			70.4		
		19.2	14.1	48.3	25.3	-3.6	36.2	40.0	32.1	49.9	60.7	32.6	87.0
	spring	15.7			8.8			50.9			45.2		
		16.4	-13.3	31.9	14.7	-4.6	32.6	25.9	-2.5	43.8	40.1	23.2	58.5
	summer	-8.9			16.2			31.8			17.4		
		-3.2	-13.7	15.2	2.4	-16.6	23.2	10.3	-15.3	36.7	-18.2	-50.2	-0.3
	autumn	12.2			28.6			24.3			52.3		
		-11.2	-33.7	7.1	17.4	-5.7	36.6	16.1	1.7	26.1	-1.3	-19.4	42.6

For RCP4.5, State-Of-The-Art data are higher than PROLINE data with the exception of summer over 2021-2050 period and spring over 2071-2100 period. For RCP8.5, this trend is enhanced.

Such a difference is partially due to the RMCs considered: in both cases, EURO-CORDEX data were adopted but in the State-Of-The-Art only 6 models were considered while in PROLINE project 19 models were used.

Table 13 points out the variations in seasonal temperature (°C) for both State-Of-The-Art data and PROLINE data as for Table 12.

Table 13: Changes in seasonal temperature (°C) in PA2.1: comparison between State-of-the-art data (in light red) and PROLINE data (in light green).

		RCP4.5						RCP8.5					
		2021-2050 distribution percentiles			2071-2100 distribution percentiles			2021-2050 distribution percentiles			2071-2100 distribution percentiles		
		50th	25th	75th	50th	25th	75th	50th	25th	75th	50th	25th	75th
Changes in seasonal temperature (°C)	winter	1.1			2.1			0.9			4.1		
		1.4	1.2	1.8	2.4	2.0	2.9	1.5	1.0	2.0	4.1	3.8	5.0
	spring	0.7			1.5			0.9			3.0		
		1.0	0.7	1.3	2.1	1.5	2.5	1.2	1.0	1.5	3.6	2.8	4.1
	summer	1.1			2.2			1.1			3.9		
		1.3	1.2	1.6	2.1	1.8	2.5	1.4	1.3	1.6	4.1	3.8	5.1
	autumn	1.0			1.8			1.3			3.6		
		1.2	0.9	1.5	2.2	1.7	2.4	1.5	1.1	1.7	3.8	3.4	4.2

Also, in this case, differences between data under different period and scenarios can be observed, but these differences are less pronounced.

Finally, Table 12 reports the yearly variations of Rx1day (mm/day), CDD (-) and CWD (-) indexes. The precipitation pattern of Table 14 can be retrieved also for RX1day, while differences in CDD and CWD are negligible.

Table 14: Changes in yearly Rx1day (mm/day), CDD (-) and CWD (-) in PA2.1: comparison between State-of-the-art data (in light red) and PROLINE data (in light green).

		RCP4.5						RCP8.5					
		2021-2050 distribution percentiles			2071-2100 distribution percentiles			2021-2050 distribution percentiles			2071-2100 distribution percentiles		
		50th	25th	75th	50th	25th	75th	50th	25th	75th	50th	25th	75th
Changes in Rx1day (mm/day)	yearly	4.4			9.3			5.8			17.7		
		3.0	1.1	4.1	6.6	2.7	7.7	4.0	0.6	6.3	11.0	6.4	15.9
Changes in CDD (-)		-0.2			-0.2			0.0			-0.2		
		-0.2	-1.3	1.3	0.5	-2.3	1.0	-0.5	-1.9	0.8	-0.1	-1.8	2.3
Changes in CWD (-)		0.0			-0.2			0.0			-0.2		
		-0.2	-0.9	0.2	-0.2	-0.6	0.1	-0.2	-1.0	0.3	-0.8	-1.3	0.1

5.3. PA2.2 Water reservoir Kozłowa Góra, PL

5.3.1. Foreword

This section is about climate change issues in Pilot Action 2.2: Water reservoir Kozłowa Góra. The pilot action area (Figure 65) represents the Brynica River sub-basin upstream the Kozlowa Gora dam and covers the area of 193.93 km2. The dam reservoir is located at km 28.000 of Brynica River water-course in the area of Silesian voivod-ship (Southern Poland). The reservoir serves mainly to provide water for the population, but as well as a flood protection of the areas located downstream of the dam.

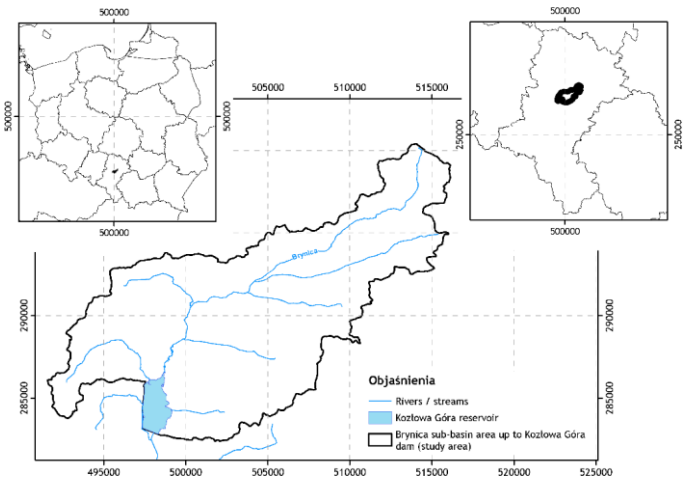

Figure 65: Location of Kozłowa Góra reservoir and Brynica River sub-basin upstream the Kozłowa Góra dam (Pilot Area) on administration map of Poland.

The analysis reported below is based on results of Miejskie Plany Adaptacji (MPA – Cities' Adaptation Plans) project co-funded by EU, leading by Polish Ministry of Environment in co-operation with Institute of Environmental Protection, Institute for Ecology of Industrial Areas, Institute of Meteorology and Water Management and Arcadis. Regarding current period analysis, historical data ranging in-between 1961 - 2015 was considered. These data were collected by Polish Institute of Meteorology and Water Management (IMGW) from meteorological station Świerklaniec, located 1.5 km southern west from PA catchment. Analysis of CC data is concerned perspective of 2030 (as average of period 2026-2035) and 2050 (avg. of 2046-2055) for the location of Bytom. The dataset is a result of Development of Urban Adaptation Plans for cities with more than 100,000 inhabitants in Poland were the CC analysis was one of the main objects. In this sense, for CC application, EURO-CORDEX data at 12.5 km of resolution are adopted under the RCP4.5 and RCP8.5 scenarios. Climate data were calibrated with observed ones provided by the nearest IMGW station. The following procedure was implemented:

- for each variable, observation vectors of daily average from period 2006 – 2015 (based on IMGW) data were created;
- for each EURO-CORDEX model, scenario, variable evaluation of comparability of results corrected with observations data (IMGW) was performed;
- for each EURO-CORDEX model, scenario, variable value vectors of an daily average (from period 2006 – 2055) were created;
- each scenario was downscaled using R (with functions from QMAP package) to minimize the systematic error (bias-correction);

- for each scenario and variable, beam analysis based on corrected values were carried out;
- for each EURO-CORDEX model and scenario, climate index set was calculated;
- based on corrected data, climate projections for 3-time horizons as an average from 10 years periods (2010: 2006-2015, 2020: 2026-2035, 2050: 2046-2055) was calculated;
- for each scenario, average values of indexes were calculated.

5.3.2. Previous state-of-the-art framework

5.3.2.1. Current climate

The climatic conditions of the Kozłowa Góra reservoir region were assessed on the base of the daily values of air temperature and precipitation obtained from the Świerklaniec station. The meteorological data include the period from 1961 to the February of 2015 (approximately 55 years) and have been made available by the Institute of Meteorology and Water Management - National Research Institute (IMGW PIB).

Regarding temperature characterization, the mean annual air temperature in the area of the Kozłowa Góra reservoir was 7.9°C and varied in individual years between 9.9°C (2014) and 6.3°C (1996). Half of all the values of the mean annual air temperature fits between 7.3°C (lower quartile) and 8.6°C (upper quartile). As in the entire Europe, summer is the warmest season with a mean temperature reaching +17.1°C. In autumn and spring, the air temperature difference is slight (8.2°C and +7.9°C, respectively) and decreases below zero only in winter (-1.4°C). In the winter, the range of air temperature variability in the period in concern was higher than in any other season. During the warmest winter (2006/07), the mean temperature reached up to +2.4°C, while in the coldest winter season, it dropped below -7.9°C (1962). In case of the remaining seasons, the variability range of the mean air temperature did not exceed 5°C. Within a year, the highest air temperature is exhibited by July (17.9°C) while the lowest is in January (-2.3°C). The lowest mean temperature of January, -10.7°C, was noted in 1987, while the highest temperature of July, namely 21.5°C occurred in 2006. More descriptive statistics for mean monthly, seasonal and annual air temperatures are included in Table 15.

Besides the mean and extreme values, the basic characteristics of the thermal conditions include also the frequency of occurrence of thermally characteristic days. Usually, such days are determined based on the maximum and minimum temperatures during the day (daily maximum and minimum air temperatures). Due to lack of such data, however, the mean daily air temperature was analysed (T_{mean}): >0°C, <0°C, ≤-10°C, ≥20°C and ≥25°C. Days with positive air temperature occur during the entire year. From May to September, the mean daily air temperature never decreased below 0°C in the period in concern. Even in the winter months, about 12-14 days with positive temperatures are noted. Relatively frosty days during which the mean daily air temperature falls below -10°C, occur from November till March, while only one such day has been noted in November in the entire studied period; In January, such days occur not more often that 2-3 times in a month. The most – 19 such days occurred in the January of 1963. Also, the February of 2013 was very frosty, when days with T_{mean} < -10°C were noted 13 times. Very warm days in which the mean temperature of air exceeds 20°C occur from May to September in Świerklaniec with a

maximum in July, that is, 9 days. The warmest months in the multiyear period were the June of 2006 (24 days with T_{mean} >20°C) and August of 1992 (18 days with T_{mean}>20°C). In Świerklaniec, very warm days with temperature over 25°C are extremely rate and only occur in summer months. Their highest frequency (4 days) was noted in the August of 1992.

Table 15: Descriptive statistics for mean monthly, seasonal and annual air temperatures for Świerklaniec 1961-2015.

	SS (±BS)	OS	Md	Max year	Min year	Amp	KwD	KwG	5p	95p
I	-2.3 (±0.4)	3.2	-1.8	2.8	-10.7	13.5	-4.8	-0.2	-8.8	2.7
II	-1.1 (±0.4)	3.1	-1.2	4.6	-8.2	12.8	-3.1	1.2	-7.3	3.5
III	+2.6 (±0.3)	2.4	+3.1	6.4	-2.7	9.2	0.8	4.4	-2.0	5.8
IV	+8.0 (±0.2)	1.6	+7.9	11.3	4.5	6.9	7.1	9.2	5.3	11.1
V	+13.1 (±0.2)	1.5	+13.4	16.4	9.7	6.8	12.1	14.0	10.3	15.2
VI	+16.2 (±0.2)	1.2	+16.2	18.5	13.7	4.8	15.5	17.0	14.1	18.4
VII	+17.9 (±0.2)	1.5	+17.9	21.5	15.0	6.5	16.8	19.1	15.6	20.3
VIII	+17.2 (±0.2)	1.2	+17.3	21.2	14.6	6.6	16.5	18.0	15.3	18.8
IX	+12.9 (±0.2)	1.4	+12.9	15.8	9.7	6.1	11.7	14.1	10.7	15.5
X	+8.3 (±0.2)	1.6	+8.3	12.2	4.7	7.5	7.5	9.2	5.5	11.2
XI	+3.4 (±0.3)	1.9	+3.8	7.1	-0.7	7.8	2.1	5.0	-0.3	6.3
XII	-0.8 (±0.3)	2.4	-0.5	2.9	-7.0	9.9	-2.2	0.9	-5.2	2.7
R	+7.9 (±0.2)	1.3	+8.0	9.9	6.3	3.6	7.3	8.6	6.5	9.2
W	+7.9 (±0.2)	1.2	+8.0	10.1	5.3	4.9	7.3	8.7	5.8	9.7
L	+17.1 (±0.1)	0.9	+17.2	19.7	15.3	4.5	16.5	17.8	15.5	18.5
J	+8.2 (±0.1)	1.0	+8.5	10.4	6.7	3.7	7.4	8.8	6.8	10.0
Z	-1.4 (±0.3)	2.2	-0.5	2.4	-7.9	10.3	-2.9	0.2	-5.3	1.7

R - year, W - spring, L - summer, J - autumn, Z - winter; SS - mean value, BS - standard error, OS - standard deviation, Md - median, Max - maximal precipitation, Min - minimal precipitation, Rok - year of occurrence, Amp - amplitude, KwD - lower quartile, KwG - upper quartile, 5p - fifth percentile, 95p - ninety fifth percentile.

It is also worth to discuss the highest daily air temperatures noted in subsequent months. The highest daily air temperature occurred not in July, which – in the Kozłowa Góra reservoir area – is one of the warmest months, but in June. The air temperature was 28.2°C. In addition, the highest temperatures in winter months are surprising – with the exception of January, the temperatures

exceeded 10°C. The lowest daily temperature occurred in January. In the coldest years, the temperature in summer months did not exceed 10°C (Table 16).

Table 16: The highest and the lowest daily air temperature and the number of days with selected air temperature threshold values.

	Max	Min	T>0°C	T<0°C	T<-10°C	T>20°C	T>25°C
I	9.8	-24.7	11.9	18.8	2.9	-	-
II	12.2	-21.1	13.2	14.9	1.6	-	-
III	14.9	-15.7	22.7	7.8	0.3	-	-
IV	21.1	-2.6	29.3	0.6	-	0	-
V	24.3	0.6	31.0	-	-	1.0	-
VI	28.2	4.6	30.0	-	-	4.6	0.2
VII	27.1	10	31.0	-	-	8.6	0.4
VIII	27.6	8.5	31.0	-	-	6.1	0.3
IX	22.6	2.6	30.0	-	-	0.3	-
X	18.7	-2.6	30.4	0.6	-	-	-
XI	15.6	-11.8	23.2	6.4	0	-	-
XII	12.5	-20.1	14.6	15.7	1.8	-	-

0 – frequency lower than 0.1; "-"- phenomenon absent

In terms of precipitation, annually, 719 mm of precipitation is noted in the area of the Kozłowa Góra reservoir. The highest annual sum of precipitation, exceeding as much as 1024 was noted in 2010; the lowest sum of less than 500 mm occurred in 1982, which results in a wide range of variability amounting to 524 mm. Precipitation in the warm half of the year, reaching a mean amount of 450.7 mm, constitute approximately 63% precipitation of the cold half of the year, amounting on average to 268.7 mm. The amount of precipitation in the warm half of the year may however vary in a wide range from 727.8 mm to 269.4 mm. The range of variability in case of the cold half of the year was significantly smaller – from 391.2 mm to 155.8 mm (Table 16).

In the studied multiyear period, in extreme cases the precipitation of the warm half of year constituted 133% (1982) and 32% (2002) of the cold half precipitation. In the Kozłowa Góra reservoir area, as in the remaining part of the country, the highest seasonal precipitation is noted in summer, while the lowest occurs in winter. Three years may be considered exceptional: 1976, 1982 and 2003, when more precipitation water reached the ground surface during winter than in summer. The mean precipitation in case of the transitional seasons indicate that spring is slightly more humid than autumn, which is the demonstration of continental features in the seasonal distribution of precipitation. In individual years, however, it was relatively often (22 times in 55 years)

that the precipitation in autumn exceeded the precipitation in spring, which, in turn, indicates a greater relevance of ocean dynamics. More descriptive statistics for annual precipitation sums, hydrological year sums, precipitation in halves of years and seasonal precipitation are presented in Table 17.

Table 17: Descriptive statistics of total atmospheric precipitation for Świerklaniec (1961-2015).

	R	RH	PC	PCh	PC%	W	L	J	Z
SS (±BS)	718.8	719.0	450.7	268.7	63.2	172.4	263.3	156.0	127.0
Wz	16.0	15.4	22.8	20.6	33.9	31.3	26.0	30.1	27.2
OS	115.2	110.7	102.6	55.3	21.4	53.9	68.5	46.9	34.5
Md	695.0	700.6	435.4	270.3	63.3	164.6	252.3	153.3	126.8
Max	1024.4	998.5	727.8	391.2	132.8	344.0	386.3	261.1	201.5
Rok	2010	2009/10	2010	1991	1982	2010	1961	1974	2005
Min	499.9	530.3	269.4	155.8	31.4	90.8	151.5	65.8	55.9
Rok	1982	1975/76	1982	1983	2002	1964	1983	2011	1977
Zz	524.5	468.2	458.5	235.4	101.4	253.2	234.8	195.3	145.6
KwD	648.7	640.2	375.5	230.3	47.9	131.9	198.8	116.2	100.1
KwG	790.5	799.5	514.0	294.7	73.9	191.1	315.6	191.7	147.7
5p	558.7	553.8	317.8	186.5	32.0	112.6	163.3	84.9	70.6
95p	942.2	934.5	675.8	360.6	111.4	283.2	384.2	241.4	193.7

R – year, RH – hydrological year, PC – warm half of the year (V-X), PCh – cold half of the year (XI-IV), PC% - precipitation in warm half of year as % of the cold half, W—spring, L – summer, J – autumn, Z - winter

SS – mean value, BS – standard error, WZ – variability factor, OS – standard deviation, Md – median, Max – maximal precipitation, Min – minimal precipitation, Rok - year of occurrence, Zz – variation range, KwD - lower quartile, KwG - upper quartile, 5p - fifth percentile, 96 - ninety fifth percentile

In the area of the Kozłowa Góra reservoir, the mean monthly total precipitation varied from 35.4 mm in February to 100.1 mm in July. The highest monthly sum of precipitation in the period in concern, however, was noted not in July, but in May of 2010 – 269.1 mm, when the high precipitation in the second half of the month led to the flood which covered the Central Europe. The highest noted sum of precipitation in July was lower by 19 mm (249.9 in 2000) than the sum of May 2010. From October to April, the monthly sums of precipitation were stable at the level of approximately 45-50 mm; between the April and May, the precipitation was clearly increasing – the sum in May was twice the precipitation of April. The decrease of precipitation in the autumn period was gradual – from month to month (Figure 66).

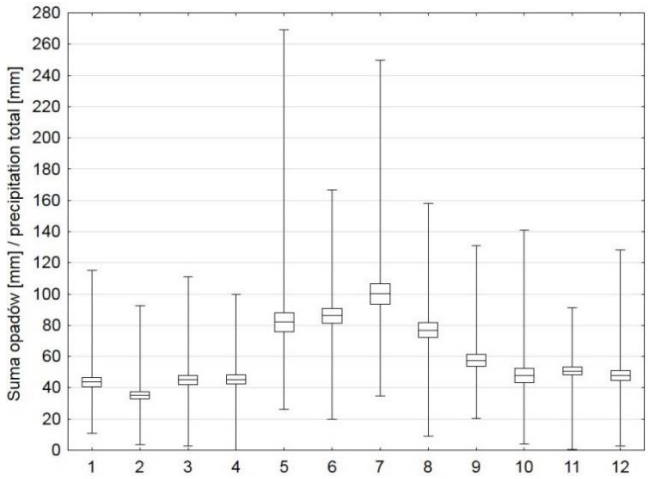

Figure 66: Annual course of precipitation: mean (line), standard error of the mean (box), max-min (whiskers).

The charts of the cumulated frequency and probability of daily precipitations indicate that approximately up to 50% of the daily precipitations in the area of the Kozłowa Góra reservoir fit in between 0-2.5 mm; precipitations ≤5mm constitute 80% of all daily precipitations while approximately 90% of precipitations do not exceed the value of 10 mm. Thus, precipitations higher than 10 mm constitute 10% of all daily sums of precipitations that have occurred in Świerklaniec in the period in concern (Figure 67). Both the frequency and the probability of precipitations was calculated based on the daily precipitation >0mm.

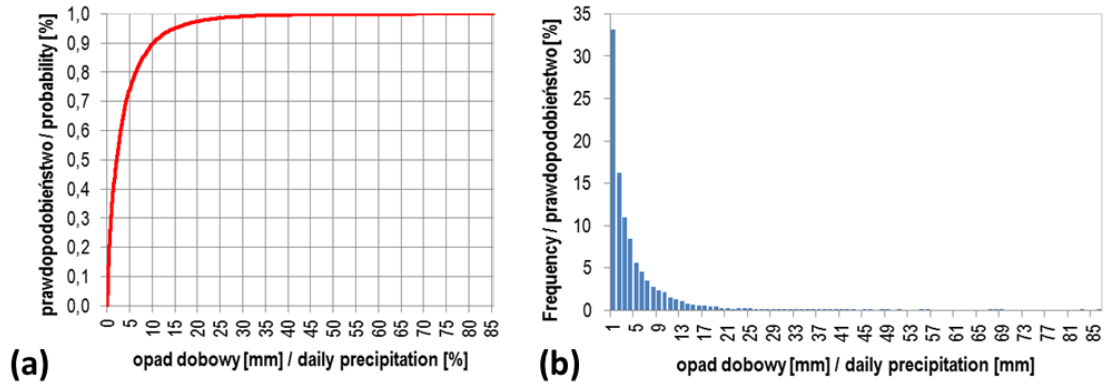

Figure 67: Cumulated probability of daily total precipitation (a) and the distribution of frequencies of daily total precipitation (b), Świerklaniec 1961-2015.

Sums of precipitation were characterized with a distinct annual cycle with a maximum in the summer period and the minimum in winter. The annual course of frequency of precipitation ≥0.1 is different. In summer, the number of days with precipitation ≥0.1 (approximately 41 days) is

smaller than in winter period (~50 days), which indicates a much higher intensity of summer precipitation. Precipitation is the least common in autumn (~41 days). One should note, however, that variability in the number of days with precipitation in the annual course is small - around days (Figure 68).

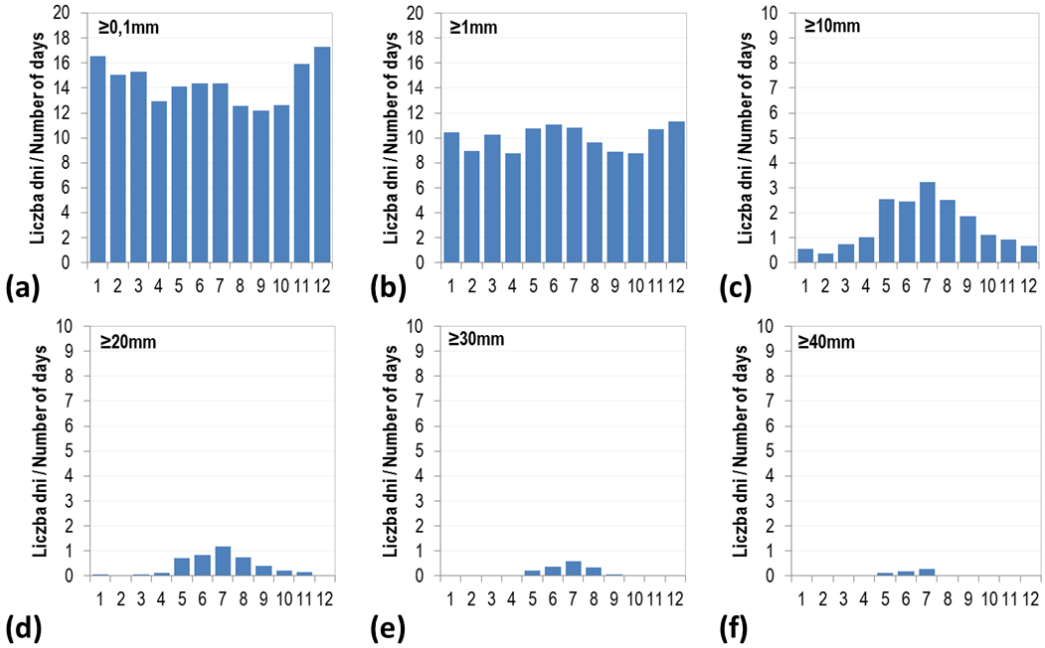

Figure 68: (a-b-c) Annual course of days with precipitation (≥0.1mm) and (d-e-f) days with specified threshold values of precipitation.

Wet days, defined as days with ≥1mm precipitation occur approximately 9-11 days in a month. Their variability in the annual course is even smaller than in case of the days with ≥0.1 mm precipitation. Most often, they occur between May and July and in December. Days with precipitation exceeding 10 mm are considered as days with high precipitation. Their annual course, as in the case of the precipitation exceeding higher threshold values, relates to the annual cycle of total precipitation. Mean number of days with precipitation ≥10 mm reaches the maximum in July, that is, 3 days. In the period from May till August, precipitations of that magnitude are noted twice a month on average, while in remaining months it occurs rarely - once a few years. In the period in concern, the ≥20 mm precipitation occurred in nearly all months with the exception of February. Their frequency reached the maximum – 5 days - in May 2010 and in July 2000. Daily precipitation ≥30 mm occurred only between May and November, while in the period between September and November – in the studied multiyear period – only 5 such days occurred. Precipitation ≥40 mm occurred 34 times in the period in concern, while precipitation ≥50 mm were noted 9 times.

5.3.2.2. Future climate

In this section, analysis of the results of MPA project, using EURO-CORDEX data, was conducted. The analysis is based on data from Bytom city, one of the subjects of the project, located nearby PA Kozłowa Góra.

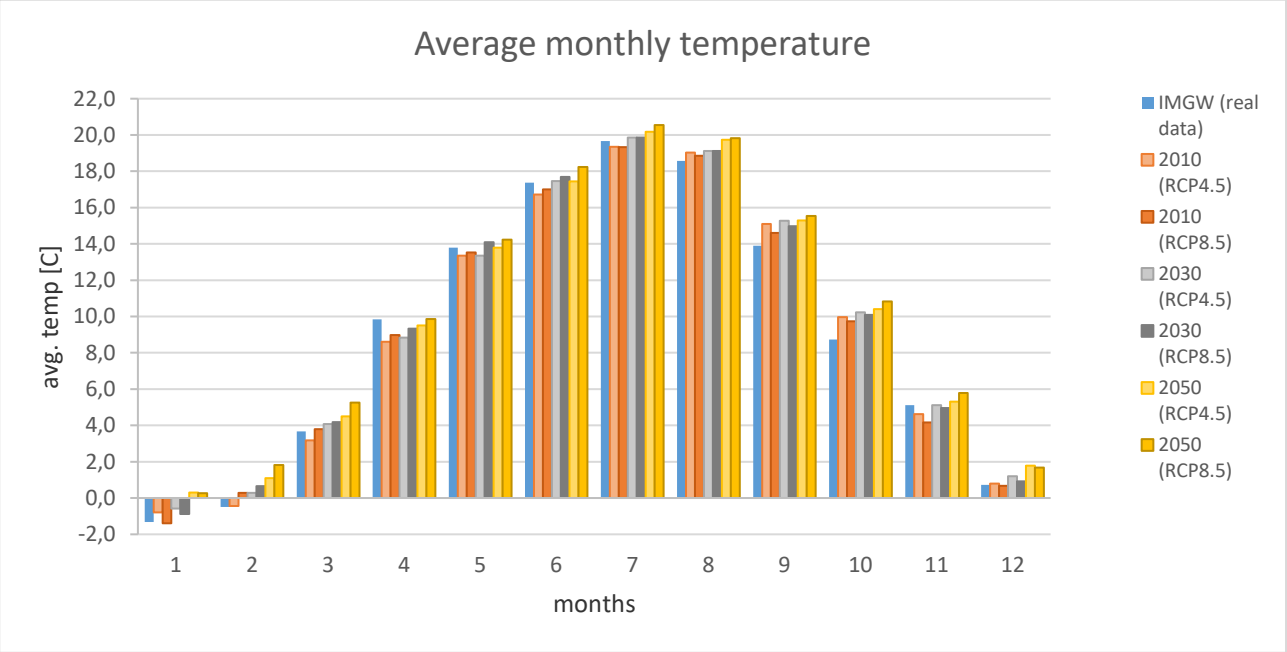

Figure 69: Average monthly temperature under RCP4.5 and RCP8.5 scenarios.

Figure 69 shows the average monthly temperature for different time horizons under RCP4.5 and RCP8.5; it reports also observed data (IMGW real data). On average, a slight increase in temperature is detectable moving from near to far long-time horizon and from RCP4.5 to RCP8.5.

5.3.2.3. PROLINE CE development for PA2.2

This section shows the variations in seasonal precipitation (Table 18), seasonal temperature (Table 19) and yearly Rx1day, CDD and CWD (Table 22) for the Pilot Action 2.2: Water reservoir Kozłowa Góra, PL. The variations are obtained considering only the EURO-CORDEX data (§4.2).

Table 18: Changes in seasonal precipitation (mm) in PA2.2 with EURO-CORDEX projections.

		RCP4.5						RCP8.5					
		2021-2050 distribution percentiles			2071-2100 distribution percentiles			2021-2050 distribution percentiles			2071-2100 distribution percentiles		
		50th	25th	75th	50th	25th	75th	50th	25th	75th	50th	25th	75th
Changes in seasonal precipitation (mm)	winter	3.1	0.5	2.6	3.2	4.6	1.4						
	spring	-2.8	-1.7	-2.2	-6.5	-0.1	-2.3						
	summer	7.7	4.1	5.6	1.8	-1.5	3.1						
	autumn	2.2	4.7	4.1	8.4	7.6	8.2						

Table 19: Changes in seasonal temperature (°C) in PA2.2 with EURO-CORDEX projections.

		RCP4.5						RCP8.5					
		2021-2050 distribution percentiles			2071-2100 distribution percentiles			2021-2050 distribution percentiles			2071-2100 distribution percentiles		
		50th	25th	75th	50th	25th	75th	50th	25th	75th	50th	25th	75th
Changes in seasonal temperature (°C)	winter	**0.7**	0.5	0.6	**1.1**	0.5	0.6	**1.5**	1.3	1.3	**1.5**	1.3	1.3
	spring	**0.2**	0.6	0.1	**0.7**	0.9	0.7	**0.9**	1.1	0.7	**0.9**	1.2	0.8
	summer	**0.1**	0.4	0.3	**0.1**	0.5	0.3	**0.7**	0.7	0.8	**1.0**	1.1	1.1
	autumn	**0.3**	0.4	0.2	**0.1**	0.2	0.0	**0.4**	0.6	0.3	**1.1**	1.4	1.0

EURO-CORDEX data projects a slight increase in seasonal precipitation with exception of spring during which a decrease can be detectable. In terms of seasonal temperature, the variations compared to the current period are negligible in line with those reported in Figure 69.

5.4. PA2.3 Tisza catchment area, HU1

5.4.1. Foreword

This section is about climate change issues in Pilot Action 2.3: Tisza Catchment area. Specifically, the pilot area is located along the Tisza River and lies on the North- and Middle Hungarian Great Plain. It includes Lake Tisza and Keleti Main Channel. The total surface of the pilot area is 7614 km2, of which is 5% covered by drinking water protection areas, and from that is 3% groundwater protection area. In the following, climate reports provided by the Hungarian Meteorological Service (OMSZ)[3] are presented. For climate change predictions, published data from OMSZ and Eötvös Loránd University (ELU) in the framework of the international project CECILIA are reported.

For numerical weather prediction (NWP), OMSZ considers ALADIN and AROME models from the ALADIN project, for past climate change modelling ALADIN and REMO models. Model results made by OMSZ (or any other Hungarian institution), for future climate change in Hungary, in their full extent are unavailable. In CECILIA (Central and Eastern Europe Climate Change Impact and Vulnerability Assessment) project ALADIN and RegCM simulations were used to predict climate change for mid-century (2021-2050) and end-of-century (2071-2100).

5.4.2. Previous state-of-the-art framework

5.4.2.1. Current climate

The general climate characteristics of the pilot area is presented in this section. For this task, open source data provided by the Hungarian Meteorological Service (OMSZ) were considered.

Figure 700 shows the climatic regions of Hungary. Due to their scale and resolution, OMSZ cannot use the global climate classifications such as Köppen or Trewartha to classify the different climate regions of Hungary, so they were using the work of Hungarian climatologists György Péczely who separated 12 climatic zones in Hungary taking into account

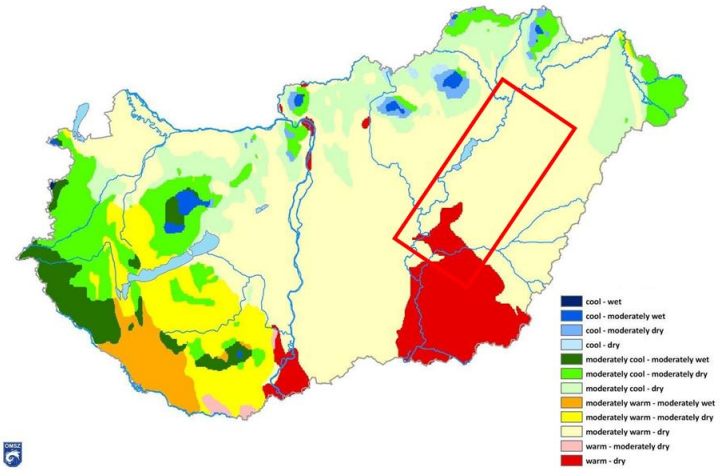

Figure 700: The climatic regions in Hungary (from Hungarian Meteorological Service [OMSZ], after György Péczely; www.met.hu).

[3] Open source datasets (for Hungary, without the possibility of downscaling) on mean temperature, maximum temperature, minimum temperature, precipitation and sunshine duration are available on www.met.hu for the 1901-2000 period. Model results for future climate change in their full extent are unavailable.

the aridity index and the growing season length. According to his classification, the majority of the country has a moderately warm, dry climate. The greater part of the pilot area lies in such climatic zone, its southern part has warm-dry climate. In case of need for further general characterisation or CC model validation, we possess a dataset provided by OMSZ and Szolnok Waterworks on local daily temperatures and daily precipitation amount for the 1981-2010 period.

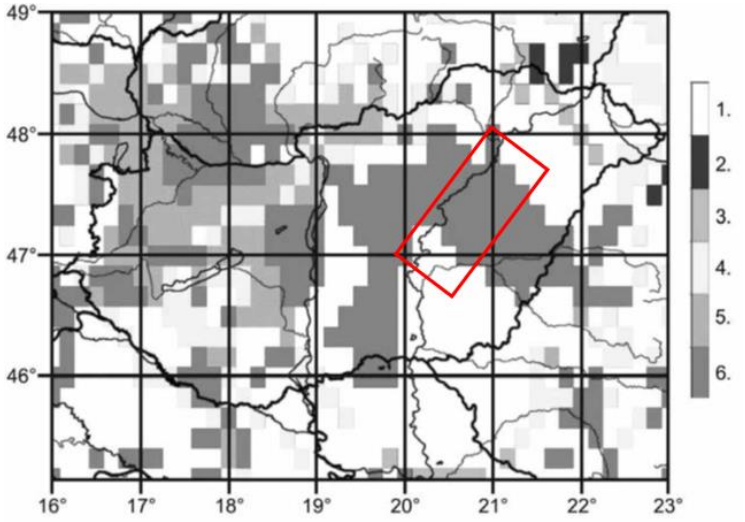

Figure 71. The change of climate in Hungary between the beginning (time period 1901-1930) and the end (time period 1971–2000) of the twentieth century according to the original method of Péczely, Gy. – 1 – no change; 2 – temperature decrease; 3 – precipitation increase; 4 – precipitation decrease; 5 – temperature increase, and precipitation decrease; 6 – temperature increase (SKARBIT et al., 2014).

Based on Péczely's work Skarbit et al. (2014) wrote a characterization of Hungary's climate for the twentieth century. In their paper they present a climate change map (Figure 3) for Hungary using climatic characteristics from time period 1901-1930 and time period 1971-2000 identified with the original method of György Péczely in Péczely (1979). According to Figure , the main process in climate change on the majority of the pilot area is temperature increase. That means that the moderately warm and dry climate became warm without any significant increase in precipitation.

5.4.2.2. Future climate

In this section, published data from OMSZ and ELU in the framework of the international project CECILIA are reported. Specifically, the already existing results by OMSZ experiments, carried out by using ALADIN and REMO simulations, are reported in Table 20. This Table shows mean annual and seasonal temperature changes in Hungary for the mid-century (2021-2051) and end-of-century (2071-2100) periods. Comparison was made using the 1961-1990 reference period. Data is from regional climate model experiments with ALADIN-Climate and REMO made by OMSZ. These models are predicting a continuous temperature increase in the Carpathian Basin, however, the increase is not constant, and it is the most intense in summer season.

Table 20: Changes in the projected mean annual and seasonal temperature (°C) for Hungary compared with the mean from the period of 1961–1990 based on the REMO and ALADIN model experiments. (SZABÓ et al., 2010).

period	year	spring	summer	autumn	winter
2021-2050	(+1.4)-(+1.9)	(+1.1)-(+1.6)	(+1.4)-(+2.6)	(+1.6)-(+2.0)	+1.3
2071-2100	(+3.5)	(+2.3)-(+3.1)	(+4.1)-(+4.9)	(+3.6)-(+3.8)	(+2.5)-(+3.9)

Moreover, Table 21 shows changes in mean annual and seasonal precipitation predicted for Hungary for the mid-century (2021-2050) and the end-of-century (2071-2100) periods. Comparison was made using the 1961-1990 reference period. Data is from regional climate model experiments with ALADIN-Climate and REMO made by OMSZ. The simulated changes in annual precipitation is not significant, however, the distribution of precipitation is likely to change more significantly. The decreasing summer and increasing winter precipitation would result an overall more homogenous distribution of the precipitation within a year (Szabó et al., 2010; Blanka et al., 2013).

Table 21: Changes in the projected mean annual and seasonal precipitation (%) for Hungary compared with the mean from the period of 1961-1990 based on the REMO and ALADIN model experiments. (SZABÓ et al., 2010).

period	year	spring	summer	autumn	winter
2021-2050	(-1)- 0	(-7)-(+3)	-5	(+ 3)-(+14)	(-10)-(+7)
2071-2100	(-5)-(+3)	(-2)-(+2)	(-26)-(-20)	(+10)-(+19)	(-3)-(+31)

Temperature and precipitation change values are interpolated and mean values and representing a situation for the country not for the pilot area.

Regarding ELU results, climate change predictions considering as reference period 1961-1990 are presented. In this perspective, Figure 71 and Figure 72 show the seasonal temperature changes. As it was for the experiments made by OMSZ the target region was also the Carpathian Basin, but the experiment has a good (10 km) horizontal resolution which allows us to draw a conclusion for the pilot area. This experiment was made by ELU using ECHAM5-driven RegCM datasets (CECILIA, Periodic activity report, 2010).

As a conclusion of the experiments made by ELU, it is evident that warming is expected in all subregions of Hungary, “the spatially averaged seasonal changes for the Hungarian grid points are projected as follows: +1.1°C in winter, +1.6°C in spring, +0.7°C in summer, and +0.8°C in autumn by 2021-2050, and +2.9°C in winter, +2.8°C in spring, +3.5 °C in summer and +3.0 °C in autumn by 2071-2100 (relative to the 1961-1990 reference period)” (CECILIA, Periodic activity report, 2010).

Seasonal changes in precipitation in the simulated climate are far more variable spatially than seasonal changes in temperature. Drier climate is projected for Hungary for the 2021-2050 period,

especially, in the eastern, and southern part of the country. For the pilot area in the near future winter and spring are expected to become drier roughly by 15-25%, and by 10-15%, respectively. Summer and autumn are expected to become wetter by 10-20%, and by 5-10%, respectively. In the second half of the century winter is expected to become wetter by 15-25%, spring will become drier by 5-10% (which means decreasing aridification processes), for summer drier climate is projected by 5-10%, and the autumn is expected to become wetter by 10-15%.

For the seasonal precipitation changes see Figure 73 and Figure 74.

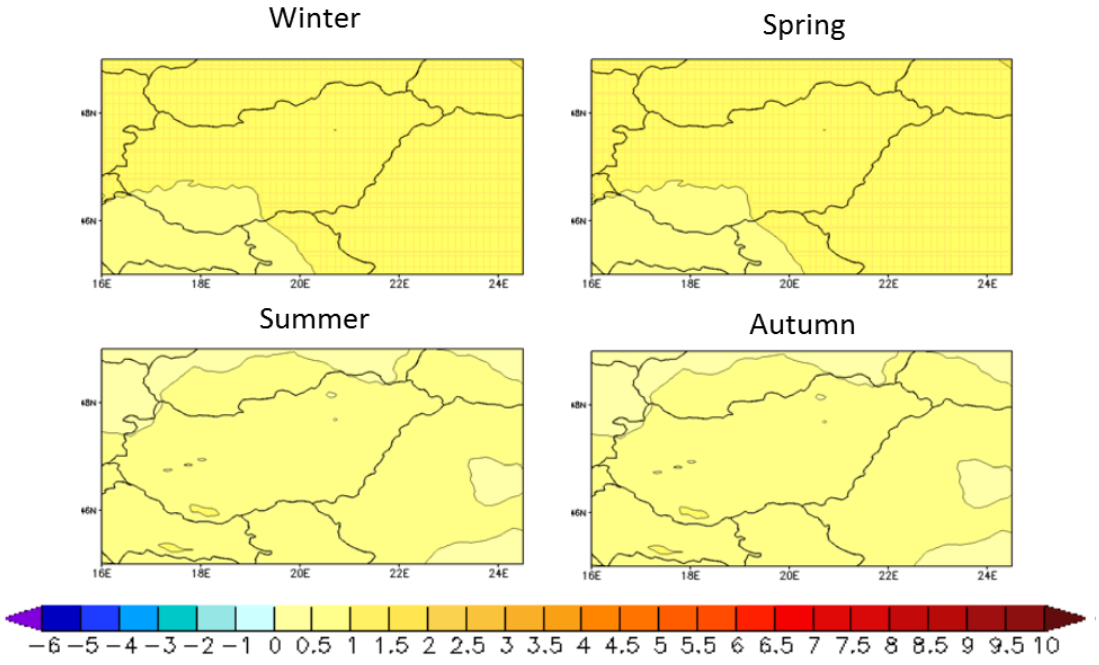

Figure 71: Simulated seasonal temperature change for the Carpathian basin for the period 2021-2050 (reference period: 1961-1990) (after experiments of ELU in CECILIA, Periodic activity report, 2010).

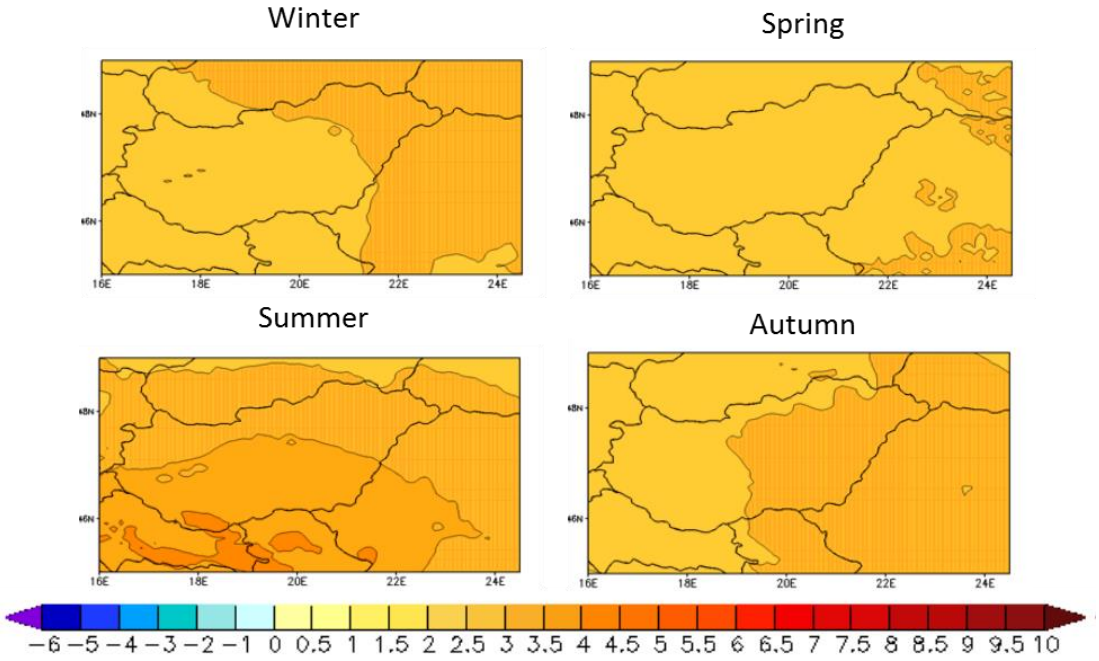

Figure 72: Simulated seasonal temperature change for the Carpathian basin for the period 2071-2100 (reference period: 1961-1990) (after experiments of ELU in CECILIA, Periodic activity report, 2010).

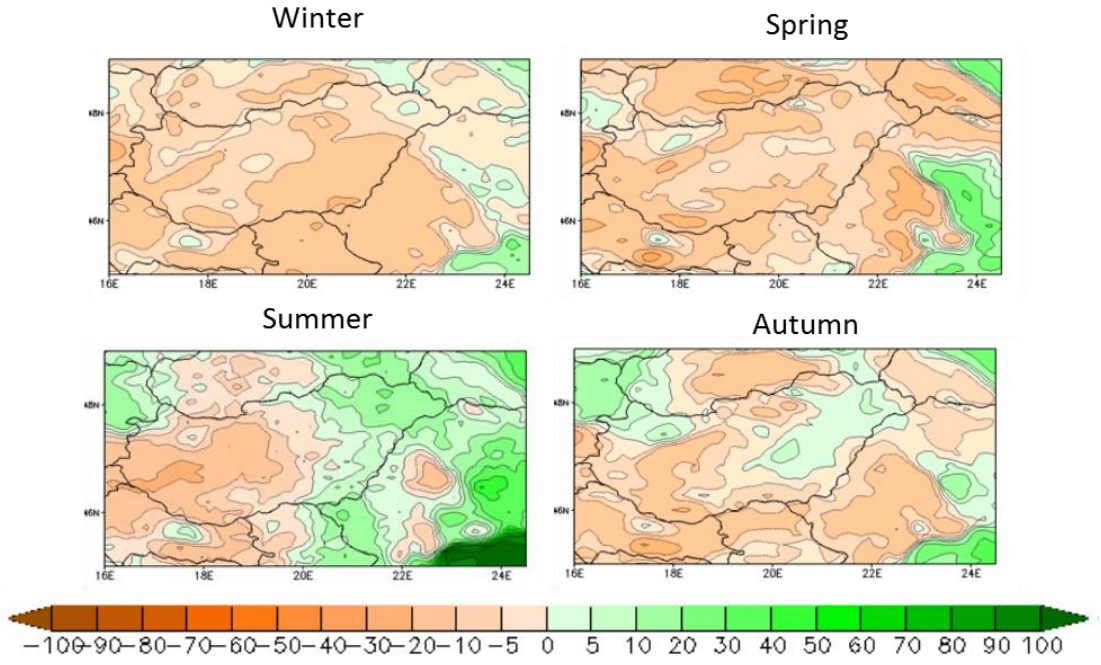

Figure 73: Simulated seasonal precipitation change for the Carpathian basin for the period 2021-2050 (reference period: 1961-1990) (after experiments of ELU in CECILIA, Periodic activity report, 2010).

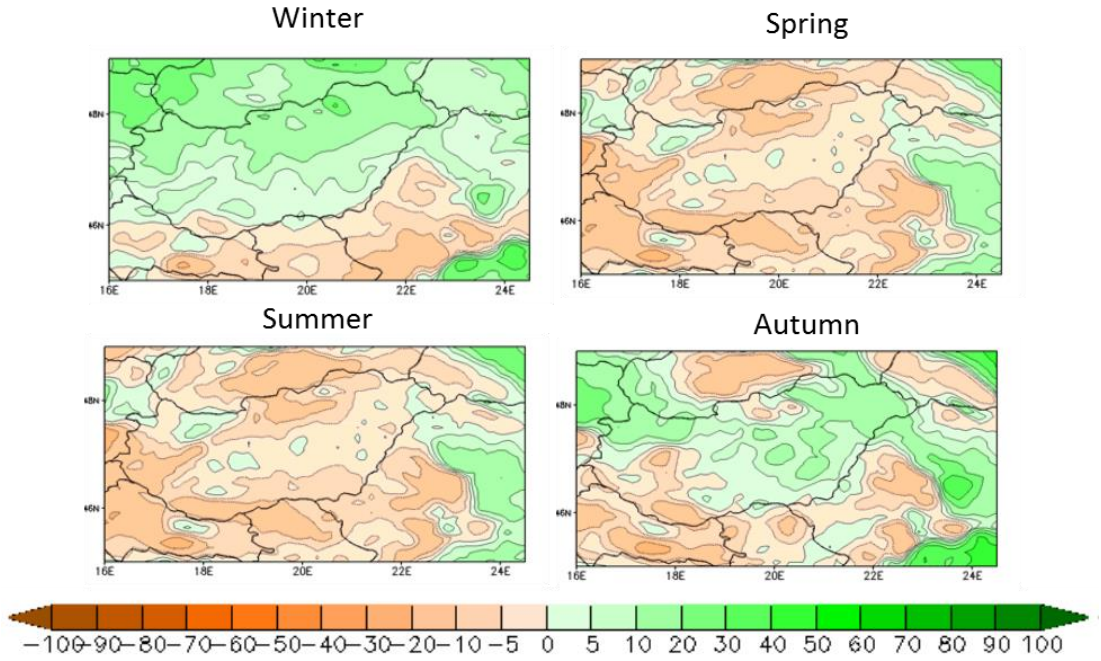

Figure 74: Simulated seasonal precipitation change for the Carpathian basin for the period 2071-2100 (reference period: 1961-1990) (after experiments of ELU in CECILIA, Periodic activity report, 2010).

5.4.3. Assessed changes in the hydrological patterns

In Kis et al. (2017) changes in hydrological processes are estimated for Upper Tisza Region using DIWA hydrological model. The necessary meteorological time series were provided by RegCM4 regional climate model (RCP8.5 scenario was used) and CARPATCLIM dataset (as reference against RegCM4). Seasonal runoff is analysed for future periods 2021-2050 and 2068-2098.

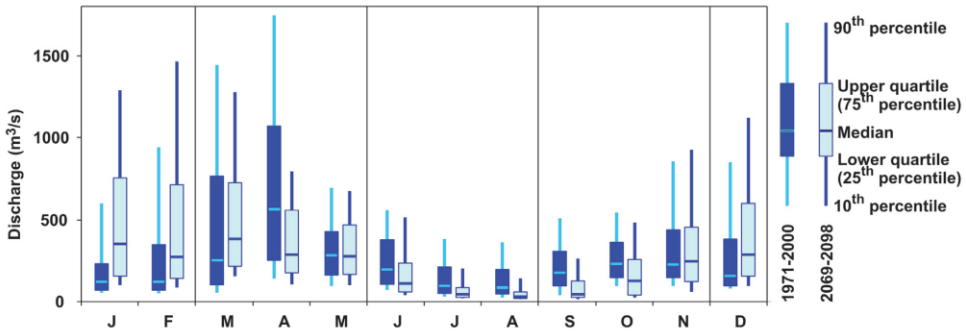

Figure 75: Annual distribution of the 10th, 25th, 50th, 75th, and 90th percentiles of runoff values calculated for each month at Tiszabecs gauge (48.1°N; 22.8°E), based on the daily averages of the 30-year-long time periods (1971–2000 and 2069–2098) (Kis et al., 2017).

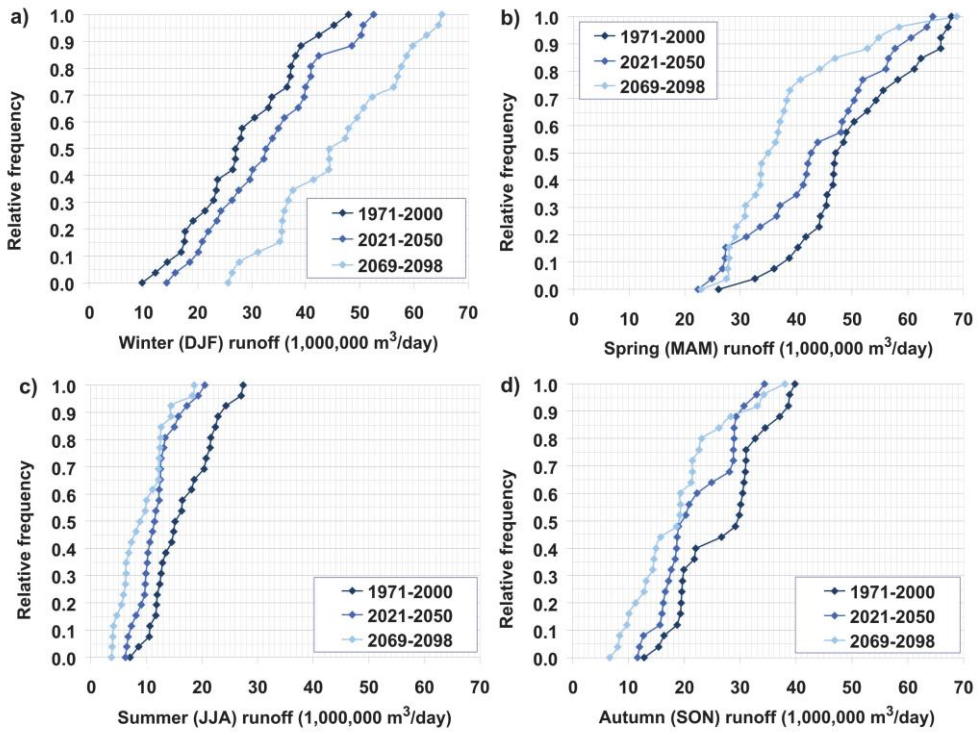

Figure 76: Comparison of simulated seasonal average runoff distributions at Tiszabecs gauge (Kis et al., 2017).

According to this paper the yearly average of runoff values is estimated to decrease, however, the trends in monthly and seasonal scales are differ within the year. Decreasing tendency in discharge values is likely to occur in spring and summer, while increased discharge values are predicted for the winter. Due to higher temperatures, their results are also predicting a runoff increase in winter and an overall decrease in spring, summer and autumn.

The upper boundary of the pilot area is at ~555 river km on the Tisza River, while in Kis et al. (2017) authors were chosen the Tiszabecs gauge - 744 river km - for presenting their results from analysing seasonal and annual runoff changes.

According to Figure 75 and Figure 76decreasing runoff values are predicted for the future except in winter (Figure 76a). The projected change of runoff is consistent with the climate model outputs described above. The decreasing trend is caused by the general increase of total precipitation and the overall warming in the area: "as a result of higher temperature values, snow accumulation will be substantially less than in the recent past. Moreover, a greater portion of precipitation is likely to occur in the form of rain instead of snow, which leads water to proceed faster into the runoff process" (Kis et al., 2017).

5.4.4. PROLINE CE development for PA2.3

This section shows the variations in seasonal precipitation (%) and temperatures (°C) for the Pilot Action 2.3: Tisza Catchment area, HU1 (Table 22). Relevant data for Tisza Catchment area were selected by coordinates using ArcMap. In this case, the variations are obtained considering only the EURO-CORDEX data (§4.2).

Table 22: Spatially averaged seasonal changes in temperature (°C) and precipitation (%) for Tisza Catchment area. Mean values were calculated from the 51 grid points which are within the pilot area.

		RCP4.5						RCP8.5					
		2021-2050			2071-2100			2021-2050			2071-2100		
		distribution percentiles			distribution percentiles			distribution percentiles			distribution percentiles		
		50th	25th	75th	50th	25th	75th	50th	25th	75th	50th	25th	75th
Changes in seasonal temperature (°C)	winter	1.6	1.2	2.0	2.6	2.1	3.0	1.5	1.1	1.9	4.4	4.1	4.8
	spring	0.9	0.6	1.3	2.0	1.4	2.6	1.2	1.0	1.4	3.4	2.6	3.8
	summer	1.3	1.1	1.6	2.0	1.7	2.8	1.4	1.2	1.7	4.0	3.4	4.8
	autumn	1.1	0.9	1.5	2.1	1.4	2.5	1.6	0.9	1.8	3.6	3.2	4.3
Changes in seasonal precipitation (%)	winter	16.8	12.4	20.6	22.0	16.4	27.6	13.6	8.4	16.8	30.7	22.4	41.5
	spring	12.8	-2.4	24.8	16.7	8.3	25.7	9.6	1.9	17.6	25.9	16.6	35.3
	summer	1.7	-8.9	13.3	3.1	-10.9	18.0	5.4	-2.9	18.3	-7.5	-17.5	7.2
	autumn	-0.9	-8.7	7.4	10.5	5.0	18.5	12.2	1.0	21.0	17.5	5.2	26.8

According to Table 22 one can see that there are small differences between temperature changes for the near future period (2021-2050) in the two different RCPs (RCP4.5 and RCP8.5) and an overall increase in temperature is expected. For the far future period (2071-2100) the RCP8.5

scenario is predicting a much more significant increase than for the near future, while the RCP4.5 scenario is predicting a more balanced temperature increase for the 21th century. Changes in precipitation are far more variable than changes in temperature. Both RCPs are predicting significant seasonal differences between changes in precipitation against the reference period, but both simulations are predicting that the winter season will become significantly wetter, and summer will likely become drier at the end of the 21th century.

A comparison of two results of climate simulation made by ELU in the framework of CECILIA project and the results of EURO-CORDEX simulation is shown in Table 23.

Table 23: Comparison of CECILIA (in light red) and EURO-CORDEX (in light green) output data for temperature and precipitation changes.

		State-Of-The-Art (CECILIA mean)		EURO-CORDEX (RCP8.5, median values)	
		2021-2050	2071-2100	2021-2050	2071-2100
Changes in seasonal temperature (°C)	winter	1.3	3.2	1.5	4.4
	spring	1.4	4.5	1.2	3.4
	summer	2.0	3.7	1.4	4.0
	autumn	1.8	3.3	1.6	3.6
Changes in seasonal precipitation (%)	winter	-17.5	15.0	13.6	30.7
	spring	-15.0	-7.5	9.6	25.9
	summer	7.5	-7.5	5.4	-7.5
	autumn	2.5	7.5	12.2	17.5

The predicted relative change values for temperature are quite similar in both results. A significant warming is expected especially for the 2071-2100 period. Although, it is conspicuous, that the estimated changes in precipitation by the two simulation are very different in their measure except for the summer season. This could be due to the comparison of *mean* and *median* values (for EURO-CORDEX no mean values were available), however, taking into account the first and the third quartiles, the difference is still significant, and EURO-CORDEX predicts a much wetter future than CECILIA.

An increase in annual mean temperature is projected for the 21th century, therefore, in the pilot area the demand for irrigation will probably increase. Also, climate change is likely to cause a decrease in total annual runoff, which is highly disadvantageous for maintaining water supply in the area. Thus, concerned water managements will have to consider that water resources are likely to decrease in the following decades, and at the same time, the demand for water for irrigation and probably the demand for drinking water will increase.

Furthermore, water management strategies have to focus on flood risk management as well, because of the predicted increase in the number of flood events in the winter and early spring seasons. The flood mitigation strategies and facilities are quite suitable for the current state of the flood hazard in the pilot area, but it is highly probable that there will be a shift in the seasonal distribution of those events which requires new strategies.

5.5. PA2.4 Groundwater protection in karst area, HR

5.5.1. Foreword

This section is about climate change issues in Pilot Action 2.4: Groundwater protection in karst area and specifically on the South Dalmatia (Prud, Klokun and Mandina spring, code 2.4.1) and Imotsko polje springs (2.4.2). In both cases, hydrological analysis in relation to the projected climate change, were performed by the hydrologist PhD Josip Rubinić, as an external associate of the PROLINE-CE project.

Figure 78: South Dalmatia pilot action.

More specifically, the pilot action of South Dalmatia (Figure) includes the springs Prud, Klokun and Mandina. Such springs represent the discharge area of a large catchment that goes deep into the neighbouring Bosnia and Herzegovina. The entire catchment area, from which a part of the water flows through the surface and/or underground pathways to the considered discharge area, extends to about 1,700 km2, most of which is located in Bosnia and Herzegovina. The area is poor in surface hydrography, and the springs, which are involved in water supply, are mainly located in the lower, south-eastern part.

Figure 77: Imotsko polje pilot action.

The other considered pilot action falls in the area of Imotsko polje springs (Figure 77). lmotsko field is a Karstic field partially situated in Croatia and partly in Bosnia and Herzegovina. Its total surface area is 92 km2, of which 48% is in Croatia. The pilot area of the spring catchment area of the Imotski field is a typical karst catchment characterized by very complex and intricate hydrogeological features. This area is faced with two basic problems, on the one hand by the flooding of certain areas, on the other hand, by the intensive agricultural activity. Both areas were partly investigated within two previous EU projects - CCWaterS (http://www.ccwaters.eu/) and DrinkAdria (http://www.drinkadria.eu/).

Climate changes have been projected using several regional climate models (RCM), namely Aladin (Bubnova et al., 1995), RegCM3 (Pal et al., 2007) and Promes (Castro et al., 1993), which results are contained in the DRINKADRIA project. The RCMs were forced by the observed concentrations of the greenhouse gases (GHGs) from 1951 to 2000; from 2001 onwards, the IPCC A1B scenario of the GHGs emissions 8 in line with the RCP4.5 as in IPCC AR/5) is applied. The initial and boundary data for each RCM were provided from different global climate models (GCMs): the ECHAM5 GCM data were used to force RegCM3, Aladin was forced by the Arpege GCM and Promes was forced by the HadCM3Q GCM. For the present climate, models are compared with the local DHMZ observations and with the EOBS gridded temperature and precipitation data (Haylock et al. 2008). Finally, the data used for hydrological analyses are mainly from the Croatian Meteorological and Hydrological Service (DHMZ (2002), DHMZ (2014)).

A simplified approach suitable for the available climatological and hydrological data was used in the discharge estimation in the pilot action South Dalmatia and the inflow assessment of the pilot area Imotsko polje springs. Such an approach is based on the comparison of the measured data on the balance of quantities discharged at the springs and watercourses that are within the monitoring system of Croatian Meteorological and Hydrological Service (DHMZ), as well as on the water balance data of effective precipitation that is infiltrated in the catchment area. More in detail, to assess the balance of effective precipitation in the Croatian karst, the most frequently used empirical models are Turc (1954) and Langbein (1962), modified and developed for GIS application (Horvat and Rubinić, 2006). These models allow defining the spatial distribution of effective annual precipitation, i.e. the precipitation infiltrated into the karst aquifer basin, assuming as spatially variable input parameters the average annual precipitation and air temperatures within the analysed catchment (often the only available climatological data in hydrological analysis of the runoff) and determining the catchment surface area by hydrogeological methods. The most effective model is selected comparing the measured and estimated values of the average annual discharges, or, when measured data on spring discharge is missing, considering expert estimates and regional formulas giving estimated average annual runoff coefficients. The adopted procedure is summarized in Table 24.

Table 24: Procedure adopted for Pilot Action 2.4.

Estimation of annual runoff	Estimation of annual runoff starts with the delineation of the drainage basins, based on hydrogeological estimations, followed by estimation of the spatial distribution of the meteorological parameters (precipitation and air temperatures). Then, estimation of the spatial distribution of the average annual runoff can be done, using both the Turc and Langbein methods. Based on the results, comparisons with the measured data are made. If the differences are negligible, the selected method, i.e. its results can be accepted and the third iteration, i.e. final estimation of the annual runoff can be carried out. Otherwise, a second iteration is repeated, which includes alternation of one of the input parameters (e.g. drainage basin boundaries) or methodological modifications (such as the modification of the analytical expressions used for estimation of the hydrological parameters).

Model calibration and validation	The model calibration and validation were conducted in two segments. One segment was the calibration of inputs into the hydrological model (data on the spatial distribution of average annual data on rainfall and average annual air temperature) for the reference 30-year period of 1961-1990 by identifying correction interrelations between the point data measured at the location of the selected climatological station and the values obtained on the basis of their spatial distribution. Another segment of the calibration done during the same 30-year period was the selection of the relevant model for estimating the average annual runoff/effective precipitation.
Future projection	Based on such verification of historical data, models were made for synthetic series of inflows – average annual yields of individual springs for the period 2013 - 2050 based on the three RCMs considered of generated mean average air temperature and annual precipitation values (DHMZ, 2014) and estimated runoff – effective precipitation from their catchment into the karst aquifers (Rubinić and Katalinić, 2014).

5.5.2. South Dalmatia: Prud, Klokun and Mandina spring

5.5.2.1. Current and future climate

The results overview for the South Dalmatia springs are presented in Table 25, Table 26 and Figure 78.

Table 25: Registered and model-based results for average annual air temperatures for the South Dalmatia catchment area.

	Temperature (^{0}C)		
1961- 1990 – Recorded			
Sr	12.7		
MAX	13.3		
MIN	12.0		
1991 – 2020 Partly recorded – partly modelled			
	Aladin	RegCM3	Promes
Sr	13.1	12.9	13.0
MAX	14.0	14.0	14.0
MIN	12.1	11.1	12.1
2021-2050 – Modelled			
Sr	13.3	12.8	13.6
MAX	14.6	14.1	14.7
MIN	12	11.6	12.3

Table 26: Registered and model-based results for annual precipitation for the South Dalmatia catchment area.

	Precipitation (mm)		
1961- 1990 - Recorded			
Sr	1424.8		
MAX	1888.8		
MIN	773.4		
1991 - 2020 Partly recorded - partly modelled			
	Aladin	RegCM3	Promes
Sr	1325.8	1357.1	1342.3
MAX	2040.6	2040.6	2040.6
MIN	854.2	854.2	854.2
2021-2050 - Modelled			
Sr	1369.1	1374.9	1342.1
MAX	1760.1	1763.2	1630.5
MIN	946.4	1038.2	1061.2

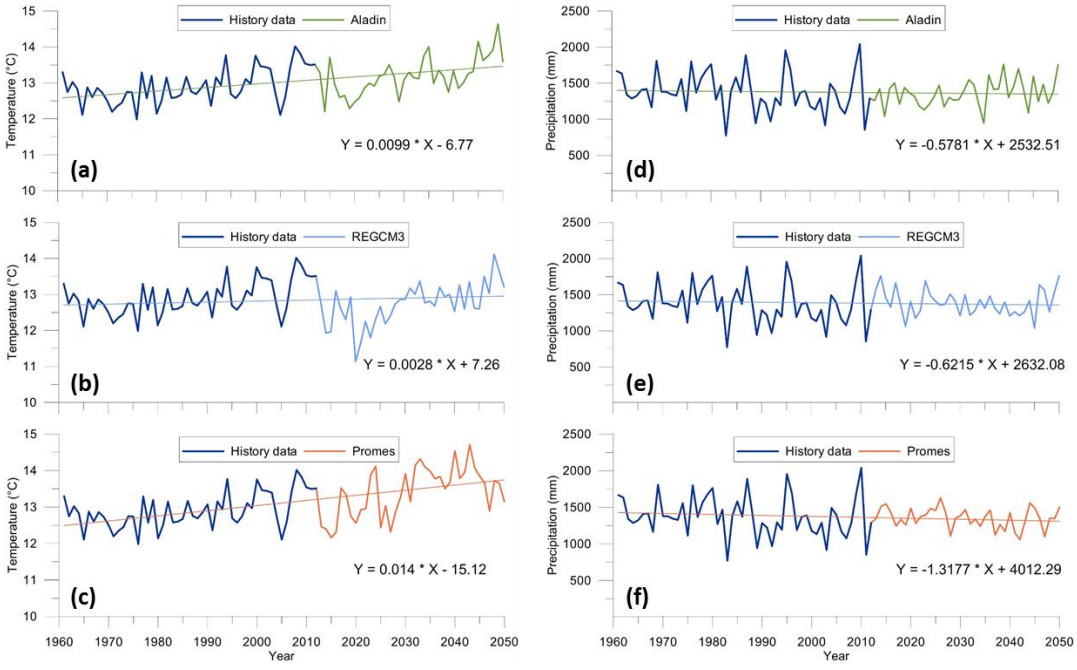

Figure 78: (a-b-c) Annual air temperature distribution (1961-2050); (d-e-f) Annual precipitation distribution (1961-2050).

According to the three models, it is visible that the air temperatures in the analysed catchment area are steadily increasing from the model RegCM3 (0.28°C/100 years) to the model Promes (1.4°C/100 years). In reference to the 30-year historical period (1961-1990), it is expected that

the average annual temperature could increase between 0.2 and 0.4°C until 2020, while an increase between 0.1 and 0.9°C is expected until 2050, where the greatest rise is developed according to the Promes model. Extreme mean annual temperatures should rapidly increase for about 0.5°C, and in Aladin and Promes model the growth is indicated within 0.3 – 0.5°C, whereas according to the RegCM3 model the temperature could decrease for 0.4°C.

Regarding the precipitation, small trends of precipitation reduction have been observed, the smallest is in the Aladin model (57.8 mm/100 years) and the highest in the Promes model (131.8 mm/100 years). When the 30-year period is compared throughout the models, a decrease of order of magnitude 100 mm is observed. And concerning precipitation extremes, a significant decline is expected up to 2050 for about 200 – 250 mm, as well as the reduction of precipitation during intense droughts for about 100 mm.

5.5.2.2. Assessed changes in the hydrological patterns

The availability of adequate data determines the application of particular runoff estimation methods. Climate data (precipitation and air temperatures) used in the analysis of basins in the South Dalmatia region is available in the form of spatial distribution of the average annual values for the 30-year period (1961-1990), in the form of a 1,000-meter spatial resolution raster prepared by experts of the Croatian Meteorological and Hydrological Service (Figure 79). This spatial resolution is identical to the spatial resolution of the digital elevation model (DEM) used.

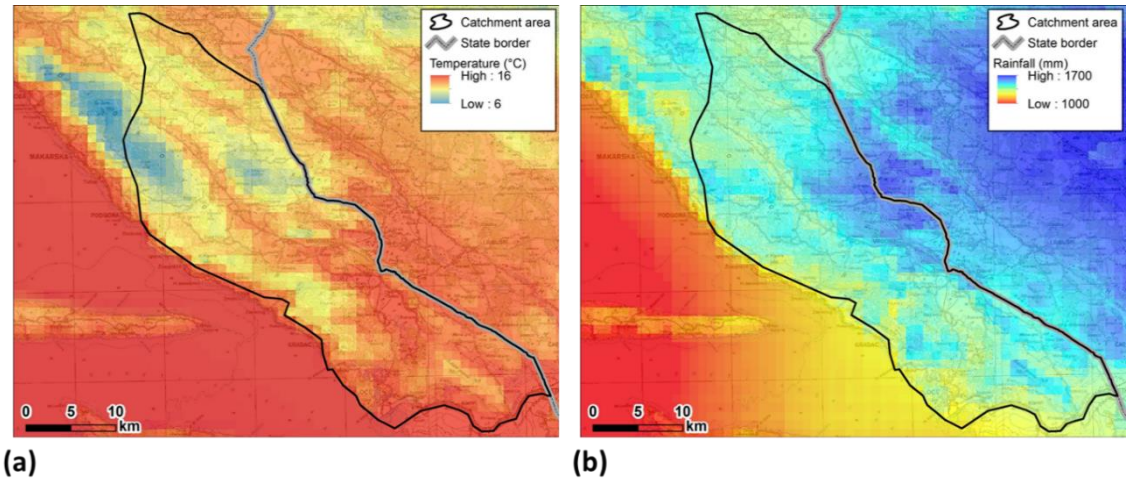

Figure 79: Spatial distribution of average annual air temperatures (a) and annual precipitation (b) in South Dalmatia (1961-1990) (DHMZ, 2002).

Based on the spatial climate data and the methodology presented above, the definition of maps of the spatial distribution of specific runoff according to the Turc (Figure 80a) and Langbein (Figure 80b) methods were defined and a map of the average values (Figure 80c) which showed that the more commonly used Turc method does not give adequate results, i.e. the method gives higher results of specific discharges in coastal areas, whereas the Langbein method gives lower specific discharge values.

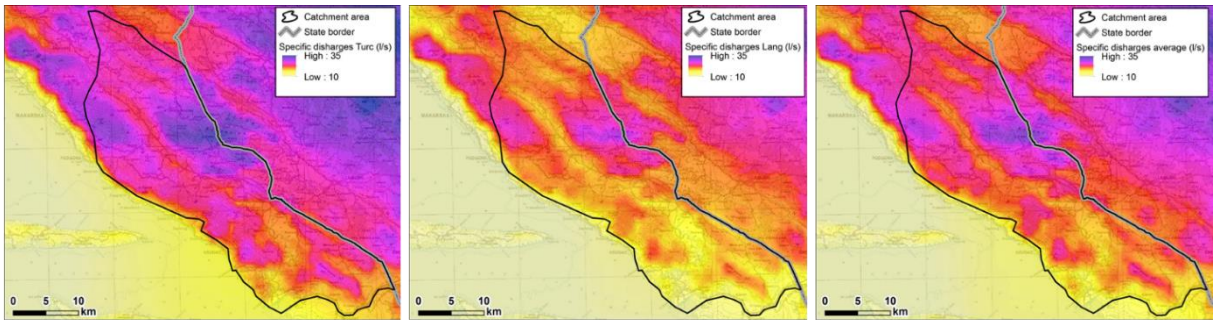

Figure 80: Spatial distribution of specific discharges in South Dalmatia for the period 1961-1990 obtained by Turc method (a), Langbein method (b) and mean results of the Turc and Langbein method (c).

Table 27: Historical data series of calculated discharges in the South Dalmatia area (1961-1990).

Average annual discharge	SR	MAX	MIN
TURC (m^3s^{-1})	24.7	38.3	7.5
LANGBEIN (m^3s^{-1})	19.9	32.7	4.3
Average TURC I LANGBEIN (m^3s^{-1})	22.3	35.5	5.9

Table 28: Generated data series of calculated mean annual discharges in South Dalmatia (1991-2050).

	Aladin			REGCM3			Promes		
	SR	MAX	MIN	SR	MAX	MIN	SR	MAX	MIN
TURC (m^3s^{-1})									
1991-2020	21.5	41.8	8.6	22.5	41.8	8,6	22.0	41.8	8.6
2021-2050	22.4	34.4	10.4	23.0	33.9	13.9	21.2	30.1	13.2
LANGBEIN (m^3s^{-1})									
1991-2020	16.8	35.9	5.1	17.9	35.9	5.1	17.3	35.9	5.1
2021-2050	17.6	29.2	6.5	18.3	28.7	9.6	16.4	25.2	8.9
Average TURC I LANGBEIN (m^3s^{-1})									
1991-2020	19.2	38.9	6.9	20.2	38.9	6.9	19.6	38.9	6.9
2021-2050	20.0	31.8	8.4	20.6	31.3	11.8	18.8	27.7	11.1

The characteristic specific discharge results calculated according to the Langbein, Turc and their average values are shown in Table 27 and

Table 28. The results of historical annual precipitation data sets and average annual air temperatures according to climate models Aladin, RegCM3 and Promes were used. In addition, for chosen discharges (averaged values according to Turc and Langbein methods) which gave an acceptable coefficient of average annual outflow for the regional area of 0.49, a depiction of historical and generated values for the period 1961-2050 is given (Figure 81).

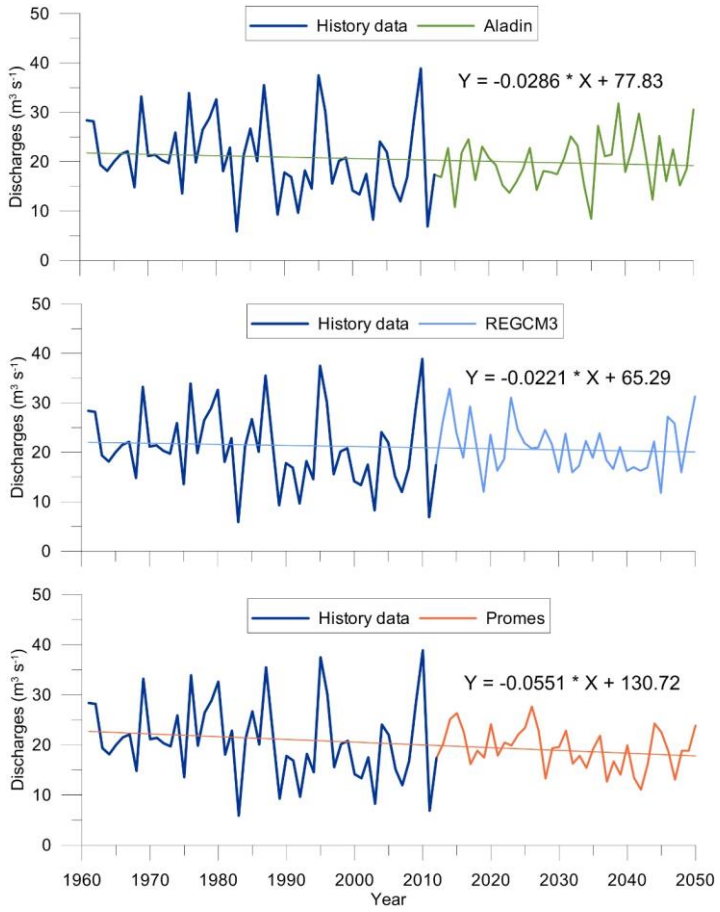

Figure 813: Historical and generated data series of average annual discharge in South Dalmatia (1961-2050).

It is evident from the previous overview that the average annual discharge from the South Dalmatia catchment area, calculated based on the average discharge values according to Turc and Langbein methods, have a reduction trend. It is most pronounced in the results determined by the Promes model, while the results of the RegCM3 model are two times less than the previous numbers. The evaluation results of the characteristical 30-year averages for the planned future 30-year periods are similar in relation to the historical period 1961-1990. The decrease of the water balance input of the analysed catchment area is expected for about 10% in average annual discharge data sets. The most emphasized reduction of the average annual inflows is according to the Promes model. Extreme annual discharges are expected more frequently in the future with an increase of the highest and lowest annual values, especially in the last 30-year period (2021-2050). According to the projections and the analysis of historical discharge data, the most significant values appeared during the period from the 1980s up until the extreme droughts in 2011 and 2012.

A test of homogeneity of average annual discharges (obtained as averaged values according to Turc and Langbein) was conducted for the historical series (1961-2012) and the generated discharge data according to the aforementioned climatological models (Aladin, RegCM3 and Promes), and nonparametric Wilcoxon test (1945). The calculated results (Table 29) show that all generated series are homogeneous compared to the historical series of mean annual discharges.

Table 29: Assessment of homogeneity of data on the average annual discharges on area of Southern Dalmatia for the historical period 1961-2012 and the period 2013-2050 generated by the climate models.

1961.-2012. / 2013.-2050.	Average annual discharges (m^3 s^{-1})
Aladin	
Standard unit deviation U_0	0.34
Homogeneity assessment	HOMOGENOUS
RegCM3	
Standard unit deviation U_0	-0.47
Homogeneity assessment	HOMOGENOUS
Promes	
Standard unit deviation U_0	0.83
Homogeneity assessment	HOMOGENOUS

5.5.3. Imotsko polje springs

5.5.3.1. Current and future climate

The results overview for the Imotsko polje springs are presented in Table 30, Table 31 and Figure 82.

Table 30: Registered and model-based results for average annual air temperatures for the Imotsko polje springs.

	Temperature (^{0}C)		
1961- 1990 - Recorded			
Sr	12.2		
MAX	12.7		
MIN	11.5		
1991 - 2020 Partly recorded - partly modelled			
	Aladin	RegCM3	Promes
Sr	12.5	12.4	12.6
MAX	13.4	13.4	13.5
MIN	11.6	10.7	11.6
2021-2050 - Modelled			
Sr	12.7	12.3	13.6
MAX	14.0	13.5	14.7
MIN	11.9	11.1	12.3

Table 31: Registered and model-based results for annual precipitation for the Imotsko polje springs.

	Precipitation (mm)		
1961- 1990 - Recorded			
Sr	1402.1		
MAX	1858.7		
MIN	761.1		
1991 - 2020 Partly recorded - partly modelled			
	Aladin	RegCM3	Promes
Sr	1304.6	1335.5	1320.9
MAX	2008.1	2008.1	2008.1
MIN	840.6	840.6	840.6
2021-2050 - Modelled			
Sr	1347.2	1353.0	1320.7
MAX	1732.0	1735.1	1604.5
MIN	931.3	1021.7	1044.3

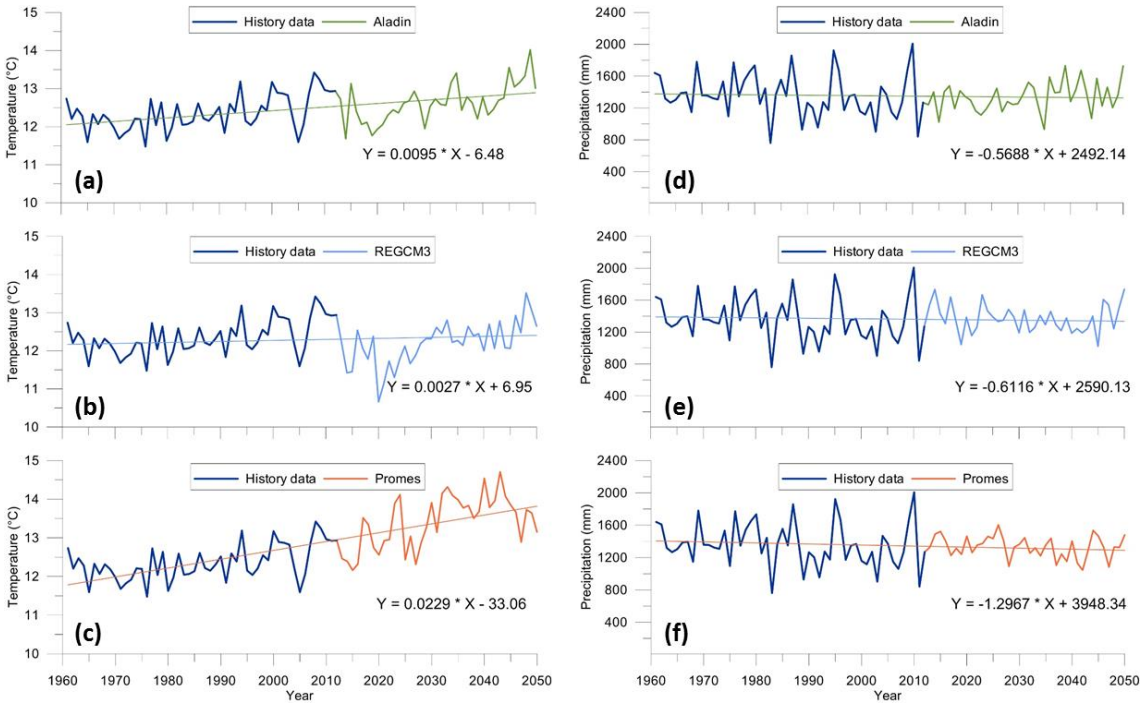

Figure 82: (a-b-c) Annual air temperature distribution (1961-2050); (d-e-f) Annual precipitation distribution (1961-2050).

According to all three mentioned models, air temperature in the catchment area tends to increase - RegCM3 model (barely 0.27 ^{0}C/100 years), Promes model (2.3 ^{0}C/100 years). In comparison to the reference 30-year period (1961-1990), the expected average annual temperature will increase until 2020 between 0.2 and 0.4 ^{0}C. The largest increase is shown with the results of Promes model – ranging from 0.1 to 1.4 ^{0}C until 2050. Extreme average annual temperature could increase more significantly up to 0.8 ^{0}C for 30-year period that is already in progress and up to 2 ^{0}C for the period until 2050, while Aladin and Promes models show a minimal increase of up to 0.1 ^{0}C for the period until 2020 and of 0.4 – 0.8 ^{0}C for the period until 2050. The RegCM3 model foresees the decrease for around 0.4 - 0.8 ^{0}C.

Concerning the precipitation, there is a slight decrease – according to the Aladin model it is around 56.9 mm/100 years, while Promes model foresees 129.7 mm/100 years. The selected 30-year periods show a decrease of 30-year average by some 50 mm. The expected significant decrease of extreme annual precipitation until 2050 is around 100 – 250 mm, while minimal annual precipitation will be increased for some 200 to 250 mm during extremely dry seasons.

5.5.3.2. Assessed changes in the hydrological patterns

The adequate data availability determines the application of particular runoff estimation methods. Climatological data (precipitation amount and air temperature), used in the analysis of the Imotsko polje catchment, is available in the form of spatial distribution of the average annual values for the 30-year period (1961-1990), with a spatial resolution raster of 1,000-meter prepared by the experts of the Croatian Meteorological and Hydrological Service (Figure 83). The spatial resolution is equivalent to spatial resolution of the digital elevation model (DEM).

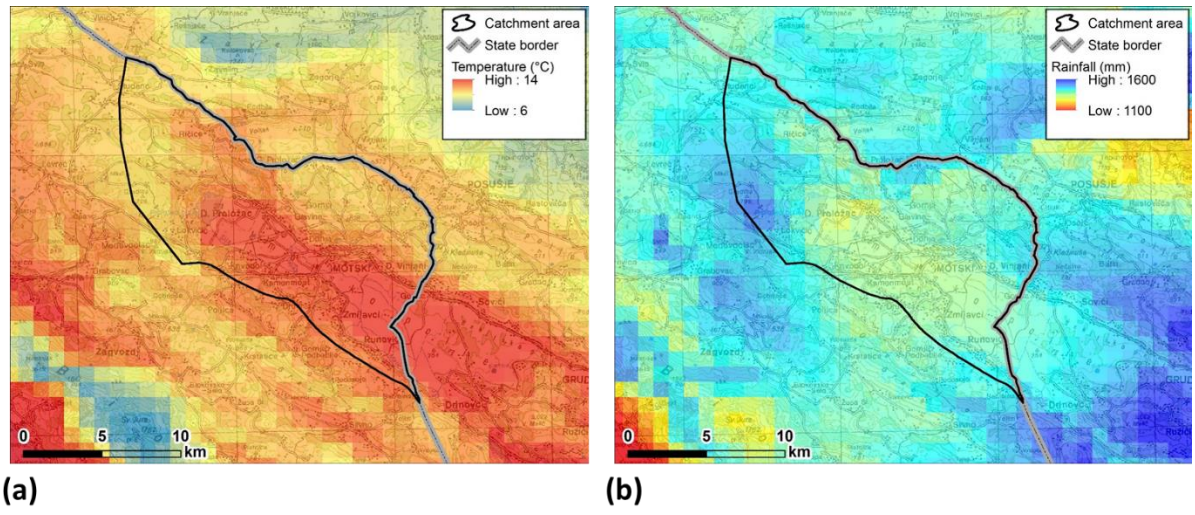

Figure 83: Spatial distribution of average annual air temperatures (a) and annual precipitation (b) in the Imotsko polje spring area (1961-1990) (DHMZ, 2002).

Based on the spatial climatological data and according to the methodology presented above, maps of spatial distribution of specific runoff were defined with the help of Turc (Figure 84a) and Langbein method (Figure 84b). Moreover, the map of average values was prepared for the analysed

area (Figure 84c) due to inadequate values obtained with the Turc method, which gives increased values of specific runoff for coastal areas, opposed to decreased specific runoff values obtained with the Langbein method.

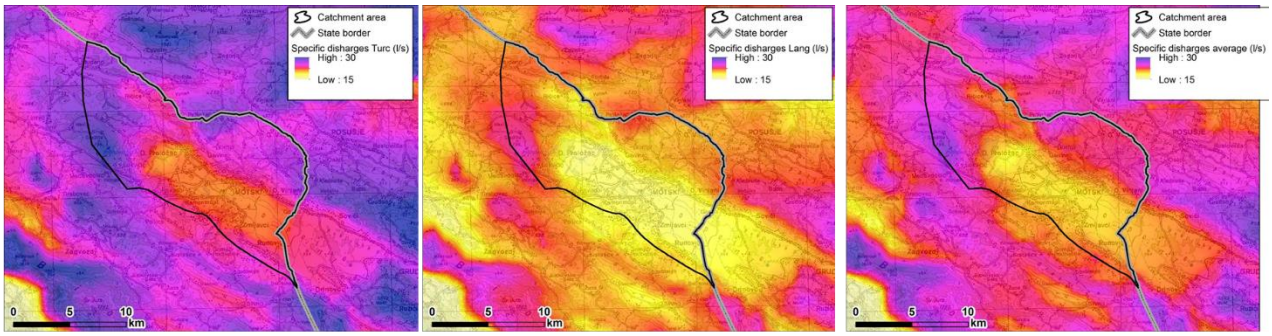

Figure 84: Spatial distribution of specific discharges in the Imotsko polje spring area for the period 1961-1990 obtained by Turc method (a), Langbein method (b) and mean results of the Turc and Langbein method (c).

Table 32: Historical data series on calculated flow within Imotsko polje catchment (1961-1990).

Average annual flow	Average	MAX	MIN
TURC (m^3s^{-1})	3.98	6.15	1.22
LANGBEIN (m^3s^{-1})	3.73	6.09	0.82
average TURC and LANGBEIN (m^3s^{-1})	3.86	6.12	1.02

Table 33: Generated data series of calculated mean annual discharges on the Imotsko polje catchment area (1991-2050).

	Aladin			RegCM3			Promes		
	SR	MAX	MIN	SR	MAX	MIN	SR	MAX	MIN
TURC (m^3s^{-1})									
1991-2020	3.48	6.73	1.41	3.64	6.73	1.41	3.53	6.73	1.41
2021-2050	3.62	5.53	1.70	3.71	5.46	2.26	3.33	4.75	2.07
LANGBEIN (m^3s^{-1})									
1991-2020	3.16	6.69	0.98	3.35	6.69	0.98	3.35	6.69	0.98
2021-2050	3.31	5.44	1.24	3.43	5.35	1.82	3.22	4.90	1.77
Average TURC and LANGBEIN (m^3s^{-1})									
1991-2020	3.32	6.71	1.20	3.49	6.71	1.20	3.44	6.71	1.20
2021-2050	3.46	5.48	1.47	3.57	5.40	2.04	3.28	4.83	1.92

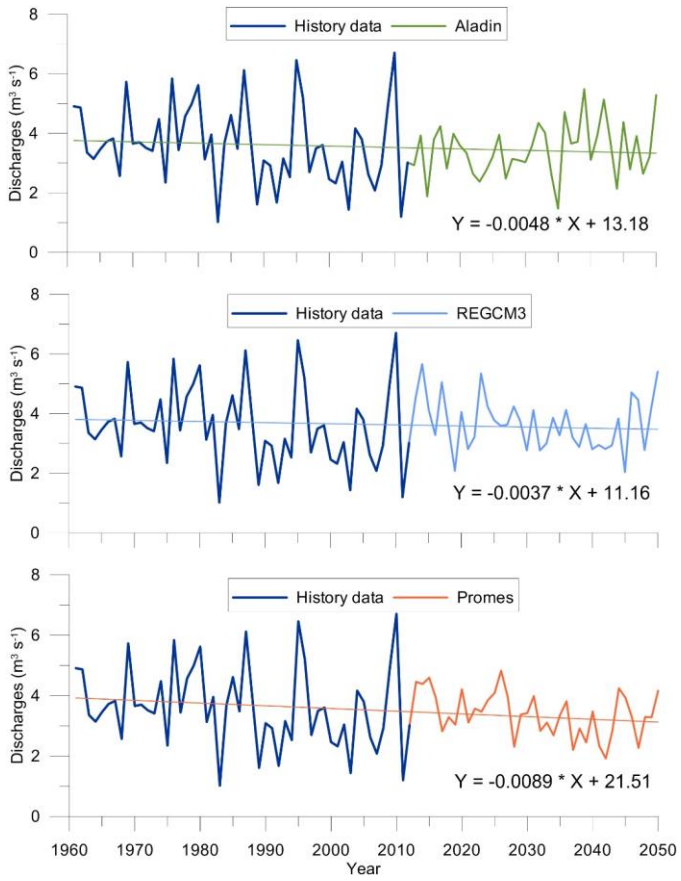

Figure 85: Distribution of historical and generated set of data on mean annual discharges in the Imotsko polje area (1961-2050).

Acquired results of calculated specific discharge defined with Langbein and Turc methods and their average values are shown in the Table 32 (historical series) and Table 33 (generated series). Historical series results of annual precipitation and average annual air temperature according to the Aladin, RegCM3 and Promes climatological models were used. Furthermore, selected reference flow values (average values obtained with Turc and Langbein methods which gave an acceptable coefficient of average annual outflow for the regional area of 0.50, a depiction of historical and generated values for the period 1961-2050 is given (Figure 85). A test of homogeneity of average annual discharges (obtained as averaged values according to Turc and Langbein) was conducted for the historical series (1961-2012) and the generated discharge data according to the aforementioned climatological models (Aladin, RegCM3 and Promes), and nonparametric Wilcoxon test (1945). The calculated results (Table 34) show that all generated series are homogeneous compared to the historical series of mean annual discharges.

Table 34: Assessment of homogeneity of data on the average annual discharges on area of Imotsko polje catchment for the historical period 1961-2012 and the period 2013-2050 generated by the climate models.

1961-2012 / 2013-2050	Average annual discharges (m^3 s^{-1})
Aladin	
Standard unit deviation U_0	0.33
Homogeneity assessment	HOMOGENOUS
RegCM3	
Standard unit deviation U_0	-0.46
Homogeneity assessment	HOMOGENOUS
Promes	
Standard unit deviation U_0	0.68
Homogeneity assessment	HOMOGENOUS

5.5.4. PROLINE CE development for PA2.4

This section reports the variations in seasonal precipitation and temperatures for the Pilot Action 2.4: Groundwater protection in karst area, HR. For the case in hand, trends are derived by comparing State-of-the-art data (HGI data) with PROLINE data obtained considering only the EURO-CORDEX data (§4.2). The comparison refers to period 2021-2050 vs 1971-2000 under RCP4.5 and RCP8.5 scenarios.

Winter season

- PROLINE CE data (EURO-CORDEX): they show an increase in temperature by 0-1.5 °C (25th, 50th percentile) and 1.5-3.0 °C for 75th percentile. This could drastically affect snow precipitation and accumulation dynamics in such short term (2021-2050). Seasonal cumulative precipitation data appears quite limited, for both models and most of percentiles the given variation of seasonal precipitation is -50 to 50 mm/season, except for RCP4.5 75th percentile, which predicts an increase of 50 – 110 mm /season
- PA2.4.1: South Dalmatia: Prud, Klokun and Mandina spring (HGI seasonal data): it partly supports this – an increase of 1.2 °C vs 1.2 (RCP4.5) and 1.3 °C (RCP8.5) for 50th percentile. Precipitation data is more variable, HGI data predicts decrease of about 4 mm, while EURO-CORDEX predicts increase of 34 (RCP4.5) and 16.8 (RCP8.5) mm
- PA2.4.2: Imotsko polje springs (HGI seasonal data): it partly supports this – an increase of 1.4 °C vs 1.2 (RCP4.5) and 1.3 °C (RCP8.5) for 50th percentile. Precipitation data is more variable, HGI data predicts decrease of 0.2 mm, while EURO-CORDEX predicts increase of 35 (RCP4.5) and 10 (RCP8.5) mm

Summer season

- PROLINE CE data (EURO-CORDEX): they show an increase in temperature by 0-1.5 °C (25th, 50th percentile) and 1.5-3.0 °C for 75th percentile. Significant variations characterize spatial patterns: southern parts have higher values (Italy and Croatia), and these variations could lead to substantial increase in atmospheric evapotranspiration demand driven also by higher humidity defects. Larger atmospheric demand driven by temperature increase could entail a substantial reduction of soil water content. All models and percentiles provide uniform data for South Dalmatia, where seasonal precipitation is expected to vary by -50 to 50 mm/season. Considering climate in pilot area (Csb warm-summer Mediterranean climate according to Koppen-Geiger classification), adaptation strategies (e.g. less water demanding crops) and irrigation practices are necessary
- PA2.4.1: South Dalmatia: Prud, Klokun and Mandina spring (HGI seasonal data): it points at an increase of 1.9 °C for summer season, which is slightly higher than EURO-CORDEX RCP4.5 and RCP8.5 increase of 1.4 and 1.7 °C. HGI predicts an increase in precipitation (10 mm) vs EURO-CORDEX decrease of 6 and 1 mm

- PA2.4.2: Imotsko polje springs (HGI seasonal data): it indicates an increase of 1.8 °C for summer season, which is slightly higher than EURO-CORDEX RCP4.5 and RCP8.5 increase of 1.4 and 1.7 °C. HGI data predicts decrease in precipitation (2.6 mm) vs EURO-CORDEX decrease of 4.9 and respectively, 4.2 mm

Spring season

- PROLINE CE data (EURO-CORDEX): they point that the expected increase should not exceed 0-1.5 °C for all percentiles. Precipitation is not highly variable according to all percentiles and models, and is expected to be in range of -50 to 50 mm/season
- PA2.4.1: South Dalmatia: Prud, Klokun and Mandina spring (HGI seasonal data): it shows 1.2 °C increase and 2 mm increase, while EURO-CORDEX models point at 0.9 and 1.1 °C increase with 4.3 mm increase (RCP4.5) and 3.3 mm decrease (RCP8.5)
- PA2.4.2: Imotsko polje springs (HGI seasonal data): it shows 1.1 °C temperature increase, and 2 mm precipitation decrease, while EURO-CORDEX models point at 0.9 and 1.1 °C increase (RCP4.5 and 8.5) with 4 mm increase (RCP4.5) and -0.1 mm decrease (RCP8.5)

Autumn season

- PROLINE CE data (EURO-CORDEX): they show an increase in temperature by 0-1.5 °C for all percentiles (RCP4.5), while with RCP8.5 predicts 0-1.5 °C for 25th and 50th percentile and 1.5-3.0 °C for 75th percentile. According to 25th percentile, both RCP4.5 and RCP8.5 predict significant decrease in precipitation, from -110 to -50 mm/season. 50th and 75th percentile shows slight variations for both models, ranging from -50 to 50 mm/season
- PA2.4.1: South Dalmatia: Prud, Klokun and Mandina spring (HGI seasonal data): it predicts 1.55 ^{0}C increase which is similar to EURO-CORDEX RCP8.5 increase of 1.6 ^{0}C. However, HGI precipitation increase amounts to 3.5 mm in contrast to EURO-CORDEX models at 11.8 mm
- PA2.4.2: Imotsko polje springs (HGI seasonal data): it predicts 1.5 °C increase which is similar to EURO-CORDEX RCP8.5 increase of 1.4 °C, while RCP4.5 predicts 1.0 increase. However, predicted HGI precipitation decrease amounts to 2.7 mm in contrast to EURO-CORDEX models increase for RCP4.5 (5.6 mm) and decrease for RCP8.5 (6.9 mm)

Data provided by CMCC foundation shows similar trends concerning temperature increase as Rubinić models (RegCM3, Promes and Aladin). Majority of CMCC models (EURO-CORDEX) point at seasonal temperature increase in range of 0-1.5 ^{0}C for South Dalmatia and for Imotsko polje, which supports data and conclusions provided in the State-of-the-art section for the case in hand.

Annual precipitation scenarios by HGI (2021-2050 vs 1991-2020) predict similar trends, with only slight increase for some models concerning mean annual precipitation. For South Dalmatia, maximum annual values are expected to decrease by 200-250 mm/year in average, while minimum annual values are expected to increase by 100-200 mm/year. On the other hand, for Imotsko polje,

maximum annual values are predicted to decrease by 100-250 mm/year, while minimum annual values are expected to increase by 200-250 mm/year

From the point of drinking water protection, interesting thing to point out is high value of CDD (consecutive dry days, 1971-2000), reaching up to 34-40 days for South Dalmatia. Future scenarios (RCP4.5 and 8.5 75th percentile, 2021-2050) predict an increase of 3-8 days for South Dalmatia, resulting in higher probability of water shortage. Such result appears quite interesting considering the recent drought events that could be already exacerbated short time horizon according 75th percentile. CWD values (consecutive wet days) are far greater in mountain regions, while for South Dalmatia, they are usually limited to 9-11 days (1971-2000). According to 25th percentile, reductions primarily affect Balkan and Alpine region, predicting -4 to -1 reduction of CWD, which could reduce flood intensity and duration in some parts of South Dalmatia (e.g. Vrgorac and Neretva fields). Concerning Rx1D parameter (yearly maximum 1-day precipitation), for PA South Dalmatia it is in the moderate range of 25-50 mm/day. 75th percentile predicts increase of 5 to 15 mm/day in period 2021-2050. It is worth recalling that Rx1D has been selected only as proxy for triggering of hydrological hazards. Their actual occurrence is strictly linked to geomorphological conditions of basins (extent, orography, land use/cover).

Hydrological modelling is pointed out that the average annual discharges from the South Dalmatia catchment area, calculated based on the average discharge values according to Turc and Langbein methods, has decreasing trend. It is most pronounced for the results determined by the Promes model, while the results of the RegCM3 model are two times less than of the Promes. The evaluation results of the characteristical 30-year averages for the planned future 30-year periods are similar in relation to the historical period 1961-1990. The decrease of the water balance input to the analysed catchment area is expected for about 10% in average annual discharge data sets. The most emphasized decreasing of the average annual discharges is resulted according to the Promes model. Extreme annual discharges are expected more frequently in the future with an increase of the highest and lowest annual values, especially in the last 30-year period (2021-2050). According to the predictions and the analysis of historical discharge data, the most significant values appeared during the period from the 1980s up until the extreme droughts in 2011 and 2012.

From the point of drinking water protection, interesting thing to point out is high value of CDD (consecutive dry days, 1971-2000), reaching up to 34-40 days for Imotsko polje. Future scenarios (RCP4.5 and 8.5 75th percentile, 2021-2050) predict an increase of 3-8 days for Imotsko polje, resulting in higher probability of water shortage. Such result appears quite interesting considering the recent drought events that could be already exacerbated short time horizon according 75th percentile. CWD values (consecutive wet days) are far greater in mountain regions, while for plain areas such as Imotsko polje, they are usually limited to 9-11 days (1971-2000). According to 25th percentile, reductions primarily affect Balkan and Alpine region, predicting -4 to -1 reduction of CWD, which could reduce flood intensity and duration in Imotsko polje. Concerning Rx1D parameter (yearly maximum 1-day precipitation), for PA Imotsko polje it is in the moderate range of 25-50 mm/day. 75th percentile predicts increase of 5 to 15 mm/day in period 2021-2050. It is worth recalling that Rx1D has been selected only as proxy for triggering of hydrological hazards. Their actual occurrence is strictly linked to geomorphological conditions of basins (extent, orography, land use/cover).

From the results of the hydrological modelling in relation with climate change predictions, it is evident that the average annual discharges from the Imotsko polje springs catchment area, calculated based on the average discharge values according to the Turc and Langbein methods have decreasing trend. It is most pronounced in the results determined by the Promes model, while the results of the RegCM3 model predict two times less discharge decreasing than determined by Promes. The evaluation results of the characteristic 30-year averages for the future 30-year periods are similar in relation to the historical period of 1961-1990.

According to all models, for the 30-year period up to 2020, a decreasing of discharge is expected for about 10 - 15% in the average annual flow rates generated in the analysed area. The Promes model shows the most drastic decrease of average annual discharge. For the period up to 2050, according to the Aladin and RegCM3 models, the discharge is expected to decrease by several percent, whereas according to the results of the Promes model further decrease is expected in comparison with the values for 2020. In the future, the maximum average annual discharges could be slightly more pronounced in the period until 2020, while for the following 30-year period, it could decrease in comparison with the 1961-1990 series. Similar changes are also expected in the minimum annual discharges that could increase in the period up to 2050. According to the projections and the analysis of historical discharge data, the most significant values appeared during the period from the 1980s up until the extreme droughts in 2011 and 2012.

5.6. PA2.5 Neufahrn bei Freising, GER

5.6.1. Foreword

This section is about climate change issues in Pilot Action 2.5: Neufahrn bei Freising. Specifically, the pilot area Neufahrn bei Freising is located 10 km north of the city of Munich.

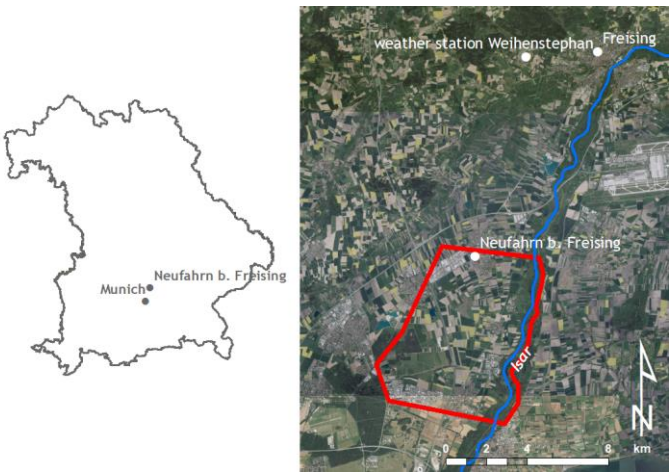

Figure 86: Location of the pilot area Neufahrn bei Freising in Bavaria.

Figure 86 illustrates the border of the pilot area as well as the locations of the city of Neufahrn and the DWD weather station in Weihenstephan (DWD, 2018). The Isar River represents the eastern boundary of the study area. Climate change investigations were performed for entire Bavaria and the pilot area Neufahrn bei Freising.

In the framework of the Bavarian climate adaptation strategies, the Bavarian Environment Agency conducted numerous studies to investigate the impacts of climate change for entire Bavaria, as well as for the major river basins (LfU, 2012a; LfU, 2012b). These studies present future climate trends and their impacts on water management. In this perspective, one Emission Scenario, three Global Climate Models (GCM) and six Regional Climate Models (RCM) were available. Four of the RCMs apply statistical models (STAR2, WETTREG 2006, WETTREG 2009, WETTREG 2010) and two use a dynamical modelling approach (CLM 2008, REMO 2006). Different combinations between the three GCM's and the six RCM's were applied. The applied GCMs are based on the A1B scenario regarding future development of greenhouse gases. On the other hand, for the pilot area Neufahrn bei Freising, state-of-the-art studies are not retrievable and then analysis performed in the PROLINE framework with Euro-CORDEX data represents a novelty.

5.6.2. Climate data

5.6.2.1. Current climate Previous state-of-the-art framework

The output of LfU (2012a; 2012b) analysis over current period for Bavaria are reported in Table 35 and Table 36. Specifically, Table 35 gives an overview of climate indicators in Bavaria as averaged for the time interval from 1971 to 2000. In general, Bavaria has a warm-moderate climate with slightly more precipitation during the hydrological summer period (May – October) as compared to the hydrological winter period (November – April). On the other side, Table 36 provides an overview of climate changes that occurred during the period from 1931 to 2010. The data shows that the mean annual temperature increased and that a temporal shift of precipitation occurred. While

the total amount of precipitation during the summer time just slightly decreased, the precipitation during the wintertime increased significantly. These observations correspond with surveys and observations for similar regions presented in IPCC (2014).

Table 35: Climate indicators for Bavaria averaged over the time period of 1971-2000 (LfU, 2012a).

Climate indicator	Bavaria
Mean annual temperature	7.8 (C°)
Number of 'ice days' (*maximal daily temperature < 0 C°*)	30 (days/year)
Number of 'frost days' (*minimal daily temperature < 0 C°*)	109 (days/year)
Number of 'hot days' (*maximal daily temperature > 30 C°*)	5 (days/year)
Number of 'summer days' (*maximal daily temperature > 25 C°*)	32 (days/year)
Averaged sum of precipitation during the hydrological winter period	400 (mm)
Averaged sum of precipitation during the hydrological summer period	533 (mm)

Table 36: Mean change of temperature and precipitation in Bavaria (LfU, 2012a).

Climate indicator	Bavaria
Mean annual temperature	+1.1 (C°)
Change of precipitation for the hydrological winter period	+22%
Change of precipitation for the hydrological summer period	-1%

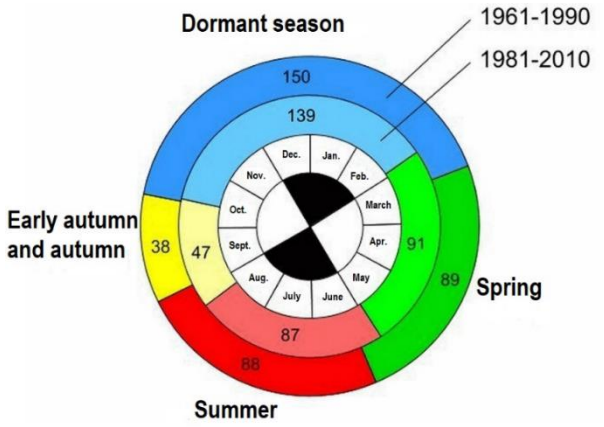

Figure 87: The phenological clock showing the shift in seasons from 1961 to 2010, (Bavarian Environmental Agency, 2017c).

5.6.2.2. Future climate

The output of LfU (2012a; 2012b) analysis over future period for Bavaria are reported in Figure 88, Figure 89 and Figure 90.

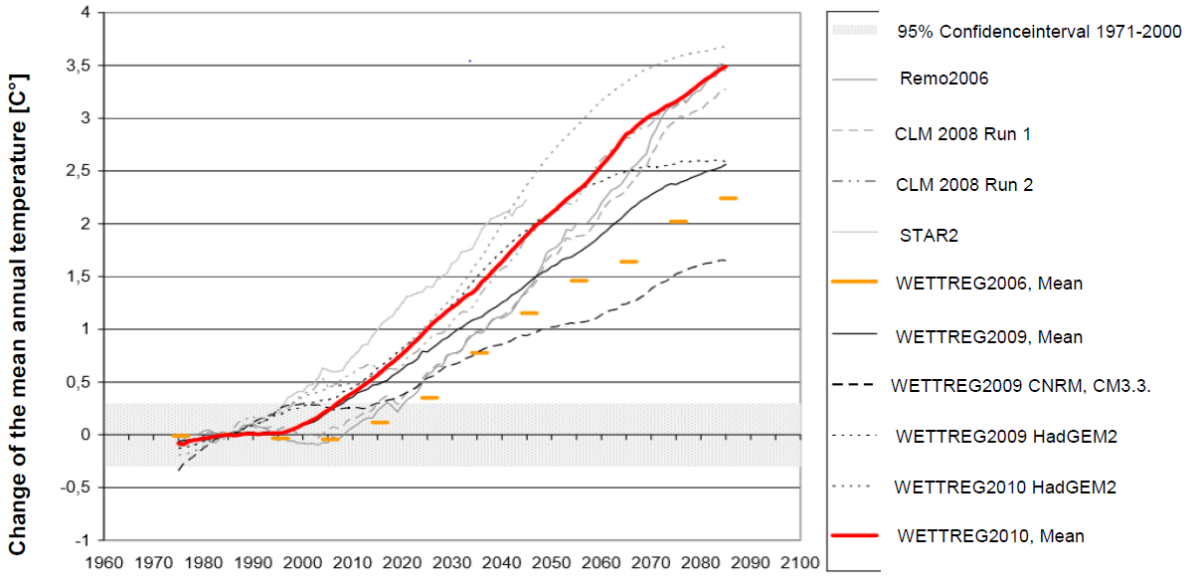

Figure 88: Change of the 30-year moving average of the annual temperature (C°) in Bavaria as com-pared to the period 1971-2000 (modified after LfU, 2012a).

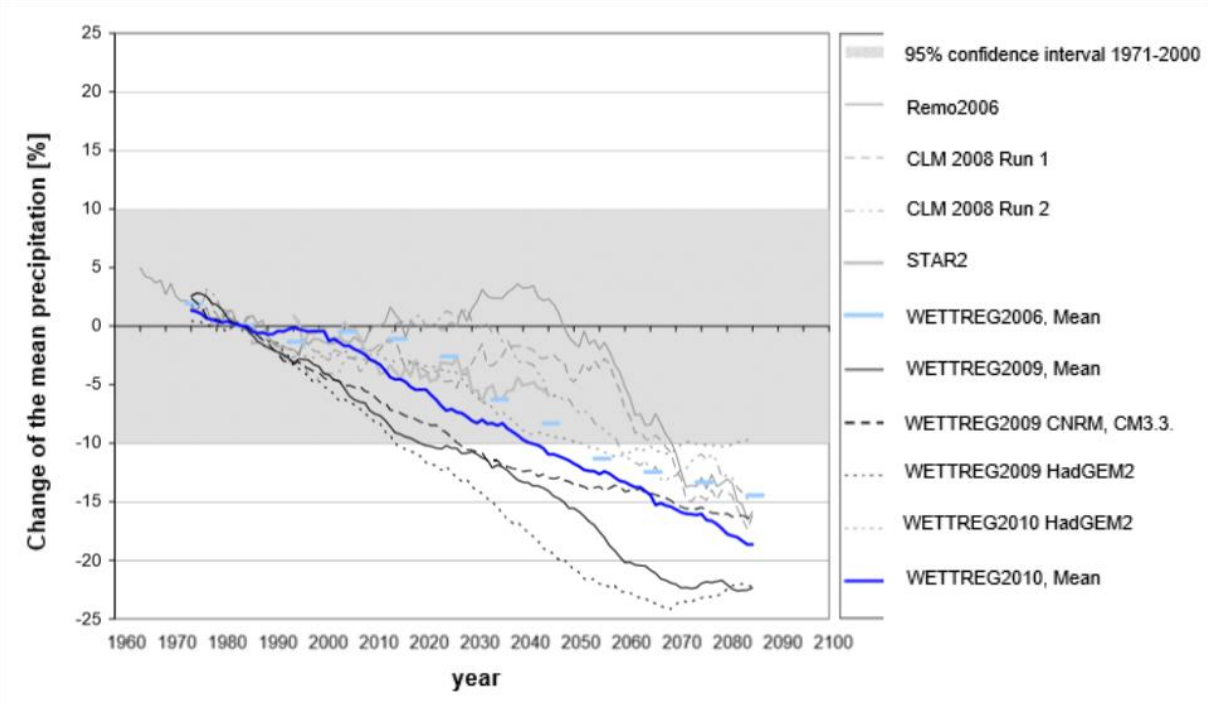

Figure 89: Relative change (%) of the 30-year moving average of the mean precipitation during the hydrological summer period in Bavaria (modified after LfU, 2012a).

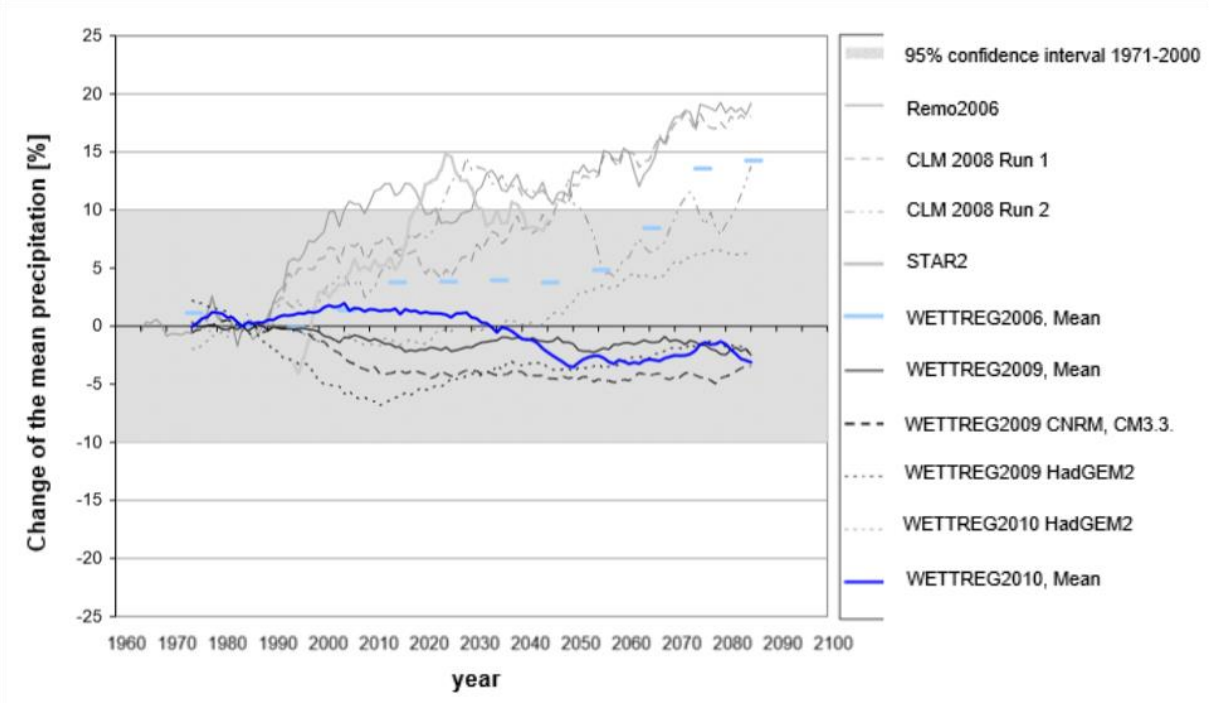

Figure 90: Relative change (%) of the 30-year moving average of the mean precipitation during the hydrological winter period in Bavaria (modified after LfU, 2012a).

As shown in Figure 88, the forecasted temperature changes in Bavaria in the period from 2021 to 2050 ranges from +0.8 C° to +1.9 C° for the ten projections. The majority of the projections predicts an increase of more than +1.2 C°. This trend is expected to continue until the end of the 21st century.

Depending on the climate projection, the number of 'ice days' (i.e. maximal daily temperature < 0 C°) decreases between -5 days/year to more than -15 days/year, while the decrease in 'frost days' (i.e. minimal daily temperature < 0 C°) varies from -7 days/year up to -28 days/year. Moreover, the amounts of 'summer days' (maximal daily temperature > 25 C°) and 'hot days' (i.e. maximal daily temperature > 30 C°) are expected to increase, ranging from +5 days/year to +25 days/year for the 'summer days' and +0 days/year to +11 days/year for the 'hot days'.

The change in the annual mean precipitation is not consistent throughout the simulations. Some modelling results indicate a slight increase towards the middle of the 21st century followed by a decrease towards the end of the century. Other simulations remain constant or show a slight decrease. However, the regarded simulation results consistently predict a decrease of the 30-year moving average of precipitation during the hydrological summer period until the end of the 21st century (Figure 89). The range of that decrease is between -15% to -22%. For what concerns the predictions of changes of the mean precipitation for the hydrological winter period (Figure 90), we can see that mostly those models based on dynamical simulations predict an increase of precipitation by up to 15%, while other model simulations forecast only slight changes.

5.6.3. Assessed changes in the hydrological patterns

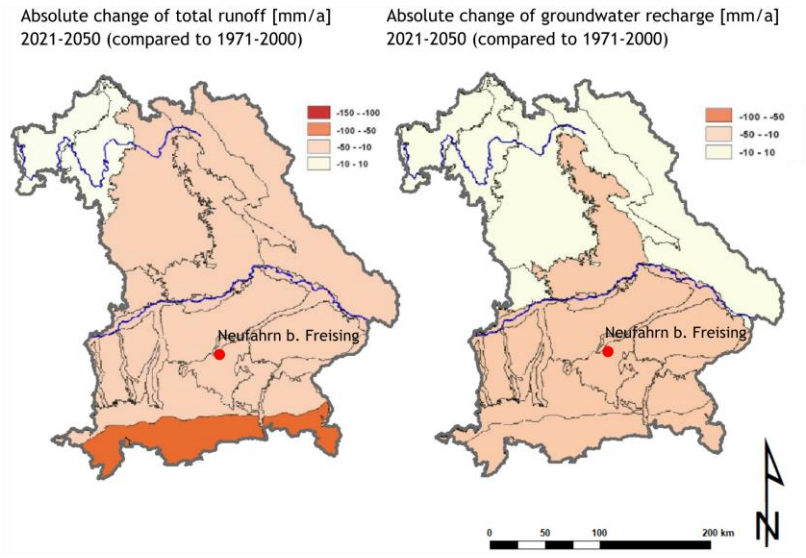

Figure 91: Absolute changes of total runoff and groundwater recharge [mm/a] in the period from 2021-2050 as compared to the reference period from 1971-2000 (modified after KLIWA, 2012).

The KLIWA working group analysed the impacts of climate changes on the soil water balance as well as on the groundwater recharge. Their simulations are based on the RCM scenarios WETTREG2003 and WETTREG2006 and are presented in KLIWA (2012). Figure 91 illustrates the impacts of climate changes on total runoff and groundwater recharge in Bavaria. The presented results are based on WETTREG2006 simulations. The figure highlights that total runoff is expected to decrease in Bavaria, however showing regional variations. Most significant changes are predicted

to occur in the Bavarian Alps. A mean decrease of about 20 mm/a in total runoff was calculated for entire Bavaria. Regarding the absolute changes of groundwater recharge, it appears that the southern parts of Bavaria will suffer a larger decrease in groundwater recharge as compared to the northern (Franconian) parts.

5.6.4. PROLINE CE development for PA2.5

As for the pilot area Neufahrn bei Fresing, bias corrected temperature and precipitation data are used. A total of 19 projection models were applied considering historic temperature and precipitation data measured at the meteorological measuring station in Weihenstephan (Germany) (Figure 86). All 19 scenarios include daily values for temperature and precipitation for the period from 2006 to 2100. The 30-years moving average from the given daily temperature and precipitation data are assessed to analyse occurring climate changes in comparison to the long-term climate observations from Weihenstephan (1971-2000). Similar to the given climate change simulations from LfU (2012a) and LfU (2012b), all 19 scenarios for climate change in Neufahrn bei Freising predict increasing temperatures until the end of the 21st century. Following the simulation results, the 30-year moving average of the predicted annual mean temperature (Figure 93) shows an increase of 3 to 5°C as compared to the reference period 1971 to 2000. In contrast, the

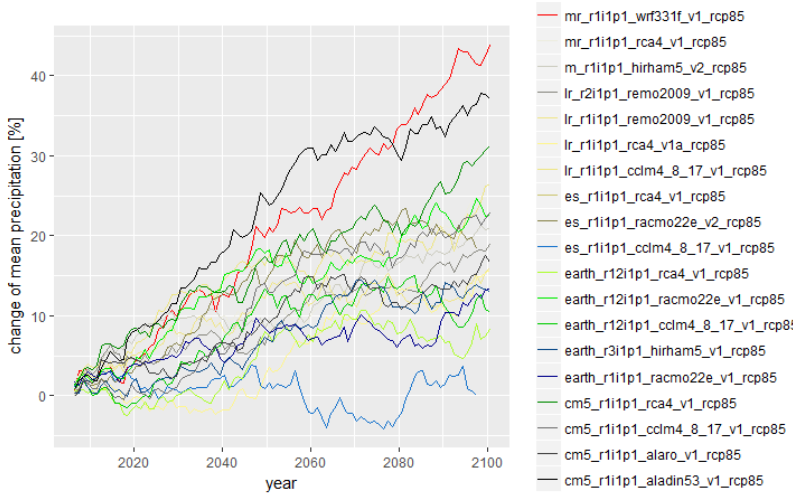

Figure 92: Relative change (%) of the 30-year moving average of the annual precipitation sums in the pilot area Neufahrn bei Freising.

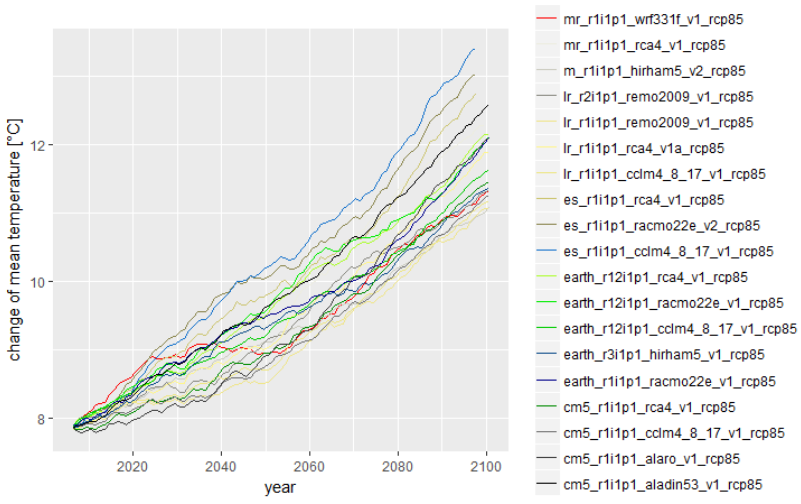

Figure 93: Absolute change of the 30-year moving average of the mean annual temperature (°C) in the pilot area Neufahrn bei Freising.

considered scenarios predict a broad range of possible developments for future annual precipitation amounts. Figure 92 illustrates the 30-year moving average of changes in the mean annual precipitation sums. The amplitude of possible changes ranges between 0% and an increase of annual precipitation by 40%.

In the following, the variations in seasonal precipitation (Table 37), seasonal temperature (Table 38) and yearly Rx1day, CDD and CWD (Table 39) for the Pilot Action 2.5 are shown. The variations are obtained considering the EURO-CORDEX data (§4.2).

Table 37: Changes in seasonal precipitation (mm) in PA2.5 with EURO-CORDEX projections.

		RCP4.5						RCP8.5					
		2021-2050 distribution percentiles			2071-2100 distribution percentiles			2021-2050 distribution percentiles			2071-2100 distribution percentiles		
		50th	25th	75th	50th	25th	75th	50th	25th	75th	50th	25th	75th
Changes in seasonal precipitation (mm)	winter	**20.1**	13.0	25.6	**30.2**	15.7	39.0	**26.9**	11.3	38.7	**51.3**	34.6	58.5
	spring	**21.6**	2.4	28.9	**20.7**	11.8	39.4	**29.5**	12.3	34.8	**47.2**	31.2	63.1
	summer	**1.2**	-5.3	17.7	**12.0**	-4.4	27.5	**11.3**	0.8	22.9	**4.6**	-14.7	29.9
	autumn	**6.2**	-2.7	10.8	**16.0**	4.4	30.7	**11.5**	2.6	33.7	**32.9**	6.7	48.3

Table 38: Changes in seasonal temperature (°C) in PA2.5 with EURO-CORDEX projections.

		RCP4.5						RCP8.5					
		2021-2050 distribution percentiles			2071-2100 distribution percentiles			2021-2050 distribution percentiles			2071-2100 distribution percentiles		
		50th	25th	75th	50th	25th	75th	50th	25th	75th	50th	25th	75th
Changes in seasonal temperature (°C)	winter	**1.3**	1.1	1.8	**2.4**	2.0	2.7	**1.4**	0.9	1.9	**4.1**	3.9	4.6
	spring	**0.8**	0.6	1.3	**1.8**	1.4	2.2	**1.1**	0.9	1.3	**3.4**	2.7	3.7
	summer	**1.3**	1.1	1.4	**1.9**	1.7	2.3	**1.3**	1.0	1.5	**3.6**	3.3	4.3
	autumn	**1.2**	0.9	1.6	**2.2**	1.7	2.5	**1.5**	1.0	1.9	**3.8**	3.3	4.3

Results of Table 37 and Table 38 are in line and consistent with those of Figure 92 and Figure 93, respectively.

Table 39: Changes in yearly Rx1day (mm/day), CDD (-) and CWD (-) in PA2.5 with EURO-CORDEX projections.

		RCP4.5						RCP8.5					
		2021-2050 distribution percentiles			2071-2100 distribution percentiles			2021-2050 distribution percentiles			2071-2100 distribution percentiles		
		50th	25th	75th	50th	25th	75th	50th	25th	75th	50th	25th	75th
Changes in Rx1day (mm)	yearly	**1.6**	-0.4	3.8	**4.3**	1.3	6.6	**3.1**	0.3	5.8	**7.9**	5.8	12.0
Changes in CDD (-)		**-0.3**	-0.8	0.9	**-0.3**	-0.8	0.3	**-0.5**	-1.3	0.1	**-0.8**	-1.6	-1.1
Changes in CWD (-)		**0.1**	-0.5	0.7	**0.5**	0.1	0.7	**0.4**	0.0	1.0	**0.4**	-0.5	1.0

In terms of yearly Rx1day, CDD and CWD the EURO-CORDEX models return:

- for Rx1day, an overall increase compared to current condition (about 8 mm for RPC8.5 for far time horizon
- for CDD, a slight decrease more enhanced for RCP8.5 over 2071-2100
- for CWD, a slight increase more enhanced for RCP4.5 over 2071-2100

5.7. PA3.1 Po river basin, IT

5.7.1. Foreword

This section is about climate change issues in Pilot Action 3.1: Po river basin. Specifically, the pilot area Po river basin (Figure 946) has an area of 74.000 km2 and among those about 71.000 km2 are in Italy, and for a small part in SWÌSS (Toce catchment) and marginally in France. With about 16 million inhabitants, territory represents an exceptionally socio-economical, landscape and geographical varied reality. The aim of the project is to consider this PA as representative of potential conflicts and their possible resolution strategies.

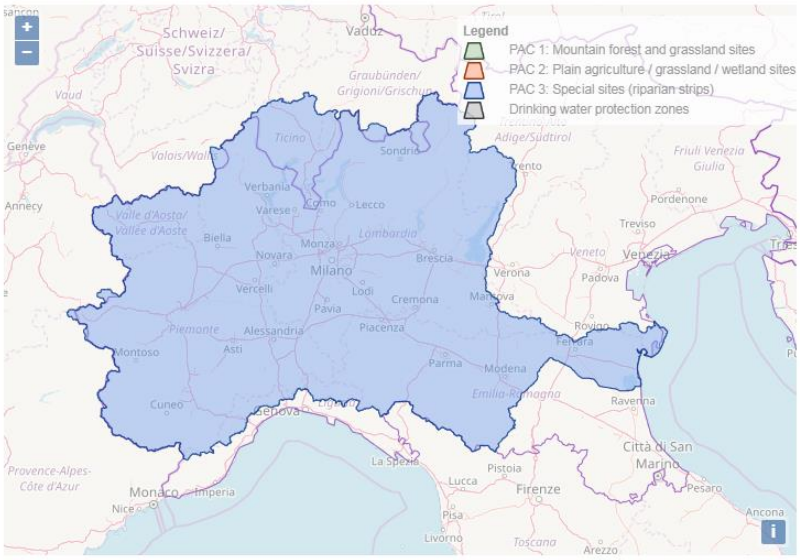

Figure 94: Location of Pilot Action 3.1: Po river basin.

Due to relevance of the area, in recent years several research works and institutional reports have been focused on the analysis of potential variations in weather patterns and associated impacts to which the territory may be exposed under the effects of climate changes (CC).

In this perspective, it is worth noting how the area was the topic of one among the "Special Cases" discussed in National Strategy for Adaptation to Climate Changes (SNACC, Castellari et al., 2014). Moreover, the potential impacts of CC on the area were investigated in Annex 1 of Po River Management Plan (MPPRB, 2016) and within several European research projects (Drought R&SPI (http://www.eu-drought.org/) and Enhance (http://enhanceproject.eu/)).

In the following sections, the main available results concerning current climate characterization, ongoing and future estimated variations in weather patterns and associated impacts are briefly reported.

5.7.2. Previous state-of-the-art framework

5.7.2.1. Current climate

The main results reported in this section are based on the extensive description provided in the SNACC (2014) and MPPRB (2016). The analysis of current conditions allows identifying according the observed values of mean temperature, three reference areas:

- < 5°C for alpine regions and Emilian Apennine;
- 5-10°C mountain areas at intermediate altitude;
- 10-15°C Alpine valleys, lake zone, Maritime Alps and the whole Po Valley.

In this regard, the link between temperature values and elevation is evident. More complex is the definition of homogeneous area in terms of rainfall regime. To this aim, AdBPo (2010) identifies five zones:

- Continental with the highest rainfall cumulative values in summer and lowest in winter; Alpine Region, including the high valleys of the Oglio, Adda and Ticino and the secondary reliefs of the Pre-Alps.
- Alpine sub-coastal type characterized by two peaks (higher in spring than in fall) and two minimums (lower in winter than in summer); it includes the plan area, the Prealpine area in Lombardy up to Toce basin and high part of the Aosta Valley.
- Western sub-coastal type characterized by two peaks (higher in spring than in winter); it includes the whole western part of the Po Basin, from Ticino to Tanaro, excluding Dora Riparia valley and the reliefs of the Maritime Alps and Monferrato.
- Sub-coastal Po Valley type characterized by two similar maxima and two minimum rainfall values: it includes the entire plain area from Pre-Alps to Po River (up to Tanaro valley in western part).
- Sub-coastal Apennine type characterized by two maxima (higher in fall than in spring) and two minimums (lower in summer than in winter); it includes a portion of the Maritime Alps and the Apennine mountains, excluding the lower Modena areas.

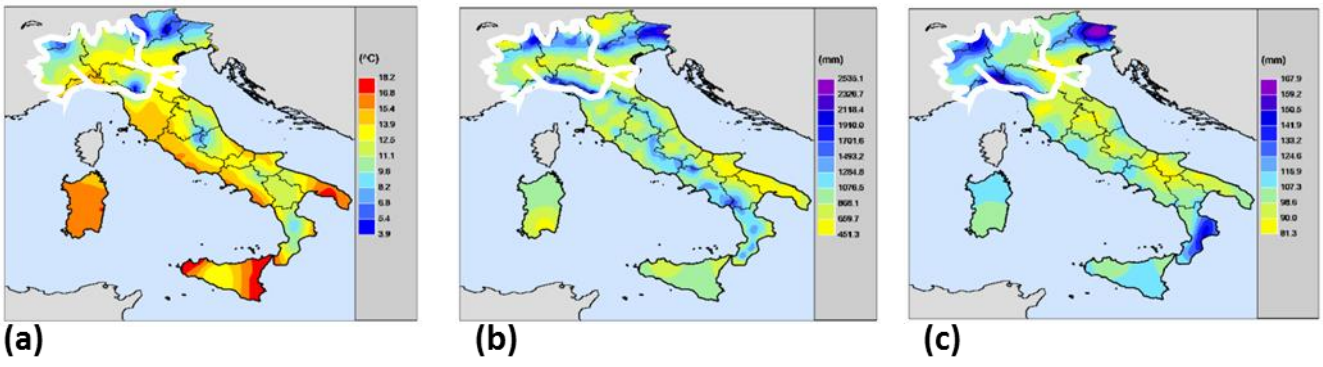

Figure 95: Thermometric and precipitation regime in Italy on the time span 1961-1990: (a) mean yearly temperature; (b) mean cumulative yearly precipitation; (c) average of maximum daily precipitation (scia.ispra.it) (white line identifies the Po River Basin).

Such patterns represent a frame of current conditions; nevertheless, remarkable efforts have been devoted to assess the presence and the extent of statistically significant trends in weather forcing

and associated hydrologic variables. To this aim, on national scale, Brunetti et al. (2006) assess an increase in temperature about equal to 1°C with slight spatial variations between 1800 and 2003 and sharper growth after 1980 and during summer and spring. Fioravanti et al. (2015) retrieve increases of comparable extent analysing 1961-1990 time span. Moreover, on the last 30 years, every annual temperature value (excluding 1991) is higher than mean on 1961-1990 (Figure 95). Concerning precipitation, "noisier" signals are observed. Brunetti et al. (2006) assess decreases of about 5% at yearly scale (9% for spring). More specifically on Po River Basin, Cacciamani et al. (2010), for example, observe an increase about equal to 2°C on Emilia Romagna (1960-2010). On the other side, regarding precipitation, for Northern Italy, Toreti et al. (2009) estimate a slight decrease in winter precipitation (1.47 mm/year) not confirmed on the other seasons while, for Po river basin, Cacciamani et al. (2008) evaluate an increase in magnitude of rainfall events but decreases quite remarkable in annual cumulative values (-20%) and Jan-Aug values (-35%) (time span 1975-2006).

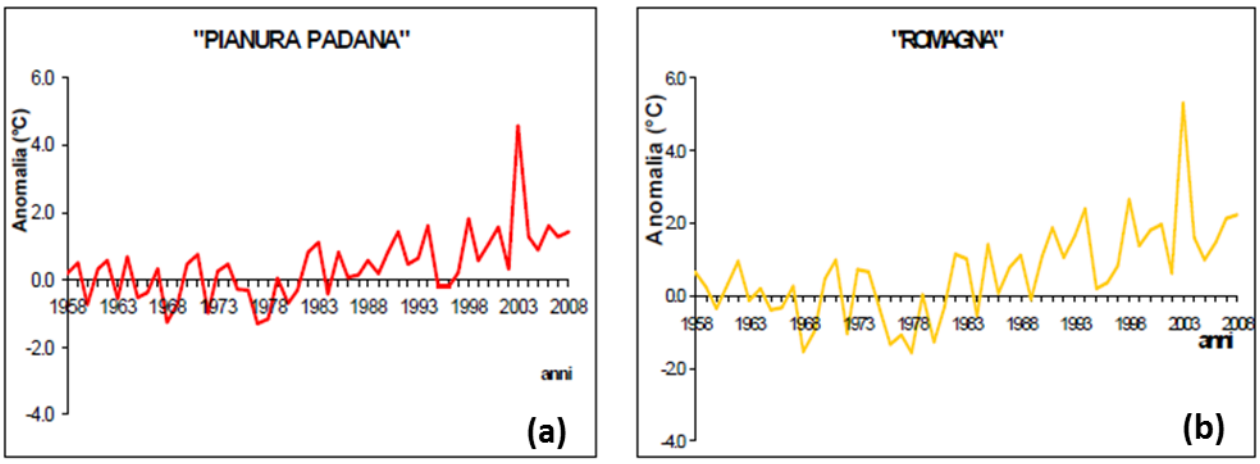

Figure 96: Yearly maximum temperature trend on Po Valley and Romagna Region (Tibaldi et al., 2014).

Such variations induce changes also in hydrological variables. Cacciamani et al. (2008) monitor a significant decrease in the average flow rate at river closure section of Pontelagoscuro. It is about 20 % on annual basis and 45 % in the summer season (1975-2006 period). However, considering a larger time span, not statistically significant variations are observed (1923-2010).

The reduction in average river flow rate jointly acting with the increase in sea level rise (about 30 cm/100 years for Northern Adriatic Sea, less than global average) and subsidence phenomena (7-8 mm/year; ARPA-DRST, 2011) entail frequent and relevant occurrence of salt intrusion phenomena at Po Delta. It reaches about 20 km during summer droughts against a mean value, during Seventies, of about 2 km inducing relevant issues not only for irrigation but also drinking water supply (for example, in Ferrara area) and withdrawal for cooling systems of thermoelectric power plants.

The ongoing variations are recognized also affecting in substantial way the high-altitude environments ("hot-spots" of climate changes at global scale). Regarding snowfalls, a decreasing trend is assessed in snow cover over the Alps in 1920-2005 time interval; it is more relevant on low altitude

(up to 40%) and in more recent times (1959-2000) (Valt et al., 2005). At the same time, the observed decrease in Alpine glaciers interested an extension about equal to 50% (1850 vs 2000) (Zemp et al., 2008). Also, in this case, the variations appear more prominent in recent years; for Lombardy, for example, they are about 100m on 1980-2000 time span. In this perspective, extreme high-temperature events, as 2003 heatwaves, are able to induce reductions (5-10%; Climalpture, 2010) in permafrost not recovered in following years.

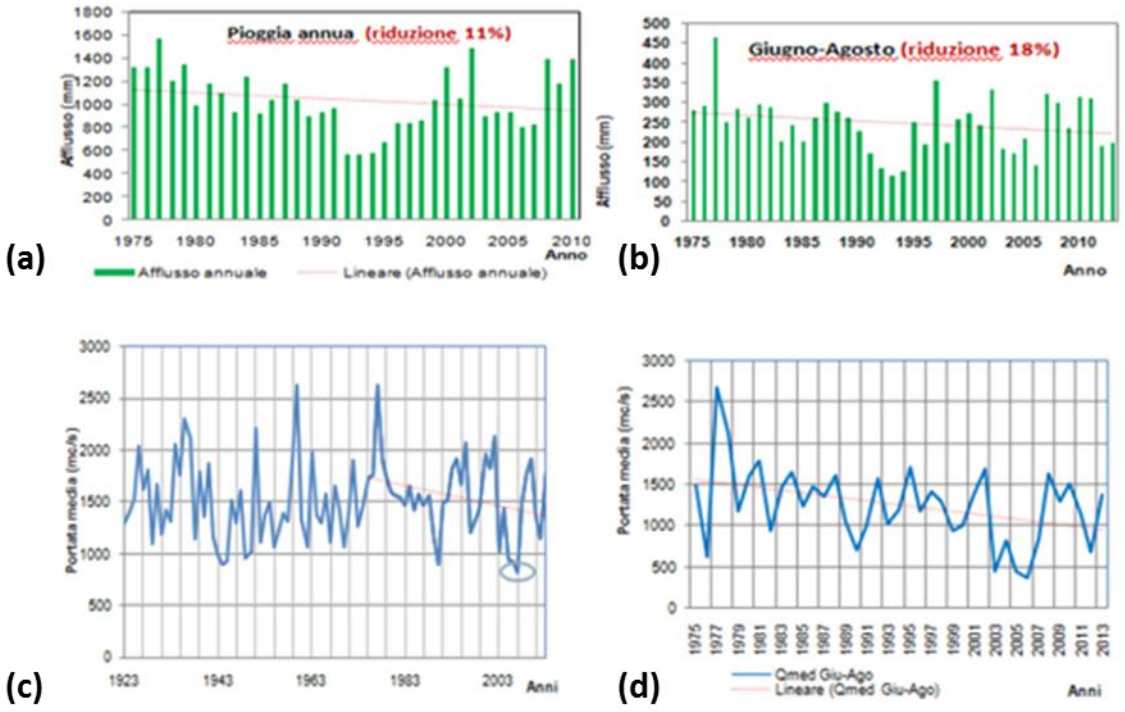

Figure 97: (a) annual precipitation on Po River Basin (estimated decrease 11% on 1975-2010); (b) summer precipitation on Po River Basin (estimated decrease 18% on 1975-2010); (c) average yearly water flow rate at Pontelagoscuro section (1923-2010); (d) average summer water flow rate at Pontelagoscuro section (1975-2010) (Tibaldi et al., 2014).

5.7.2.2. Future climate

In the previous paragraph, the main findings about ongoing trends have been displayed on Pilot Action areas. However, in order to put in place effective and adequate adaptation counter measurements, assessments about future evolutions of weather forcing and associated hydrologic variables have a crucial role.

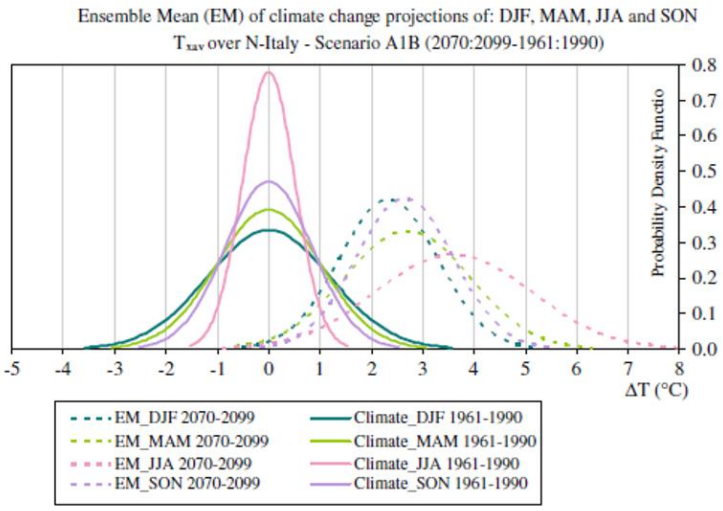

Figure 98: PDFs of CC projections of multi-model ensemble mean of seasonal Txav over N-Italy (mean over the stations), period 2070–2099 relative to 1961–1990, scenario A1B (from Tomozeiu et al., 2014).

For what concern the main findings achieved through displayed climate simulation chains on PA area, Fourth and Fifth IPCC reports, using results provided by ensembles, consider the area included in a "transition zone" between Mediterranean South area (where a decrease is expected in cumulative values) and North-Continental (where the opposite could occur). Nevertheless, an increase in heavy rainfall events is recognized likely. More robust findings regard temperatures with expected increases ranging from 2° to 4°C. Adopting statistical downscaling approaches, Tomozeiu and co-authors in different works (2007, 2011 and 2014) evaluate on the area or sub-regions the existence of future trends in weather forcing. On the Emilia Romagna, they assess a significant increase in both maximum and minimum temperatures, associated with a reduction in frost days and an increase in the duration of heat waves. Moreover, as example in Figure 100 are reported the expected variations in pdf of maximum temperature for North Italy at seasonal scale (2070-2099 vs 1961-1990).

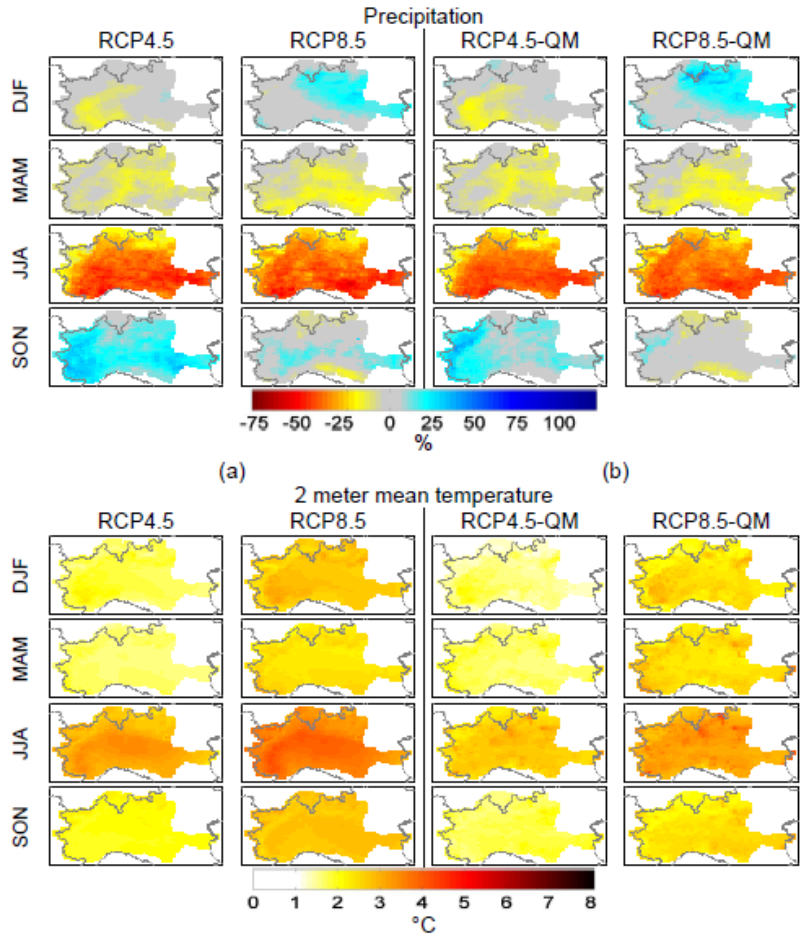

Figure 99: Anomalies in (a,b) seasonal precipitation in % and (c,d) two meter mean temperature in ◦C over Po River basin, for the period 2041-2070. Left side (a,c) refer to raw CMCC-CM/COSMO-CLM outputs; right side (b,d) to the bias corrected climate (from Vezzoli et al., 2015).

In recent years, REMHI (Regional Modelling and geo-Hydrological Impacts) Division of CMCC Foundation has deeply investigated the expected variations in hydrological regime of the area (Vezzoli et al., 2015, 2016).

To this aim, RCP4.5 and RCP8.5 are used to estimate future concentration gases. They force the Global Climate Model, CMCC_CM (Scoccimarro et al., 2011) with a horizontal resolution of about 80 km; it is dynamically downscaled using the RCM COSMO_CLM model at a horizontal resolution of 8 km, in the optimized suite on Italy carried out by Bucchignani et al. (2015). They show how, in terms of average values, the model performances are substantially in line with those achieved using ensemble approaches (e.g. EURO-CORDEX or ENSEMBLE experiments) while, in terms of extreme values, they usually perform better than the ensemble approaches also thanks to their higher resolution (Zollo et al., 2015). Lastly, model outputs are bias-corrected (BC) using a parametric quantile mapping approach. Main findings in terms of temperature and precipitation at seasonal scale are reported in Figure 99 and Figure 100 respectively for 2041-2070 and 2071-2100 vs 1982-2011. From these ones, it is clear how an increase could be expected and how it could be regulated as by time horizon (the farthest the time horizon, the higher the growth), as by concentration scenario (the more severe the scenario, the higher the increase). The expected variations, quite homogeneous on the area, are about 2-4°C on 2041-2070 an up to 6-7°C (in summer). In this regard, the adoption of bias correction approach appears affecting in minor way the expected changes. Precipitation projections deeply differ at seasonal scale; during the summer, a strong reduction (mainly under

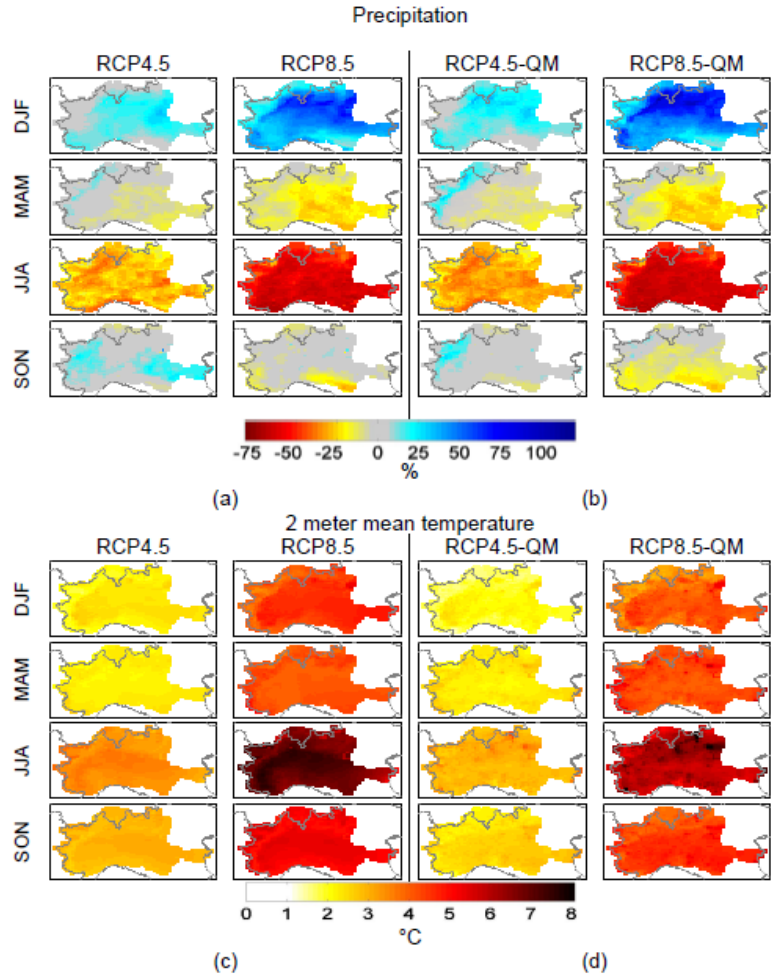

Figure 100: Anomalies in (a, b) seasonal precipitation in % and (c, d) two-meter mean temperature in °C over Po River basin, for the period 2071-2100. Left side (a, c) refer to raw CMCC-CM/COSMO-CLM outputs; right side (b, d) to the bias corrected climate (from Vezzoli et al., 2015).

RCP8.5 and farthest time horizon) is assessed; it is less evident for Spring while the opposite is estimated for the "wet season" in the area with increases quite significant in special way during the Winter and RCP8.5. The output variables (temperature and precipitation) of climate simulation chain are used to couple the hydrological module at daily timescale.

5.7.3. Assessed changes in the hydrological patterns

The hydrological module includes a spatially distributed and physically based hydrological model, TOPographic Kinematic Approximation and Integration (TOPKAPI, Liu and Todini, 2002) and, to account for the anthropogenic pressure on Po River basin (Garcia-Ruiz et al., 2011), a water balance model, River Basin SIMulation (RIBASIM; Delft Hydraulics (2006)). Such tools have been calibrated and validated on control period through observations by ARPAE as they are used for monitoring the hydraulic regime on PA areas.

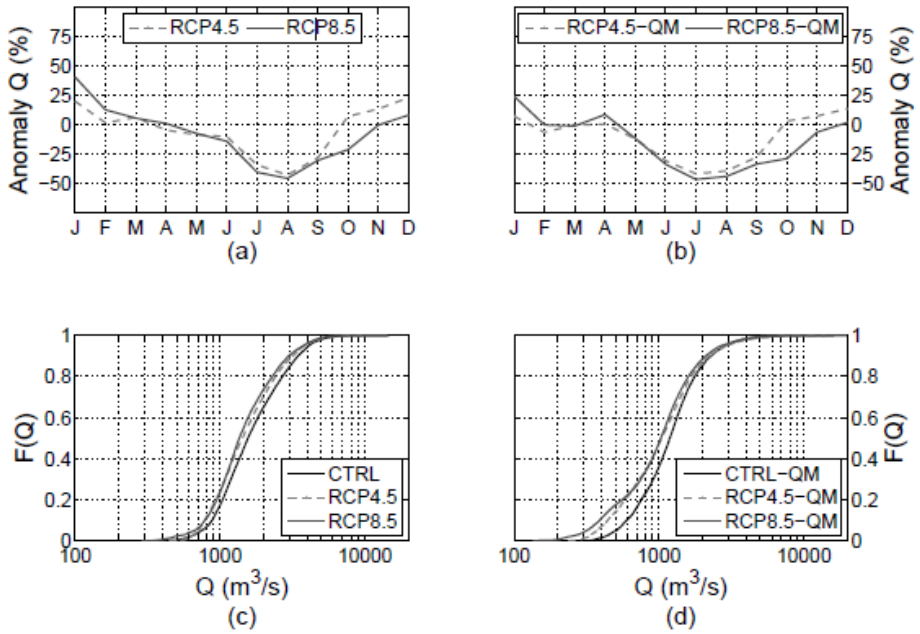

Figure 101: Anomaly (in %) in monthly average discharge (a, b) and cumulative distribution function (c, d) of Po River discharges at Pontelagoscuro under RCP4.5 (dashed grey) and RCP8.5 (continuous grey) scenarios, for the period 2041-2070 with respect to 1982-2011 (in black in panels (c, d)). Discharges simulated using raw RCM outputs are in panels (a, c) and those obtained from bias corrected climate are in panels (b, d) (from Vezzoli et al., 2015).

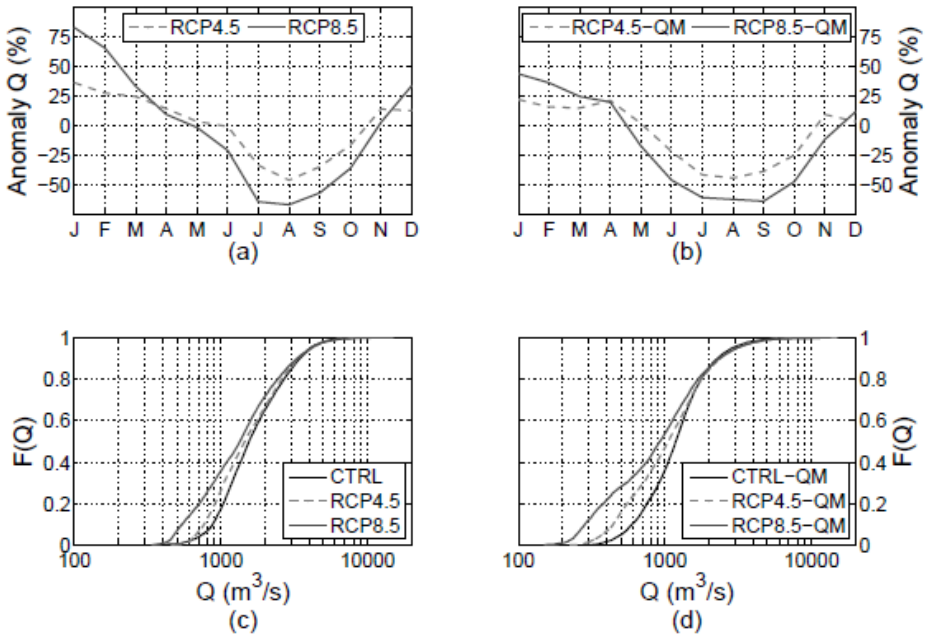

Figure 102: Anomaly (in %) in monthly average discharge (a, b) and cumulative distribution function (c, d) of Po River discharges at Pontelagoscuro under RCP4.5 (dashed grey) and RCP8.5 (continuous grey) scenarios, for the period 2071-2100 with respect to 1982-2011 (inblack in panels (c, d)). Discharges simulated using raw RCM outputs are in panels (a, c) and those obtained from bias corrected climate are in panels (b, d) (from Vezzoli et al., 2015).

Figure 101 reports the changes (2041-2070 vs 1982-2011) in Po River discharge at Pontelagoscuro in terms of monthly anomaly (a, b) and CDF (c, d) considering both scenarios and raw (a, c)/bias corrected (b, d) climate data. Simulations show a general agreement on the shape of anomalies while more differences are present in the anomaly magnitude. In particular, from October to September, RCP4.5 (-QM) simulation returns more consistent discharges with respect to RCP8.5 (-QM) one, while between January and March the behaviour is opposite. This is, in agreement with the associated precipitation anomalies, higher in autumn for RCP4.5 (-QM) and in winter for RCP8.5 (-QM). A discharge reduction is projected in dry season (April-September) up to 40% in August. Similar results are retrievable in Coppola et al. (2014) and Ravazzani et al. (2015) projections at 2050 of Upper Po River discharges. Moreover, the slight differences between the two scenarios are induced by short term time horizon investigated. The results concerning the comparison between the 30 years at the end of XXI century and 1982-2011 control period are reported in Figure 102. Similar patterns arise between the two RCPs while more differences are found in the magnitude of variations. In particular, from April to November, RCP4.5 (-QM) simulations show higher discharges than RCP8.5 (-QM), while between December and March the behaviour is opposite, in agreement with the precipitation anomaly. Between March and October, the discharges reduce of 11% (14%) under RCP4.5 (-QM) and of 27% (29%) under RCP8.5 (-QM) on average but with values exceeding 40% (50%) in August under RCP4.5 (RCP8.5). In this perspective, the role of temperature increase that reduces the solid fraction of the precipitation, increasing the winter runoff (less snow is accumulated) and reducing the spring snow-melting (Garcia-Ruiz et al., 2011) is recognized relevant.

Finally, for what concern Alpine Region, in terms of snow cover, future scenarios at 2100 estimate an average reduction of 35 %. The persistence of the snowpack could be significantly reduced: about 35 % for each degree of increase in average temperature below 1,400 m, 15 % up to 1850 and 12 % at 2,300 m (Beniston 2007). For elevation less than 500m, the snowpack could completely disappear (Jacob et al. 2007). The total extent of glaciers could be reduced of about 80% at 2060 (compared to 1971-2000 time span) under the effect of temperature increase (Zemp et al. 2006; EEA report, 2008).

5.7.4. PROLINE CE development for PA3.1

This section shows the variations in seasonal precipitation (Table 40), seasonal temperature (Table 41) and yearly Rx1day, CDD and CWD (Table 42) for the Pilot Action 3.1: Po River Basin, IT. The variations are obtained considering only the EURO-CORDEX data (§4.2) for Pontelagoscuro.

Table 40: Changes in seasonal precipitation (mm) in PA3.1 with EURO-CORDEX projections.

		RCP4.5						RCP8.5					
		2021-2050 distribution percentiles			2071-2100 distribution percentiles			2021-2050 distribution percentiles			2071-2100 distribution percentiles		
		50th	25th	75th	50th	25th	75th	50th	25th	75th	50th	25th	75th
	winter	**6.8**	0.8	16.4	**14.0**	5.9	21.8	**8.7**	1.2	21.3	**13.8**	5.3	24.0
	spring	**-6.7**	-17.1	9.1	**1.8**	-9.2	7.6	**9.5**	-15.4	25.2	**-0.5**	-18.9	7.9

Changes in seasonal precipitation (mm)	summer	-4.0	-14.2	10.0	0.8	-9.4	15.8	3.5	-13.3	19.6	-30.3	-39.5	0.0
	autumn	-2.8	-9.1	16.6	7.5	2.3	21.2	12.0	-4.6	18.9	13.1	5.1	30.4

Table 41: Changes in seasonal temperature (°C) in PA3.1 with EURO-CORDEX projections.

		RCP4.5						RCP8.5					
		2021-2050 distribution percentiles			2071-2100 distribution percentiles			2021-2050 distribution percentiles			2071-2100 distribution percentiles		
		50th	25th	75th	50th	25th	75th	50th	25th	75th	50th	25th	75th
Changes in seasonal temperature (°C)	winter	1.4	1.0	1.5	2.2	1.9	2.5	1.4	1.1	1.7	4.0	3.6	4.2
	spring	0.9	0.6	1.2	1.8	1.5	2.1	1.0	0.9	1.3	3.2	2.9	3.7
	summer	1.5	1.3	1.8	2.2	2.0	2.7	1.5	1.3	1.8	4.4	4.0	5.2
	autumn	1.4	0.9	1.5	2.3	1.9	2.5	1.4	1.3	1.9	4.2	3.6	4.5

Table 42: Changes in yearly Rx1day (mm/day), CDD (-) and CWD (-) in PA3.1 with EURO-CORDEX projections.

		RCP4.5						RCP8.5					
		2021-2050 distribution percentiles			2071-2100 distribution percentiles			2021-2050 distribution percentiles			2071-2100 distribution percentiles		
		50th	25th	75th	50th	25th	75th	50th	25th	75th	50th	25th	75th
Changes in Rx1day (mm)	yearly	4.3	-4.2	6.7	3.6	1.6	6.2	5.0	1.5	6.1	8.6	5.7	12.8
Changes in CDD (-)		0.2	-0.7	2.4	-0.8	-1.8	2.3	0.3	-0.9	1.7	2.5	0.8	4.3
Changes in CWD (-)		-0.2	-0.4	0.3	-0.1	-0.4	0.3	-0.2	-0.7	0.2	-0.6	-1.0	-0.3

Table 40 returns an increase in seasonal precipitation mainly during winter and autumn with a decrease in summer. The absolute values of these variations depend on the time period and concentration scenario considered. Moreover, the signs of these variations are in agreement with previous studies (Figure 99 and Figure 100).

In terms of temperature (Table 41), generally a widespread increase can be detected for all time periods and concentration scenario with values up to 4.5 °C and in line with the previous projections performed by CMCC (Figure 99 and Figure 100).

Finally, for Rx1day an increase can be projected with concentration scenario and time period while as for CDD and CWD slight variations can be observed excepting for CDD over 2071-2100 under RCP8.5.

5.8. PA3.2 Along Danube Bend, HU2

5.8.1. Foreword

This section is about climate change issues in Pilot Action 3.2: Along Danube Bend. Specifically, the pilot area is located in the northern part of Central Hungary, in section of Danube between Szob and Tass. It includes the municipality Budapest, the Szentendre Island, in north of it, and the Csepel Island, in south of the capital. On these islands are located the two most important bank-filtered drinking water resources of Hungary, that provide the drinking water supply of the capital.

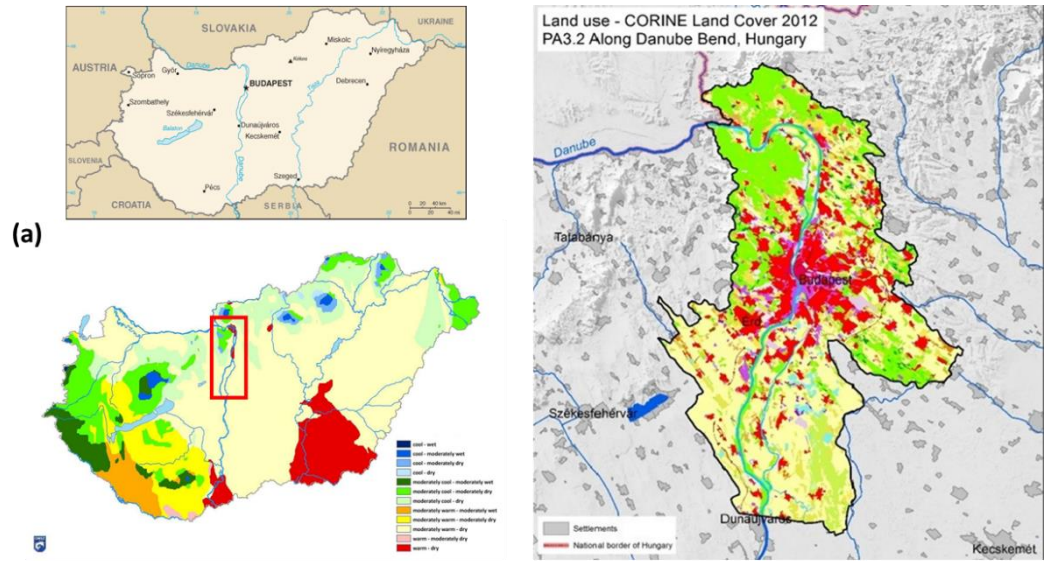

Figure 103: (a) - (b) Location of the pilot area 3.2, Along Danube Bend; (c) climatic regions in Hungary (from Hungarian Meteorological Service [OMSZ], after György Péczely; www.met.hu).

This section is partly included in paragraph 5.4 and sub-paragraph 5.4.2. Details about the predicted changes in hydrological patterns for the pilot site in hand are reported in the following paragraph.

5.8.2. Assessed changes in the hydrological patterns

In the Danube river basin in Germany and Austria, a 30% decrease in summer low water is possible, which can have an impact on small water flows in the Hungarian section of the river. In the winter semester, a larger proportion of the current precipitation may be rainfall, especially in lower-lying river basins, and therefore some increase in winter runoff cannot be excluded, but this does not compensate the decrease in summer runoff. Similar changes can be expected at the Tisza and its tributaries, i.e. the decrease of medium and low water discharge, which can be significant in unfavourable circumstances. (National Water Strategy 2013).

The utilizable water resources compared to water resources appearing in the country is significantly fewer and it is affected by numerous mitigating factors, such as temporal variability (floods that are a significant part of the runoff cannot be utilized due to lack of storage), territorial accessibility or its shortage and ecological water demand.

As a result of climate change, the effects of warming increase territorial and temporal extremes, which reduce the utilizable resources and increases our vulnerability to the amount of water arriving from abroad. The utilization of surface water is currently around 30% on the average during the critical August conditions. However, it should be noted that a significant increase in agricultural demand is expected, and in particular, the demand for irrigation and aquaculture may increase (may reach 50%). (Somlyódy 2011)

As a result of the privatization of land, big farms have split, land sizes and production patterns have changed. Most of the irrigation systems established have not been further operated, their technical condition has deteriorated and ruined. The size of irrigated land has decreased significantly, at present it is 100.000 ha, 1.8% of the total cultivated area, which is still very low in international comparison. It is necessary to increase the size of irrigated areas in order to properly exploit our intensive cultivated areas, to raise production levels and to maintain and increase the competitiveness of our agricultural production. In view of the fact that the precipitation conditions of our country are in many cases at the border in terms of the water demand of our crops, cultivation is risky without irrigation. In years with low precipitation, there is significant harvest loss due to drought damage. As a result of climate change, the security of agricultural production decreases and its risk increases.

During the quantitative evaluation of surface water bodies the second Water Resources Management Plan determines the 80% water discharge of August (natural water resources: Qnat) and the ecological low water discharge (Qecol) that are to be left in the watercourse and on the basis of which the utilizable resources (Qutil) can be determined and water resource management assessment for water bodies without ecological or natural water resources can be carried out. From the proportion of water drainage and the utilizable water resources the availability of ecological demand can be determined and on its basis the water body can be classified in quantitative terms. (VKGTT 20174)

It is necessary to improve the current technical status of surface irrigation systems established to satisfy increasing demands as well as to modify the operating method. Public utilization is very low among the surface water uses.

Regarding surface water utilization and on the basis of the figures it is not a strained situation neither in the Tisza, nor in the Danube water catchment. At the same time, we need to prepare for unfavourable changes, increasing demands, decreasing water resources and quality degradation. The importance of retention and water transfer is increasing. During summer there will be no water resources available on small rivers without retention, while the otherwise unfavourable hydrological conditions of retention will deteriorate.

[4] VKGTT: Territorial Water Supply Management Plan

5.8.3. PROLINE CE development for PA3.2

Variations in seasonal mean temperatures (˚C) and precipitation (%) for Along Danube Bend area are shown in Table 43. Relevant data for Along Danube Bend area were selected by coordinates using ArcMap.

Table 43: Spatially averaged seasonal changes in temperature (°C) and precipitation (%) for Along Danube Bend area. Mean values were calculated from the 51 grid points which are within the pilot area.

		RCP4.5						RCP8.5					
		2021-2050			2071-2100			2021-2050			2071-2100		
		distribution percentiles			distribution percentiles			distribution percentiles			distribution percentiles		
		50th	25th	75th	50th	25th	75th	50th	25th	75th	50th	25th	75th
Changes in seasonal temperature (˚C)	winter	1.6	1.1	1.9	2.5	2.09*	3.0	1.5	1.0	1.9	4.3	3.9	4.7
	spring	1.0	0.7	1.3	1.9	1.4	2.5	1.2	1.0	1.4	3.4	2.5	3.8
	summer	1.4	1.2	1.5	2.0	1.7	2.8	1.3	1.2	1.7	4.0	3.4	4.8
	autumn	1.1	1.0	1.5	2.1	1.5	2.5	1.5	0.9	1.8	3.6	3.2	4.3
Changes in seasonal precipitation (%)	winter	18.8	11.6	25.2	20.9	15.8	32.1	14.5	11.4	18.3	31.6	22.8	49.2
	spring	13.8	-1.7	27.2	19.2	9.1	28.3	8.8	3.3	20.6	25.1	16.3	37.1
	summer	0.3	-13.5	11.5	4.0	-8.0	22.7	6.5	-1.1	14.1	-6.8	-18.3	5.0
	autumn	-4.8	-12.4	2.3	10.4	4.5	18.3	7.7	2.3	20.5	14.3	2.9	31.3

According to Table 43, one can see that there are small differences between temperature changes for the near future period (2021-2050) in the two different RCPs (RCP4.5 and RCP8.5). For the far future period (2071-2100) the RCP8.5 scenario is predicting a much more significant increase than for period 2021-2050, while the RCP4.5 scenario is predicting a more balanced temperature increase for the 21th century.

Related to changes in precipitation both RCPs are predicting significant seasonal differences between changes in precipitation against the reference period, but both simulations are predicting that the winter season will become significantly wetter, and autumn will likely become drier at the end of the 21th century.

A comparison of two results of climate simulation made by ELU in the framework of CECILIA project and the results of EURO-CORDEX simulation is shown in Table 44.

Table 44: Comparison of CECILIA (in light red) and EURO-CORDEX (in light green) output data for temperature and precipitation changes.

		State-Of-The-Art (CECILIA mean)		EURO-CORDEX (RCP8.5, median values)	
		2021-2051	2071-2100	2021-2050	2071-2100
Changes in seasonal temperature (°C)	winter	1.3	2.5	1.5	4.3
	spring	1.3	2.5	1.2	3.4
	summer	0.7	3.5	1.3	4.0
	autumn	0.7	2.7	1.5	3.6
Changes in seasonal precipitation (%)	winter	-7.5	14.7	14.5	31.6
	spring	-17.0	-12.5	8.8	25.1
	summer	-12.8	-12.5	6.5	-6.8
	autumn	-6.5	4.8	7.7	14.3

An increase in annual mean temperature is predicted for the 21th century, therefore, in the pilot area the demand for irrigation will probably increase. Also, climate change is likely to cause a decrease in total annual runoff, which is highly disadvantageous for maintaining water supply in the area. Thus, concerned water managements will have to consider that water resources are likely to decrease in the following decades, and at the same time, the demand for water for irrigation and probably the demand for drinking water will increase.

Climate change is expected to increase the size of water scarcity areas, mainly in the karstic areas of the Transdanubian Hills, at the North Hungarian Mountains and the Great Plains, at areas far from large rivers. Water shortage, however, raises competition and conflicts, and leads to restrictions, or to illegal water use in the absence of effective control, as well as it increases the importance of water transfer and storage (which is not always justified). (Somlyódy 2011). The decline in groundwater resources can be mentioned as a general trend, which raises the importance of soil storage and stresses the urgency of its application. However, it becomes more and more obvious that groundwater should not be considered as a water supply reserve alone but should also be protected for its environmental value. Groundwater plays an essential role in the hydrological cycle, it has a critical role in maintaining wetlands and watercourses and serving as a buffer in dry periods. Local reduction of extreme weather phenomena and more balanced provision of available water resources should also play an increasing role in our water management.

Drinking water demands can be safely met at present and in the future since they are expected to have a slight decline, but spatial rearrangement and rearrangement according to the types of resources are possible and even desirable. In addition to the current water consumption, it is not expected that the level of water level after the completion of mining will be such that higher springs will operate again.

6. Conclusion

This report provides an overview about expected changes under Climate Change over Central Europe with a special focus on the Pilot Action sites considered in the PROLINE CE project. In this sense, data provided by an ensemble of different climate modelling chains included in EURO-CORDEX initiative and characterized by very high horizontal resolution (0.11°, about 12 km over the Europe) are adopted to evaluate expeditiously future changes in quantity and quality of water resources and occurrence and severity of hydrological/hydraulic hazards. The ensemble allows accounting for uncertainties currently associated to climate projections (also function of time horizon of interest). For the Pilot Action sites, the report tries comparing state-of-the-art data with EURO-CORDEX data to retrieve analogies or not between these data.

Over Central Europe domain, in general, the increase in temperature is clearly detectable over the entire domain; nevertheless, it results strictly linked to the time horizon (the farthest, the higher the increase) and concentration scenario (the more severe, the highest the increase). On the other hand, changes in seasonal cumulative rainfall pattern do not return clear trends or spatial patterns. Moreover, climate simulations display significant differences in projections in terms of magnitude and direction of climate signals. However, in terms of rainfall distribution, an increase in Consecutive Dry Days can be expected in special way in the southern part of the CE domain while an increase in CWD is assessed in high altitude areas of Alpine Region. Finally, the increase in maximum daily rainfalls clearly arise over a large part of the domain in special way under the more pessimistic, but business as usual, RCP8.5 scenario.

Such variations could affect the availability of water resources and weather-induced hazards through different feedbacks mechanisms and with different magnitude according the area, the time horizon and the selected scenario. In particular, strong increases in evaporative atmospheric demand could be expected over the entire hydrological year. Nevertheless, it could be fulfilled by soil water also taking into account the actual rainfall regime and the expected variations (considered in this work), the soil texture and current/future land use (out of the topic). Furthermore, the strong variations expected in high altitude areas could entail strong variations also in snow dynamics (duration of snow cover, snow elevation during the year, melting mechanisms and timing). Of course, it could strongly affect water balances and occurrences of hydrological hazards also in areas close to those directly interested by such variations.

In the work, the findings are reported in terms of variations comparing the outputs of climate simulations on future and current period under the assumption that any bias could be quite equivalent (no time varying) and then could be cancelled when the simulations are considered in terms of anomaly. Nevertheless, in more complex simulation chains in which the findings of climate simulations are used as input for impact studies, such approach could be not applicable and statistical approaches are used in attempt to remove systematic biases.

7. References

- AdBPo (Autorita di Bacino del fiume Po) (2010). Piano di gestione del distretto idrografico del fiume Po. Autorita di Bacino del Fiume Po. Parma.
- Ahmed, S., De Marsily, G. 1987. Comparison of Geostatistical Methods for Estimating Transmissivity Using data on Transmissivity and Specific Capacity. Water Ressources Research, 23 / 9
- Allen, R.G., Pereira, L.S., Raes, D. Smith, M. 1998. Crop evapotranspiration - Guidelines for computing crop water requirements - FAO Irrigation and drainage paper 56. FAO - Food and Agriculture Organization of the United Nations, Rome.
- ARPAV-DRST, 2011 - L'innalzamento del mare nel Delta del Po - Contributo a incontro tematico scarsità e cambiamenti climatici. Autorità di Bacino del fiume Po, 23/06/2011 - http://www.adbpo.it/onmulti/ADBPO/Home/PianodiBilancioIdrico/Informazioneconsultazioneepartecipazione/artCatPBIPartecipazioneattivaprimocicloaprile-luglio2011.8407.1.40.1.html
- Bakonyi, P. (2010): Flood and drought strategy of the Tisza river basin. VITUKI, Budapest, www.icpdr.org/icpdr-files/15494
- Beniston, M., Stephenson, D., Christensen, O., Ferro, C., Frei, C., et al, 2007. Future extreme events in European climate: an exploration of regional climate model projections. Climatic Change 81 (Suppl. 1), 71–95.
- Bíró Nagy, A., Boros, T. (2011): Climate Change Policy in Hungary. Friedrich Ebert Stiftung Büro Budapest
- Blanka, V., Mezősi, G., Meyer, B. (2013): Projected changes in the drought hazard in Hungary due to climate change. IDŐJÁRÁS, Quarterly Journal of the Hungarian Meteorological Service. Vol. 117, No. 2, April – June, 2013, pp. 219–237
- BMU (2018): Klimaschutzziele in Zahlen: Klimaschutzziele Deutschland und EU. https://www.bmu.de/fileadmin/Daten_BMU/Download_PDF/Klimaschutz/klimaschutz_in_zahlen_klimaziele_bf.pdf (May 9th, 2018)
- Breugem W.P., Hazeleger W. e Haarsma R.J. (2007) Mecha- nisms of northern tropical Atlantic variability and response to CO2 doubling. Journal of Climate vol 20(11): 2691-2705.
- Brunetti, M., Maugeri, M.. Monti, F., Nanni, T. (2006). Temperature and precipitation variability in Italy in the last two centuries from homogenized instrumental time series, Int. J. Climatol., 26, 345-381. doi: 10.1002/joc.1251.
- Bubnova, R.; Hello, G.; Benard, P.; Geleyn, J. (1995): Integration of the Fully Elastic Equations Cast in the Hydrostatic Pressure Terrain - Following Coordinate in the Framework of the ARPEGE/ Aladin NWP System. Monthly Weather Review, 123, pg. 515-35.
- Bubnova, R.; Hello, G.; Benard, P.; Geleyn, J. (1995): Integration of the Fully Elastic Equations Cast in the Hydrostatic Pressure Terrain - Following Coordinate in the Framework of the ARPEGE/ Aladin NWP System. Monthly Weather Review, 123, pg. 515-35.
- Bucchignani, E.; Montesarchio, M.; Zollo, A.L.; Mercogliano, P. High-resolution climate simulations with COSMO-CLM over Italy: performance evaluation and climate projections for the 21st century. International Journal of Climatology 2015 doi: 10.1002/joc.4379.

- Cacciamani, C., Tibaldi, S. and Pecora, S. (2008). Quanto il clima pesa sul bacino del Po. Available at http://www.arpa.emr.it/documenti/arparivista/pdf2008n3/CacciamaniAR3_08.pdf
- Cacciamani, C., Tomozeiu, R. and Pavan, V. (2010). Cambiamenti climatici, impatti e adattamento. Ecoscienza Numero 2, Anno 2010.
- Castellari S., Venturini S., Ballarin Denti A., Bigano A., Bindi M., Bosello F., Carrera L., Chiriacò M.V., Danovaro R., Desiato F., Filpa A., Gatto M., Gaudioso D., Giovanardi O., Giupponi C., Gualdi S., Guzzetti F., Lapi M., Luise A., Marino G., Mysiak J., Montanari A., Ricchiuti A., Rudari R., Sabbioni C., Sciortino M., Sinisi L., Valentini R., Viaroli P., Vurro M., Zavatarelli M. (a cura di.) (2014). Rapporto sullo stato delle conoscenze scientifiche su impatti, vulnerabilità ed adattamento ai cambiamenti climatici in Italia. Ministero dell'Ambiente e della Tutela del Territorio e del Mare, Roma.
- Castro, M., Fernandez, C.; Gaertner, M.A. (1993): Description of a mesoscale atmospheric numerical model. Mathematics, Climate, and Environment, Rech. Math. Appl. Ser., 27, pg. 230-153.
- Castro, M., Fernandez, C.; Gaertner, M.A. (1993): Description of a mesoscale atmospheric numerical model. Mathematics, Climate, and Environment, Rech. Math. Appl. Ser., 27, pg. 230-153.
- Christensen JH, Christensen OB. 2007. A summary of the PRUDENCE model projections of changes in European climate by the end of this century. Climatic Change (81): 7-30
- ClimAlpTour (2010). Cambiamento climatico e turismo, un progetto europeo per guardare al futuro.
- Coppola E., Verdecchia M., Giorgi F. et al. (2014) Changing hydrological conditions in the Po basin under global war- ming. Science of The Total Environment 493: 1183-1196.
- Delft Hydraulics (2006) RIBASIM River basin planning and management simulation program. In: Proceedings of the iEMSs Third Biennial Meeting: "Summit on Environmen- tal Modelling and Software". Burlington, USA: Interna- tional Environmental Modelling and Software Society.
- Déqué, M., D.P. Rowell, D. Lüthi, F. Giorgi, J. H. Christensen, B. Rockel, D. Jacob, E. Kjellström, M. de Castro and B. van den Hurk, 2007. An intercomparison of regional climate simulations for Europe: assessing uncertainties in model projections. Climatic Change (81): 53-70
- DHMZ ((Croatian Meteorological and hydrological service)) (2002): Meteorološka podloga za vodnogospodarsku osnovu Hrvatske (Voditelj zadatka: Gajić-Čapka, M.), Zagreb, unpublished.
- DHMZ ((Croatian Meteorological and hydrological service)) (2002): Meteorološka podloga za vodnogospodarsku osnovu Hrvatske (Voditelj zadatka: Gajić-Čapka, M.), Zagreb, unpublished.
- DHMZ (Croatian Meteorological and hydrological service) (2014): Klimatske podloge za dva pilot područja u Hrvatskoj u okviru EU projekta DRINK-ADRIA (Autori: Branković Č, Cindrić, K., Gajić-Čapka, M., Güttler I.), Zagreb, unpublished.

- DHMZ (Croatian Meteorological and hydrological service) (2014): Klimatske podloge za dva pilot područja u Hrvatskoj u okviru EU projekta DRINK-ADRIA (Autori: Branković Č, Cindrić, K., Gajić-Čapka, M., Güttler I.), Zagreb, unpublished.
- DWD (2018): Climate Data Center. Deutscher Wetterdienst.
- EEA, European Environment Agency (2008). Impacts of Europe's changing climate-based assessment. EEA Report No 4/2008.
- Ehret, U.; Zehe, E.; Wulfmeyer, V.; Warrach-Sagi, K.; Liebert, J. Should we apply bias correction to global and regional climate model data? Hydrol. Earth System Sci. 2012, 16, 3391–3404, doi:10.5194/hess-16-3391-2012.
- Feiler, J., Ürge-Vorsatz, D. (2010): Hosszú távú (2050) kibocsátás csökkentési célok Magyarország vonatkozásában [Long-term (2050) emissions reduction targets in the Hungarian context]
- Feser, F., Rockel, B., von Storch, H., Winterfeldt, J., and Zahn, M.: Regional Climate Models Add Value to Global Model Data: A Review and Selected Examples, B. Am. Meteorol. Soc., 92, 1181–1192, 2011.
- Fioravanti, G., Desiato, F., Fraschetti, P., Perconti, W., & Piervitali, E. (2013). Time series requirements and trends of temperature and precipitation extremes over Italy. In EGU General Assembly Conference Abstracts (Vol. 15, p. 1173).
- Fowler, H.J., Blenkinsopa, S., Tebaldib C. 2007 Linking climate change modelling to impacts studies: recent advances in downscaling techniques for hydrological modelling. Int. J. Climatol. 27: 1547-1578
- Frei, C. and Schär, C.1998. A precipitation climatology of the alps from high-resolution rain-guage observations. Int. J. Climatol. 18: 873–900
- García-Ruiz J.M., López-Moreno J.I., Vicente-Serrano S.M. et al. (2011) Mediterranean water resources in a global change scenario. Earth-Science Reviews 105(3-4): 121-139.
- Giorgi, F., Jones, C., Asrar, G., 2009. Addressing climate information needs at the regional level: the CORDEX framework. WMO Bull. 58 (3), 175e183.
- Harpham, C. und Wilby, R.L. 2005. Multi-site downscaling of heavy daily precipitation occurrence and amounts, Journal of Hydrology 312/1-4, 235-255
- Haylock, M.R., Hofstra, N., Klein Tank, A.M.G., Klok, E.J., Jones, P.D. and New M. 2008. A European daily high-resolution gridded data set of surface temperature and precipitation for 1950–2006. J. Geophys. Res. 113, D20119
- Horvat, B., Rubinić, J. (2003): Primjena GIS-a na procjenu otjecanja (GIS Application in Surface Runoff Estimation), Proc. 3rd Croatian Conference on Waters, 265-271, Osijek, Croatia.
- Horvat, B., Rubinić, J. (2003): Primjena GIS-a na procjenu otjecanja (GIS Application in Surface Runoff Estimation), Proc. 3rd Croatian Conference on Waters, 265-271, Osijek, Croatia.
- Horvat, B., Rubinić, J. (2006): Annual runoff estimate - an example of karstic aquifers in the transboundary region of Croatia and Slovenia, Hydrological Sciences Journal, 51(2). pg. 314-324.

- Horvat, B., Rubinić, J. (2006): Annual runoff estimate - an example of karstic aquifers in the transboundary region of Croatia and Slovenia, Hydrological Sciences Journal, 51(2). pg. 314-324.
- IMGW dataset, Świerklaniec meteorological station, data period: 1961-2015 (unpublished)
- Institute for Electrical and Power Engineering (Institut za elektroprivredu i energetiku d.d. –IEE) (2007): Hidrološka obrada malih voda sliva Neretve sa slivnim područjem Baćinskih jezera i Imotskog polja (nos. Zad. Petričec, M., Ričković, V.). Zagreb, unpublished.
- Institute for Electrical and Power Engineering (Institut za elektroprivredu i energetiku d.d. –IEE) (2007): Hidrološka obrada malih voda sliva Neretve sa slivnim područjem Baćinskih jezera i Imotskog polja (nos. Zad. Petričec, M., Ričković, V.). Zagreb, unpublished.
- Intergovernmental Panel on Climate Change. Climate Change 2014: Synthesis Report. Contribution of Working Groups I, II and III to the Fifth Assessment Report of the Intergovernmental Panel on Climate Change. Geneva, Switzerland, 2014; (151 pp.).
- IPCC (2014): Climate Change 2014: Synthesis Report. Contribution of Working Groups I, II and III to the Fifth Assessment Report of the Intergovernmental Panel on Climate Change.
- Jacob D, et al. 2007. An inter-comparison of regional climate models for Europe: model performance in present-day climate. Climatic Change (81): 31-52
- Kis, A., Pongrácz, R., Bartholy, J., Szabó, J. A. (2017): Application of RCM results to hydrological analysis. IDŐJÁRÁS, Quarterly Journal of the Hungarian Meteorological Service. Vol. 121, No. 4, October – December, 2017, pp. 437–452
- KLIWA (2012): Auswirkungen des Klimawandels auf Bodenwasserhaushalt und Grundwasserneubildung in Baden-Württemberg, Bayern und Rheinland-Pfalz. Untersuchungen auf Grundlage von WETTREG2003- und WETTREG2006-Klimaszenarien. Klimaveränderung und Wasserwirtschaft. https://www.kliwa.de/_download/KLIWAHeft17.pdf (May 11th, 2018)
- Lafon, T.; Dadson, S.; Buys, G.; Prudhomme, C. Bias correction of daily precipitation simulated by a regional climate model: a comparison of methods. Int. J. Climatol. 2013, 33, 1367-1381.
- Langbein, W.B. (1962): The Water Supply of Arid Valleys in Intermountain Regions in Relation to Climate, IAHS Bull., Vol.7/1.
- Langbein, W.B. (1962): The Water Supply of Arid Valleys in Intermountain Regions in Relation to Climate, IAHS Bull., Vol.7/1.
- LfU (2012a): Auswertung regionaler Klimaprojektionen Klimabericht Bayern. Landesamt für Umwelt, Bayern. https://www.bestellen.bayern.de/application/eshop_app000004?SID=486602276&ACTIONxSESSxSHOWPIC(BILDxKEY:'lfu_klima_00082',BILDxCLASS:'Artikel',BILDxTYPE:'PDF') (May 11th, 2018)
- LfU (2012b): Auswertung regionaler Klimaprojektionen Regionalbericht Isar. Der Klimawandel in Bayern. Landesamt für Umwelt, Bayern. https://www.bestellen.bayern.de/application/eshop_app000000?SID=1393969176&ACTIONxSESSxSHOWPIC(BILDxKEY:'lfu_klima_00082',BILDxCLASS:'Artikel',BILDxTYPE:'PDF') (May 11th, 2018)
- LfU (2017): Klimabeobachtung - Phänologie. https://www.lfu.bayern.de/klima/klimabeobachtung/beobachtung_bayern/phaenologie/index.htm (May 11th, 2018)

- Liu Z. e Todini E. (2002) Towards a comprehensive physical- ly-based rainfall-runoff model. Hydrology and Earth Sy- stem Sciences 6 (5): 859-881.
- Maraun, D. Bias Correcting Climate Change Simulations - a Critical Review. Curr Clim Chang Reports 2016, doi:10.1007/s40641-016-0050-x.
- Maraun, D.; Widmann, M.; Gutiérrez, J.M.; Kotlarski, S.; Chandler, R.E.; Hertig, E.; Wibig, J.; Huth, R.; Wilcke R.A.I. VALUE: A framework to validate downscaling approaches for climate change studies, Earth's Future 2015, 3, 1–14, doi:10.1002/2014EF000259.
- Markart G., Kohl B., Sotier B., Schauer T., Bunza G., Stern R., (2004). Provisorische Geländeanleitung zur Abschätzung des Oberflächenabflussbeiwertes auf alpinen Boden-/Vegetationseinheiten bei konvektiven Starkregen. –BFW –Dokumentation, 89 S.
- Meinshausen, M., S. J. Smith, K. V. Calvin, J. S. Daniel, M. L. T. Kainuma, J.-F. Lamarque, K. Matsumoto, S. A. Montzka, S. C. B. Raper, K. Riahi, A. M. Thomson, G. J. M. Velders and D. van Vuuren (2011). "The RCP Greenhouse Gas Concentrations and their Extension from 1765 to 2300." Climatic Change (Special Issue), DOI: 10.1007/s10584-011-0156-z
- MOP (2016): Strategic Framework for Adaptation to Climate Change (in Slovenian: Strateški okvir prilagajanja podnebnim spremembam). - Ministry of the Environment and Spatial Planning.
- http://www.mop.gov.si/fileadmin/mop.gov.si/pageuploads/podrocja/podnebne_spremembe/SOzP.pdf (November 7th, 2018)
- MPA project - Development of Urban Adaptation Plans for cities with more than 100,000 inhabitants in Poland – Bytom, Institute of Environmental Protection – State Research Institute.
- MPPRB, Management Plan of Po River Basin (Piano di Gestione del Distretto Idrografico del Fiume Po: Stato delle Risorse Idriche) (2016)
- National Water Strategy on Water Management, Irrigation and Draughtsmanship. Ministry of Rural Development, 2013
- Pal, J. et al. (2007): Regional Climate Modelling for the Developing World: The ICTP RegCM3 and RegCNEt. Bulletin of the American Meteorological Society, 88(9), pg. 1395-1409.
- Plaut, G., Schuepbach, E., Doctor M. 2001. Heavy precipitation events over a few Alpine sub-regions and the links with large-scale circulation, 1971–1995. Clim. Res. 17, 285-302.
- Ravazzani G., Barbero S., Saladin A. et al. (2015) An integrated hydrological model for assessing climate change impacts on water resources of the Upper Po River basin. Water Resources Management, 29(4): 1193-1215.
- Rubinić, J.; Katalinić, A. (2014): Water regime of Vrana Lake in Dalmatia (Croatia): changes, risks and problems, Hydrological Sciences Journal, 59(10), pg. 1908-1924.
- Scoccimarro, E.; Gualdi, S.; Bellucci, A.; Sanna, A.; Fogli, P.; Manzini, E.; Vichi, M.; Oddo, P.; Navarra, A. Effects of Tropical Cyclones on Ocean Heat Transport in a High Resolution Coupled General Circulation Model. J. Climate 2011, 24, 4368–4384.
- Skarbit, N., Ács, F., Breuer, H., Krakker, D. (2014): Magyarország éghajlatának változásai a 20. században [The climate of Hungary in the twentieth century based on Péczely's method]. Földrajzi Közlemények 2014. 138. 4. pp. 261–276. (In Hungarian)

- Skoda, G. und Lorenz, P. 2003. Mittlere Jahresniederschlagshöhe – Modellrechnung mit unkorrigierten Daten. In: BMLFUW (Hrsg.), Hydrologischer Atlas Österreichs, 1. Lieferung, Kartentafel 2.2. Wien, Bundesministerium für Land- und Forstwirtschaft, Umwelt und Wasserwirtschaft
- Slovenian Environment Agency 2017. Climate data - result of the project Assessment of climate change in Slovenia until the end of 21st century. Slovenian Environment Agency and Ministry of the Environment and Spatial Planning.
- Somlyódy, L.: Public Corporate Strategic Programs, Water Management of Hungary: Situation and Strategic Tasks. Hungarian Academy of Sciences, Budapest, 2011
- Spiegel Online (2018): Union und SPD wollen Klimaschutzziel aufgeben. http://www.spiegel.de/wirtschaft/soziales/grosse-koalition-zu-klimaschutz-union-und-spd-wollen-ziel-2020-aufgeben-a-1186785.html (May 9th, 2018)
- StMUV (2007): Klimaprogramm Bayern 2020. Bayerisches Staatsministerium für Umwelt und Verbraucherschutz.
- Szabó, P., Horányi, A., Krüzselyi, I., and Szépszó, G., (2010): Az Országos Meteorológiai Szolgálat regionális klímamodellezési tevékenysége: ALADINClimate és REMO. 36. Meteorológiai Tudományos Napok, OMSZ, Budapest, 87–101 (In Hungarian)
- Teutschbein, C.; Seibert, J. Bias correction of regional climate model simulations for hydrological climate change impact studies: Review and evaluation of different methods. J. Hydrol 2012, 456-457, 12-29.
- Tibaldi, S, Cacciamani C, Tomozeiu R. "Il cambiamento climatico dalla scala globale a quella di bacino del Po" – I Conferenza annuale EU.WATERCENTRE, 2014 - Proceedings
- Tolson BA, Shoemaker CA. 2007. Dynamically dimensioned search algorithm for computationally efficient watershed model calibration. Water Resources Research 43: 16 pp
- Tomozeiu R., Agrillo G., Cacciamani C., Pavan. V (2014). Statistically downscaled climate change projections of surface temperature over Northern Italy for the periods 2021–2050 and 2070–2099. Natural Hazards DOI: 10.1007/s11069-013-0552-y.
- Tomozeiu R., Agrillo G., Villani G., Tomei F, Marletto V., Botarelli L (2011). Scenari di cambiamento climatico di temperatura e precipitazioni in Italia per il periodo 2021-2050, ottenuti attraverso tecniche di regionalizzazione statistica e loro impatto sull'irrigazione. Atti del XIV Convegno Nazionale di Agrometeorologia - Rivista Italiana di Agrometeorologia, pag. 29-30, PATRON EDITORE, edizione maggio 2011.
- Tomozeiu R., Pavan V., Cacciamani C., Amici M. (2007). Observed temperature changes in Emilia-Romagna: mean values and extremes. Theor. Appli. Climatol. (2007).
- Toreti, A., Fioravanti, G., Perconti, W., Desiato, F. (2009). Annual and seasonal precipitation over Italy from 1961 to 2006, Int. J. Climatol., 29, 1976-1987. doi: 10.1002/joc.1840.
- Turc, L. (1954): Le bilan d'eau des sols, relation entre les précipitations, l'evaporation et l'écoulement, Troisiémes journées de l'hydraulique à Alger.
- Valt, M., Cagnati, A., Crepaz, A., Marigo, G. (2005). Neve sulle Alpi. Neve e Valanghe, 56, 24-31.

- van der Linden P., and J.F.B. Mitchell (eds.) 2009: ENSEMBLES: Climate Change and its Impacts: Summary of research and results from the ENSEMBLES project. Met Office Hadley Centre, FitzRoy Road, Exeter EX1 3PB, UK. 160pp.
- Vezzoli, R. et al. 2015. "Hydrological Simulation of Po River (North Italy) Discharge under Climate Change Scenarios Using the RCM COSMO-CLM." Science of the Total Environment 521-522: 346–58.
- Vezzoli, Renata, Paola Mercogliano, and Sergio Castellari. 2016. "2050: quale disponibilità idrica nel bacino del fiume Po ?" Ingegneria dell'Ambiente 3: 44–52.
- VKGTT: Territorial Water Supply Management Plan
- Wilby R. (2017) Climate change in practice Cambridge Press
- Wilcoxon, F. (1945): Individual Comparisons by Ranking Methods. Biometrics Bulletin, 1(6), pg. 80-83.
- Woolhiser DA, Pegram GGS. 1979. Maximum Likelihood estimation of Fourier coefficients to describe seasonal variations of parameters in stochastic daily precipitation models. Journal of Applied Meteorology 18: 34-42
- Zemp, M., Haeberli, W., Hoelzle, M., Paul, F. (2006). Alpine glaciers to disappear within decades? Geophysical Research Letters, 33, L13504.
- Zemp, M., Paul, F., Hoelzle, M., Haeberli, W. (2008). Glacier fluctuations in the European Alps,1850-2000. An overview and a spatiotemporal analysis of available data. In: Darkening Peaks: Glacier Retreat, Science, and Society (Orlove, B., Wiegandt, E., Luckman, B.H., eds.), 152-167. University of California Press, Los Angeles.
- Zollo A.L.; Rillo, V.; Bucchignani, E.; Montesarchio, M.; Mercogliano, P. Extreme temperature and precipitation events over Italy: assessment of high-resolution simulations with COSMO-CLM and future scenarios. International Journal of Climatology 2015, doi: 10.1002/joc.4401.